Master of Science Thesis in Electrical Engineering
Department of Electrical Engineering, Linköping University, 2017

Powertrain Control for Improved Driver Comfort During Automated Gear Shifts

Viktor Dahlgren and Oskar Lindahl

Master of Science Thesis in Electrical Engineering

Powertrain Control for Improved Driver Comfort During Automated Gear Shifts

Viktor Dahlgren and Oskar Lindahl

LiTH-ISY-EX--17/5084--SE

Supervisor: **Viktor Leek**
ISY, Linköpings universitet
Marcus Engman
Scania CV AB

Examiner: **Lars Eriksson**
ISY, Linköpings universitet

Division of Vehicular Systems
Department of Electrical Engineering
Linköping University
SE-581 83 Linköping, Sweden

Sammanfattning

Körbarhet är ett relevant problem vid utveckling av moderna lastbilar. Komfort och att ha en känsla av kontroll över fordonet är nyckelfaktorer för föraren. Under en växling sänks svänghjulsmomentet till noll före frikoppling och höjs sedan igen efter koppling. Sättet att utföra sänkningen och höjningen av momentet skapar rörelser i hytten. Tidigare utveckling av växlingens funktionalitet har haft syftet att behålla ett bra beteende i drivlinan under växlingen. Detta examensarbete har istället undersökt möjligheterna att förbättra hyttkomforten under autonoma växlingar genom att ändra sättet växlingen utförs.

Ett mått på komfort har tagits fram i arbetet genom experiment och samarbete med testförare. De viktigaste skillnaderna mellan bra och dåliga växlingar identifierades som amplituden för hyttaccelerationer och jerk. Därför var målet att minska hyttaccelerationer och jerk för att förbättra hyttkomforten.

En modell över hur drivlinan påverkar hyttrörelser har tagits fram. Delmodeller av drivlina, chassi och hytt har utvecklats var för sig för att kombineras till en sammansatt modell. Delmodellerna presterade bra individuellt och den kombinerade modellen bedömdes tillräckligt bra för att användas vid regulatorutveckling.

Vid tiden för exjobbet använde Scania en regulator med syftet att motverka oscillationer och jerk i drivlinan. För att undvika att behöva ta hänsyn till beteendet i drivlinan användes den existerande regulatorn i kombination med regulatorn framtagen i examensarbetet. Två ansatser undersöktes, öppen styrning och återkoppling. Funktionen för den öppna styrningen var att lågpassfiltrera insignalerna till den existerande regulatorn. Den andra ansatsen var att återkoppla z-accelerationen (uppåt). Syftet var att hålla accelerationen låg genom att använda en referens framtagen med erfarenheter från komfortexperimenten.

Simuleringar av den öppna styrningen visade att det var möjligt att påverka hyttkomforten genom att ändra motormomentet. Komforten var förbättrad i större delen av växlingen men även försämrad i en fas mot slutet av växlingen. Regulatorn med återkoppling visade lovande resultat i simuleringar. Det var problematiskt att kombinera den existerande regulatorn med den utvecklade regulatorn eftersom de hade olika mål. Genom en sammanslagning av de två regulatorerna skulle det finnas goda möjligheter att förbättra växlingen med avseende på både drivlinebeteende och hyttkomfort.

Abstract

Driveability is an important issue in the development of modern trucks. Comfort and sense of control are key for the driver. During a gear shift, the flywheel torque is lowered to zero before disengaging the clutch and then increased again after engaging the clutch. Lowering and increasing the flywheel torque creates movements in the cab. The previous developments of the gear shift functionality has had the purpose to maintain a good behaviour in the powertrain. This Master's thesis has instead investigated whether it was possible to improve the cab comfort during autonomous gear shifts by altering the way it is performed.

A measure of cab comfort has been developed through experiments and cooperation a test driver. The main differences between good and bad gear shifts were identified as the amplitudes of cab accelerations and jerk. Therefore, the goal was to minimize acceleration and jerk in order to improve the cab comfort.

A model of how the powertrain affects the cab movements has been developed. Sub models of the powertrain, chassis and cab were developed individually and combined into one large model. The models performed well individually and the combined model was judged to be good enough for developing a controller.

At the time of writing the existing controller had the purpose of preventing oscillations and jerk in the driveline. To avoid having to consider behaviour in the powertrain the developed controller were to control the existing controller. Two approaches have been investigated, open loop control and feedback control. The functionality of the open loop controller was to low pass filter inputs to the existing controller. The other approach was a feedback controller using the z-acceleration (upwards) as feedback. The purpose was to keep the acceleration low using a reference developed with experience from the comfort experiments.

Simulations of the open loop controller showed that it was possible to alter the cab comfort by altering the engine torque. The comfort was improved in most parts of the gear shift and worsend in some parts. The feedback controller showed promising results in simulations. It was problematic to combine the existing controller with the developed controller since they have different purposes. By a fusion of the controllers there would be good opportunities to improve the gear shift with respect to both powertrain behaviour and cab comfort.

Acknowledgments

We would like to direct our gratitude to our examiner, Lars Eriksson, and our supervisor at Linköping University, Viktor Leek, for their guidance and encouragement throughout this thesis. We would also like to thank our colleagues at Scania, especially our supervisor, Marcus Engman, for countless productive discussions and lots of support.

Linköping, August 2017
Viktor Dahlgren and Oskar Lindahl

Contents

Nomenclature

Parameter	Description
F	Force
W	Normal force
m	mass
a	acceleration
θ	angle
ϕ	chassis angle relative to the ground
v	Speed
J	Inertia
M	Torque
r	Radius
k	Spring constant.
c	Damper constant
i	Conversion ratio
g	Gravitational acceleration
General subscripts	
x	x-direction
z	z-direction
a	air
r	Rolling resistance.
g	gravity
DR	Driving resistance.
ch	Chassis
p	Propulsion.
Powertrain subscripts	
a	Air resistance.
w	Wheel
t	Transmission.
f	Final drive
e	Engine
d	Driveshaft
Chassis subscripts	
tr	trailer
R	rear
F	front
Cab subscripts	
s	Spring
c	Cab

1. Introduction

This introductory section aims at giving the reader an overview of why this Master's thesis was conducted and what the scope was. The first part is a background to the problem. It gives a brief description of how a gear shift is performed and how the powertrain is defined. The background also states what is unique with this thesis compared to previous work.

The objective is stated pointwise. These points describe the different parts that was worked with and was developed to state what had to be done in order to improve the cab comfort.

Delimitations are introduced to make the thesis viable.

1.1 Background

Driveability is an important issue in the development of modern trucks. Comfort and sense of control are key for the driver. It is therefore important that the vehicle acts as the driver desires. The concept of control is an excellent way to improve the driveability for example by improving the software instead of altering expensive hardware.

How to perform a gear shift is one of the areas where different approaches of control might be used. A common way to shift gear is manual transmission with gear shifting by engine control which is described in [1]. In short, the transmitted torque from the engine to the clutch is controlled down to zero and then the neutral gear is engaged. The engine speed is controlled to track the transmission speed, the new gear is engaged and the transmitted torque rises again.

The powertrain is defined as *the group of components that generate power and deliver it to the road* in [2]. Typically it consists of the engine, transmission, propeller shaft, differential, driveshafts and wheels, thus the driveline and the engine. The function of the powertrain is to deliver the power desired by the driver to the wheels. Due to different characteristics and torsional effects in the driveline components, oscillations might occur when the torque is changed. Such oscillations might transfer into a jerky drive.

Previous work has been done in controlling the engine and driveline during a gear shift with the focus on behaviour in the powertrain. The change in torque during the gear shift means a change in propulsion force. The truck driver is linked to the powertrain through large masses and long levers, cab and chassis, which could lead to large movements and forces in the seat induced by the powertrain. Therefore it is reasonable to investigate how the gear shift affects the cab movements from a comfort and driveability perspective. This is the motivation of this thesis.

A further advantage of reducing the cab movements is the reduced wear of components used in the suspension system of the cab. Sustainability of dampers and springs could be much improved if the movements are controlled and suppressed.

1.2 Objective

The purpose of this thesis was to improve the comfort in the cab by looking at the functionality of autonomous gear shifts. A powertrain model extended with a model describing the movements of the cab were to be developed. A control algorithm was to be developed to control the cab movements and eventually implemented and validated on a Scania truck. More specifically the objective of the thesis was the following:

1. Develop a complete powertrain model extended with cab movements.
   (a) Parameterize an existing powertrain model with parameters specific for the vehicle in this thesis.
   (b) Develop a model describing the cab pitch and heave movements.
   (c) Assemble the powertrain model and the cab movement model into a complete model.
2. Investigate which variables affect the comfort.
   (a) By experiments, identify the variables affecting the comfort.
   (b) Define how cab comfort is seen in this thesis.
3. Develop a control algorithm with the goal of improving driver comfort regarding the identified variables in 2.(a).
   (a) Control the propulsion unit and transmission during a gear shift subject to cab movements.
   (b) Try different control structures and compare them.
4. Implement and verify the control algorithms.

(a) Implement the control algorithm in a simulation environment.

(b) Implement and verify the control algorithm on a Scania truck.

(c) Compare the performance of the developed control algorithm to that of the new generation Scania trucks.

1.3 Delimitations

Scania combines different modules so that each customer might adapt their truck to their specific need. This means that the number of possible setups for a truck is large. In order to reach the goals in the short time available one vehicle configuration was chosen.

Frame twisting was not considered in this thesis. Chassis and cab were considered as stiff bodies. Only forces and movements in the xz-plane was considered leading to pitch and heave cab movements.

Wheel slip and backlash were not considered in the powertrain model.

2. Problem description

The purpose of this section is to present information needed to understand this report. The system available to work with to improve the cab comfort is presented, where truck and driveline components are defined. It is also described how a general automated manual transmission gear shift is performed which was used in this thesis.

The end of the section describes how the model and controller was implemented and used.

2.1 System introduction

Initially, a truck definition is given in order to minimize the risk of misconception between the reader and the authors. The vehicle of interest, the driving area where data collection was performed, and also how a gear shift is performed in this thesis are described.

2.1.1 Vehicle

Figure 2.1 shows the different truck components and how they will be referred to throughout this report. The xz-plane is defined such that x is straight forward parallel to the ground and z is straight upwards perpendicular to the ground.

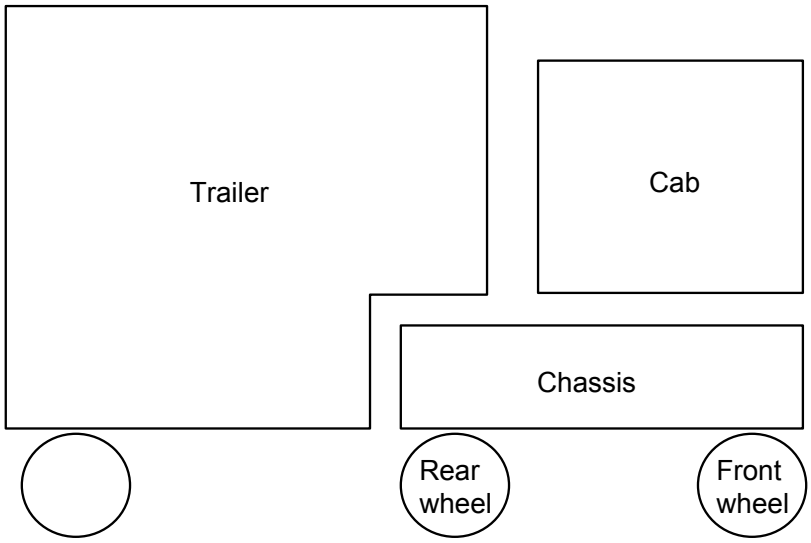

Figure 2.1: Definitions of the different truck components used in this thesis. The wheels, chassis and cab are defined as the tractor, while the truck is the tractor with the trailer.

The vehicle that was used in this thesis was a tractor with a trailer. The tractor is defined as the cab and the chassis together. There are many possible tractor configurations. Number of axles, choice of driving wheels, chassis and cab suspensions are all parameters in defining a tractor composition. One specific setup was chosen for this project. It was used to collect data to analyze movements, develop models and controllers. When choosing a setup, it was of interest to have a vehicle with a lot of cab movements during a gear shift. The choice fell on a tractor named *Monaco*. The main parameters of interest that determined the choice were that it had a powerful engine with 6 cylinders and 500 hp, 4-bellow air suspension system, and finally a large cab of S-type. With this setup the chance of getting a lot of cab movement during a gear shift was high.

As mentioned in 1.1 the powertrain is the group of components of the vehicle that generate power and deliver it to the road. The composition of the components in the powertrain is illustrated in Figure 2.2.

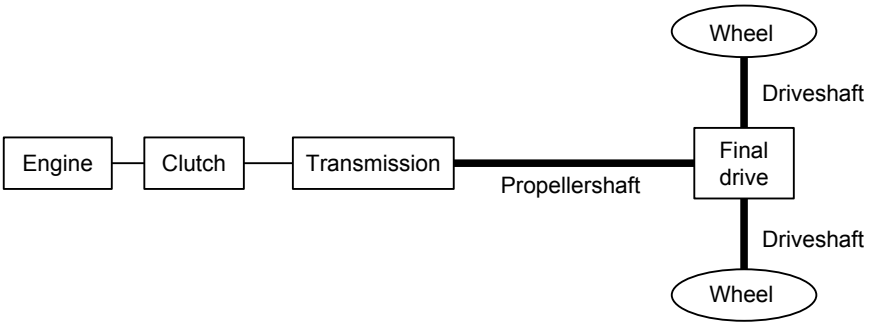

Figure 2.2: Composition of the powertrain components.

2.1.2 Driving area

The test track at Scania was used to collect the data needed. For this thesis the relevant parts were straights, parts with inclination and parts with no inclination. The test track offered a good opportunity to make relevant experiments.

2.1.3 Gear shift

In this thesis, a gear shift was performed as described in [3] and shown in Figure 2.3. The figure shows the different phases of an autonomous gear shift.

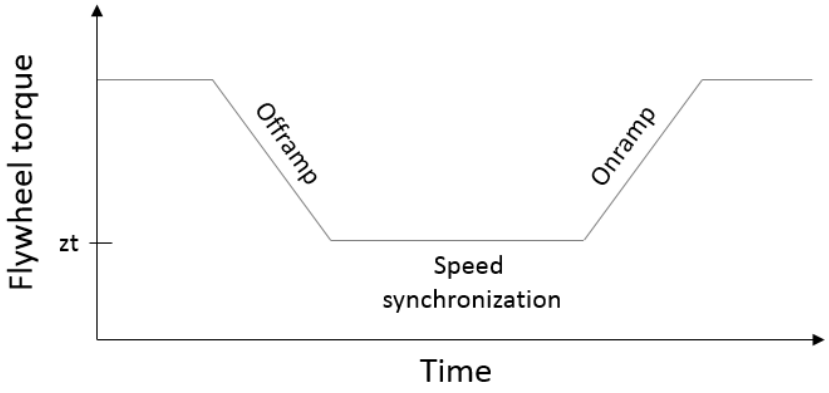

Figure 2.3: A sketch of the flywheel torque in an autonomous gear shift. The neutral gear is engaged after the offramp and the new gear is engaged before the onramp. zt is the flywheel torque level which represents zero transferred torque in the transmission.

To perform the gear shift the transmitted torque in the transmission should be controlled down to zero transmitted torque, this part will be referred to as the offramp. Then the neutral gear is engaged and the engine speed is controlled to match the transmission speed. The last part is to engage the gear and return the torque level to the driver demands, this will be referred to as the onramp.

The controller used to control the onramp and the offramp in this thesis controlled it in a way that the oscillations of the powertrain were suppressed. In this thesis the on and offramp were modified to improve

the comfort. Oscillations in the powertrain also affects the comfort. Therefore the controller developed in this thesis was used in combination with the existing controller. It was the shape of the offramp and onramp of the gear shift that was modified in order to improve the cab comfort. The time is crucial in some situations, for example in an upwards slope it is important to perform the gear shift in a short time in order to keep the velocity and propulsion gained before the gear shift. Therefore the time that the onramp and offramp can be performed on cannot be extended to much.

2.2 Implementation

The system, model and controller, was developed and verified in a simulation environment. The implementation in truck was cancelled due to a combination of time limitation and vehicle problems.

2.2.1 Simulation environment

The system was implemented in Simulink in order to develop and validate the control algorithm in a safe and cheap way. The system was divided into subsystems, with a vehicle model and a controller as the highest sub systems. The vehicle model consisted of two parts, the powertrain and the movement model, where the movement model consisted of a chassis model and a cab model.

3. Related research

This section presents research related to this project. Why it is related and how it is different to this work is explained. The related research includes areas such as modelling the driveline in different ways, modelling the truck and different work about controlling cab movements. Some investigations about vehicle comfort are also brought up.

3.1 Modelling

The driveline configuration differs between different vehicles. It is however truck standard to be rear-wheel-driven. Such a driveline, described in [2], consists of clutch, transmission, propeller shaft, final drive, driveshafts and wheels. The driveline together with the engine constitutes the powertrain and every component needs to be modelled in order to describe the powertrain behaviour.

3.1.1 Rigid powertrain model

One way to model the driveline is to neglect the oscillative characteristics of the driveline by using a rigid model. According to [2] this approach is suited for studies in propulsion where it is sufficient to neglect the internal states of the driveline. This is interesting to this thesis since it is a simple model and the focus is how the propulsion affects the cab movements. An approach to derive rigid model equations describing the components mentioned above is also presented in [2].

[4] derives a rigid powertrain model where the engine torque transfers through the driveline resulting in a propulsion force to accelerate the wheels. The force is calculated under the assumption that there is no wheel slip. This assumption applies to this thesis as well. The propulsion force on the wheels is thought to be one of the forces inducing movements in the cab movement model.

A first approach in this thesis was to use the rigid driveline model since the focus was on the cab movements affected by the propulsion. It was also assumed that the existing controller handled the oscillations.

3.1.2 Powertrain model with flexible components

Another approach to the driveline model is a model that describes the flexibility of components in the driveline. [3] concludes that in order to control the oscillations in the driveline it is necessary to have a model that captures the oscillations. Such a model is derived in [1]. In [2] different approaches are used where different components in the powertrain are considered flexible. One approach is to lump all the flexibilities into the driveshaft which has the most flexibility in the powertrain. This model could be extended by adding flexible components and states.

3.1.3 Cab movement

There has been previous investigations about how the road influences the cab movements. For example in [5], a three-degree-of-freedom truck cab model is presented describing the pitch, heave and roll movements. The objective was to control the movements induced by road excitations, thus forces acting in z-direction. An active suspension system was used to control the movements. Another investigation about controlling cab movements induced by road excitations with an active suspension system is made in [6].

Unlike above, where the forces acting on the system are induced by the road, in this thesis the movements are induced by the change in propulsion force in the powertrain during a gear shift. This thesis did only focus on the pitch and heave (xz-plane) movements which motivates a choice of a two-dimensional model.

A two-dimensional truck model is presented in [7]. It is stated that such a model has one major limitation in that the sprung mass (here, cab and chassis) is modelled as one rigid body. Though in reality, the truck has a flexible frame and chassis. In this thesis however, structural elements was considered stiff and phenomena such as frame twisting were not considered. Therefore a two-dimensional model is motivated also by this example.

[8] also derives a two-dimensional truck model. Just like in [7], the chassis and cab are modelled as one stiff body. A trailer is attached to the chassis and expressions of trailer forces acting on the chassis are derived

using Newton's second law and Euler's laws of motion. A trailer was also used in this thesis and the same approach to calculate the forces from the trailer on the chassis was used.

3.2 Control

Work on controlling the powertrain has previously been done with respect to the oscillations in the driveline. In [2] the driveline is modelled with dynamics and controlled in order to suppress the oscillations that occur because of these. In [9] different approaches of engine torque control to minimize oscillations in the driveline are tested.

A popular way of controlling the cab movement is by using active suspension to reduce the effect of road excitation. In [5] a three-degree-of-freedom cab model is used to control the cab movements with active suspension. In [6] the cab movements are also controlled with active suspension. The goal is to optimize the driver comfort when driving in a straight line while still following a compensation strategy adapted for braking, accelerating and turning.

The objective in this thesis work was to improve driver comfort by controlling the propulsion unit. The onramp and the offramp were the focus in this thesis. Using the model of the chassis, the model of the driveline in combination with the cab model the ramps would be controlled with the goal of reducing the effects on the cab from the gear shift.

3.3 Comfort measurement

Since comfort has a subjective element to it, a measurement of comfort is hard to define. In [10] it is stated that the goal should be to eliminate all vibrations in a vehicle for good comfort. The book uses different measures and concludes that the vertical vibrations in the region of 4 and 8 Hz and the horizontal vibrations in the region of 1 and 2 Hz are what the human body is most sensitive too.

The road is not the only source of uncomfortable vehicle movements. In [11] a speed planner for an autonomous car is derived. It uses a quintic Bézier curve for a smoother profile of acceleration and jerk. In [12] a control strategy for an autonomous gear shift in a sport motorcycle is derived. The goal was to minimize the jerk while limiting the duration of the gear shift by keeping track of the clutch position. [13] derived a ride comfort prediction method which was applied on a rail vehicle. The method that was used to evaluate comfort was to minimize the square root of the summed squared accelerations in x-, y- and z-direction. This measurement evaluates the size of the acceleration vector instead of investigating the acceleration in each direction respectively.

In order to obtain a comfort measure experiments were performed in cooperation with a test driver. The driver gave the verdict good, bad or undefined for different gear shifts and the collected data was then analyzed.

4. Method

This section gives an overview of the work done throughout the thesis. First, experiments were performed in order to analyze the movements of the tractor components. A measurement system was developed in order to register these movements. With the goal of the thesis being to improve the cab comfort it had to be defined for this thesis. The experiments, measurement system and thesis comfort definition are described in the beginning of this section.

A large part of the thesis was to develop models. The truck and powertrain consists of many parts. These had to be modelled and connected in order to describe how the propulsion force is generated and affecting the cab movements. An overview of the modelled components and how they were connected to each other is described. How each component was modelled is presented. Alternative models that were considered and why they were not chosen for the complete model are brought up.

Different controller structures developed and investigated are presented in the end of the section.

4.1 Experiments

In order to learn how the different parts of the truck were moving a number of experiments were done. The measurement equipment and the experiments performed are explained. To improve the comfort in the cab measurements were performed and analyzed to define comfort for this thesis.

4.1.1 Measurement system

A measurement system was developed in order to receive the data needed to analyze the truck movement and to use when developing the vehicle model. Only movements in the xz-plane were considered in this thesis. This meant that the movements of interest were the cab and chassis movements up, down, forward, backward and rotations. The sensors needed and their positions were decided through discussions with the vehicle dynamics department at Scania. The measurement system developed to catch the relevant movements is shown in Figure 4.1.

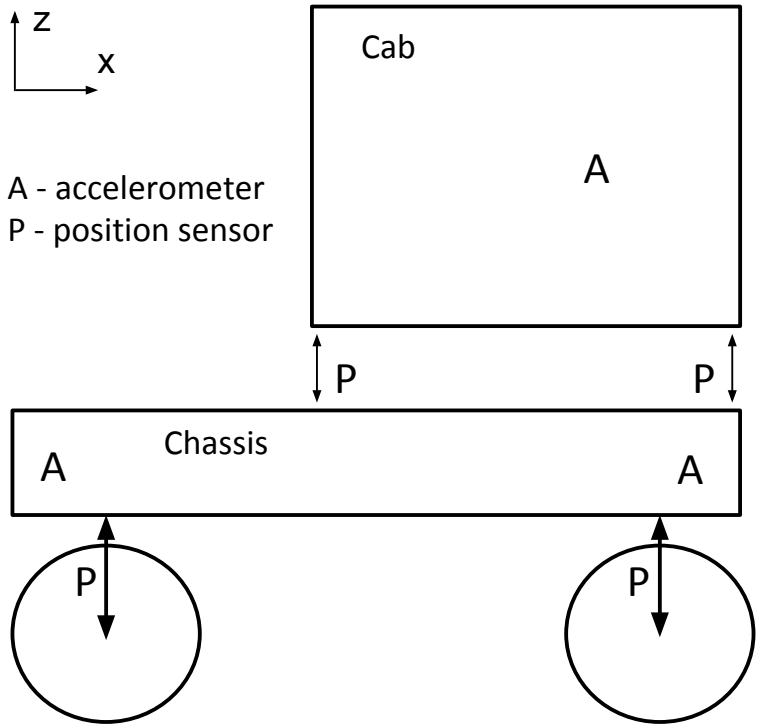

Figure 4.1: Placements of the sensors used for data collection. An "A" means an accelerometer and a "P" stands for a position sensor. The position sensors at the wheels measured the distance between the wheel axle and the chassis frame. The position sensors between the chassis and the cab measured the distances between the cab front and chassis frame, and the cab rear and chassis frame. Each position denoted by an "A" contained two accelerometers, one measured acceleration in x-direction and one in z-direction. The accelerometers in the cab were placed on the base of the seat to ignore effects from the driver and damping of the seat was not considered.

There were a number of existing sensors already installed on the truck. However the installed sensor system only contained the two position sensors at the wheels out of the sensors in Figure 4.1. The data from the existing sensors was registered with a software called $Vision$. The remaining sensors had to be installed on

the truck. The software $Vision$ did not handle external sensors easy. Instead, another measurement system, called $DEWEsoft$, was used to register the data from the external sensors.

In order to synchronize the signals from the different measurement systems, the engine speed was registered by both systems. The engine speed was measured by an existing sensor, and therefore $Vision$ received the signal straight away. To register the engine speed in $DEWEsoft$, the signal had to be transferred to the external measurement system. This resulted in a delayed engine speed. [14] is a thesis work that investigates and compensates for time-delays on the data bus used by Scania. The delay that was used was 10-15 ms. This also had to be taken into account when synchronizing the signals. How the signals were synchronized is explained in Appendix A.

4.1.2 Driving situations

Measurements could only be performed in the beginning of the thesis. Therefore it was important to carefully decide the experiments needed to receive the desired data. The data was needed for modelling and developing of controller, but also for knowledge of the system. Table 4.1 summarizes the driving situations and explains the thought of what to use them for.

Table 4.1: The table consists of the experiments performed to collect data.

Driving situation	**Function**
Standing still, 0 % inclination	Used for noise estimation and to remove sensor offset.
Constant velocity, 0 % inclination	Find an equilibrium that could be used to estimate spring and damper constants.
Acceleration from 0 m/s^2, in slope	Capture the movements during gear shifts.
Decouple at different velocities, 0 % inclination with and without the trailer	Estimate driving resistances.
Comfort measurements	Perform good and bad gear shifts to define what comfort was in this thesis.

4.1.3 Comfort

The goal of the thesis was to make gear shifts more comfortable. To identify variables which could be used to identify comfort, measurements had to be performed and analyzed. One assumption that was made regarding comfort was that the stronger forces acting on the human body, the more uncomfortable it feels. The force is proportional to the acceleration according to Newton's second law of motion, F=ma. This lead to the conclusion that the acceleration should be measured and analyzed. In [11] the acceleration was used as a measurement of comfort which further strengthened the case for investigating the acceleration. Jerk is the time derivative of acceleration and should therefore be interesting to investigate to see if it affects the driver comfort. Another measurement of interest was the frequencies present during the gear shift. According to [10] the goal should be to eliminate the vibrations of the system.

To measure the acceleration, jerk and frequencies accelerometers had to be placed on the truck. The driver is located in the seat while driving. It was therefore important to investigate the behaviour by the seat. Since effects induced by the driver should not affect the measurement the sensors were placed at the base of the seat which is connected to the floor but are separated from the suspended moving parts of the seat.

An experienced driver was appointed to identify which gear shifts were good and which were bad. In this case, "good" was a gear shift which the driver considered comfortable and "bad" was uncomfortable. The measurements were performed in slopes at low speeds. This because the movements in the cab were most distinct at these conditions. After the experiments the collected data was matched to the corresponding verdicts from the driver.

The acceleration measurements were low passed filtered with the cut-off frequency 10 Hz. The reason behind the cut-off frequency is explained in Appendix A. To calculate the jerk the numerical differentiation method *Finite difference method forward*, described in [15], was used. In some plots there are a red and a black line. The red line represents a limit for bad gear shifts while the black represents the limit for a good gear shift. These lines are reference points to be able to compare plots to each other. The lines are different for acceleration and jerk. They are also different for the z- and x-direction.

Acceleration and jerk in x-direction

Figure 4.2a and Figure 4.2b shows the acceleration and jerk in x-direction in two different measurements. One measurement contains three bad gear shifts and the other contains one bad and three good gear shifts.

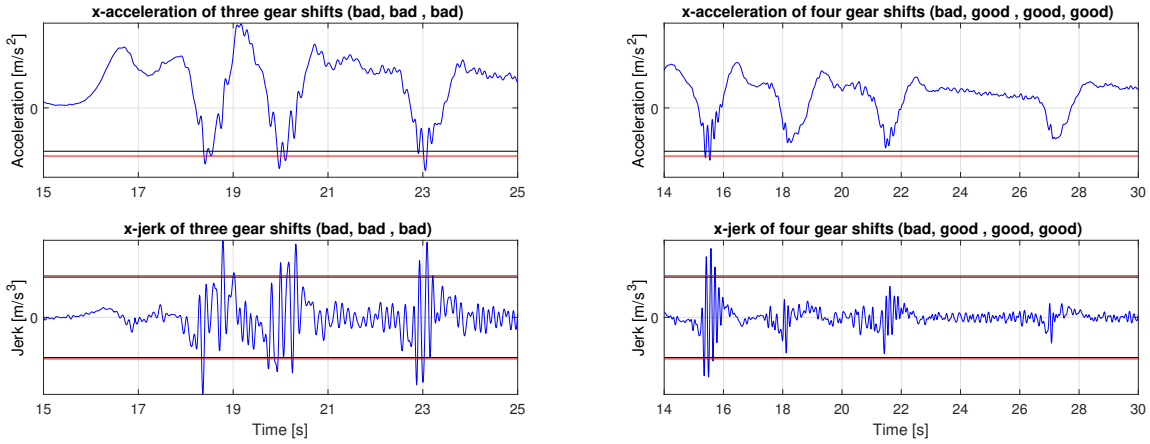

(a) The figure includes three bad gear shifts.

(b) The figure includes one bad and three good gear shifts.

Figure 4.2: Measured acceleration (above) and calculated jerk by the seat (below). The red line represents a limit for bad gear shifts and the black line represents a limit for good gear shifts.

The case in these two figures was that if the acceleration and jerk were above (acceleration) or within (jerk) the black line they were considered comfortable. If they were outside the red line the gear shift was not considered comfortable. As seen in the figures the space between the lines that defined good (black) and bad (red) gear shifts was small. This led to the conclusion that a good and bad gear shift were not always easy to separate.

The lines were based on multiple measurements. Figure 4.3a and Figure 4.3b however, shows that there were contradicting measurements of good and bad gear shifts.

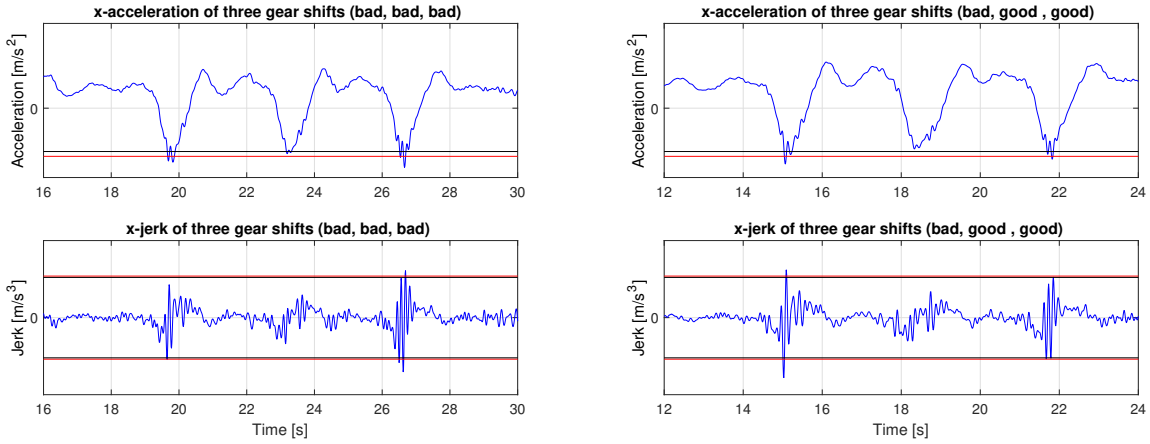

(a) The figure includes three bad gear shifts.

(b) The figure includes one bad and two good gear shifts.

Figure 4.3: Measured acceleration (above) and calculated jerk by the seat (below). The red line represents a limit for bad gear shifts and the black line represents a limit for good gear shifts.

The acceleration of the second gear shift (bad) in Figure 4.3a should according to the lines go below the red line which it did not. The jerk of the second gear shift should be greater if the lines were to be absolute limits between good and bad gear shifts. Looking at the acceleration of the third gear shift (good) in Figure 4.3b, the acceleration goes below the red line. The jerk of the third gear shift should be smaller if the lines were to be absolute limits between good and bad gear shifts.

This led to the conclusion that in the general case the acceleration and the jerk should be small if the gear shift was to be considered comfortable. But even if the acceleration and jerk in the x-direction were within the defined lines it did not guarantee that the driver found it comfortable.

Acceleration and jerk in z-direction

The measurements and calculations in the z-direction are displayed in this section. Figure 4.4a and Figure 4.4b shows acceleration and jerk of two different measurements.

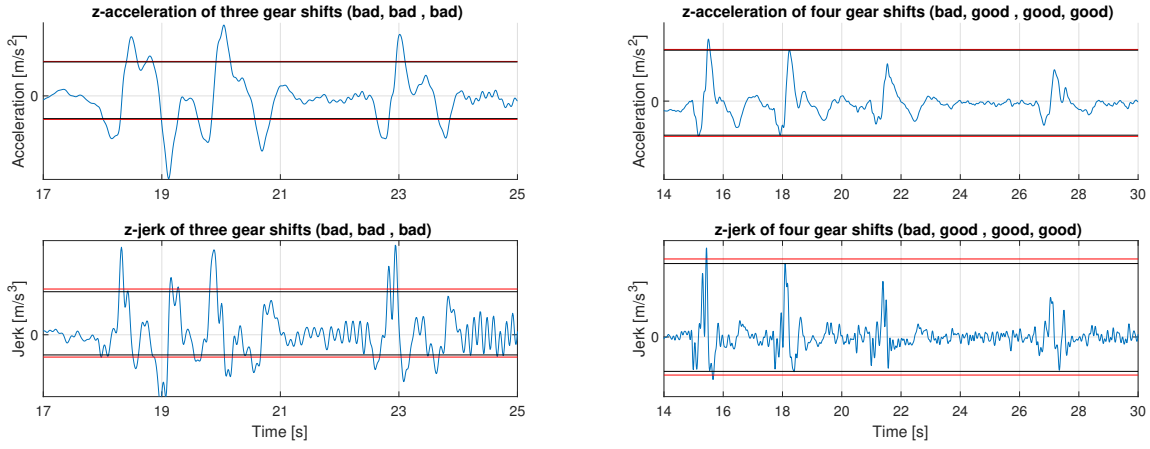

(a) The figure includes three bad gear shifts.

(b) The figure includes one bad and three good gear shifts.

Figure 4.4: Measured acceleration (above) and calculated jerk by the seat (below). The red line represents a limit for bad gear shifts and the black line represents a limit for good gear shifts.

The figures show the same general principle as in the x-direction. That is when the acceleration was not too big and the jerk was kept small the gear shifts could be considered good. The separation of the good and bad gear shifts were not distinct for the z-direction either. It could be noticed that the positive jerk was generally higher in the z-direction compared to the negative one. As for the x-direction there were contradicting measurements which are displayed in the Figure 4.5a and Figure 4.5b.

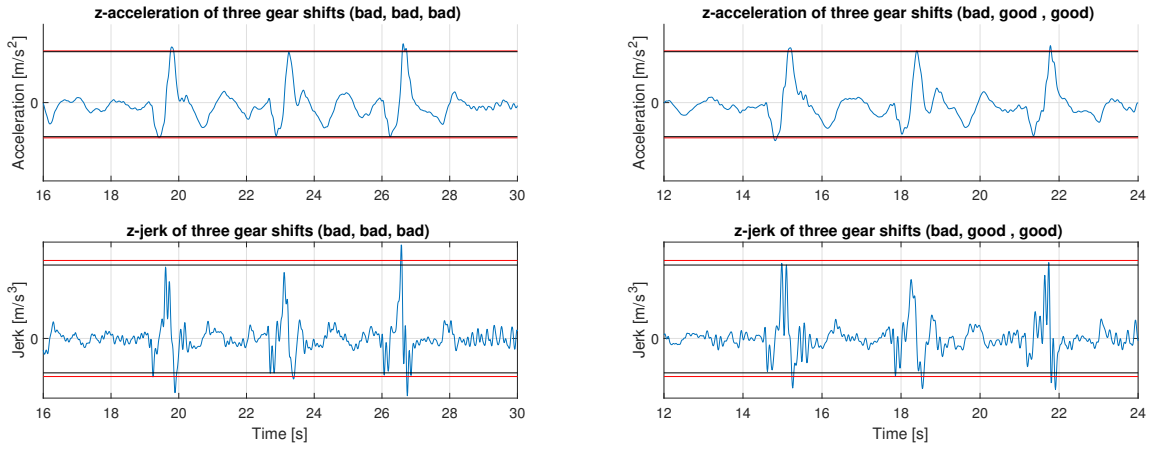

(a) The figure includes three bad gear shifts.

(b) The figure includes one bad and two good gear shifts.

Figure 4.5: Measured acceleration (above) and calculated jerk by the seat (below). The red line represents a limit for bad gear shifts and the black line represents a limit for good gear shifts.

Looking at the second gear shift (bad) in Figure 4.5a, the acceleration should go below the red line, which it did not. In Figure 4.5b, the acceleration and jerk of the third gear shift (good) should have been smaller if the lines would have been absolute.

Since there were contradicting measurements an absolute limit between good and bad acceleration and jerk in z-direction could not be drawn. In the general case it was desirable to minimize acceleration and jerk.

Frequencies during gear shifts

The frequencies present during a gear shift were investigated by calculating the *Fast Fourier Transform* of the measured accelerations. In Figure 4.6 and Figure 4.7 the frequencies in x- and z-direction respectively are displayed. All measurements shown were during gear shifts, from when the offramp started until the onramp ended.

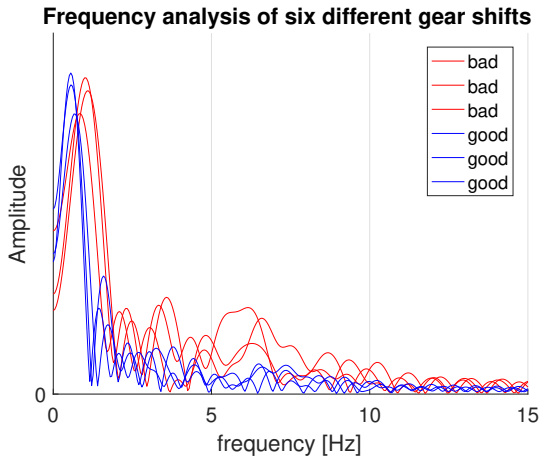

(a) Three bad and three good gear shifts.

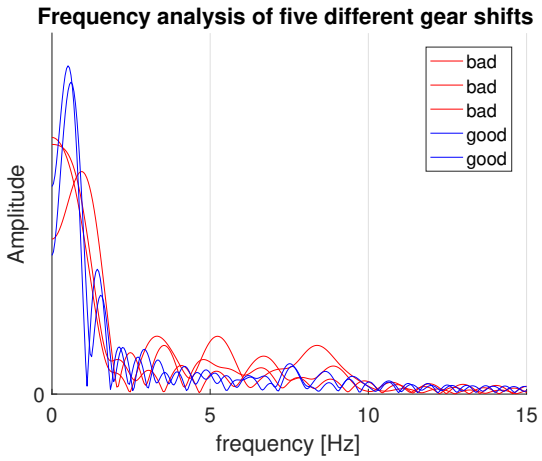

(b) Three bad and two good gear shifts.

Figure 4.6: Frequency analysis of good and bad gear shifts in x-direction. The red represents bad gear shifts and the blue represents good gear shifts. Both of them had a peak at about 1 Hz but the bad gear shifts had more energy in the frequencies above 1 Hz.

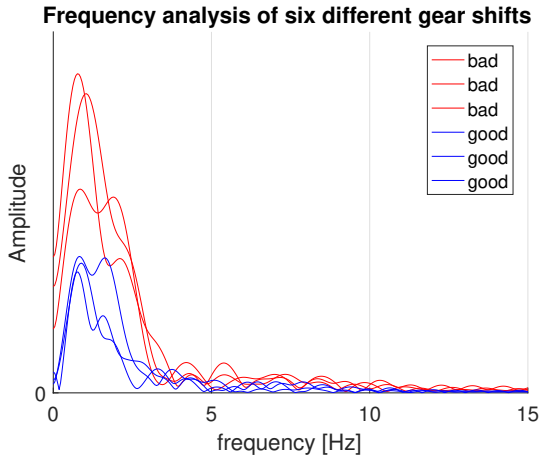

(a) Three good and three bad gear shifts.

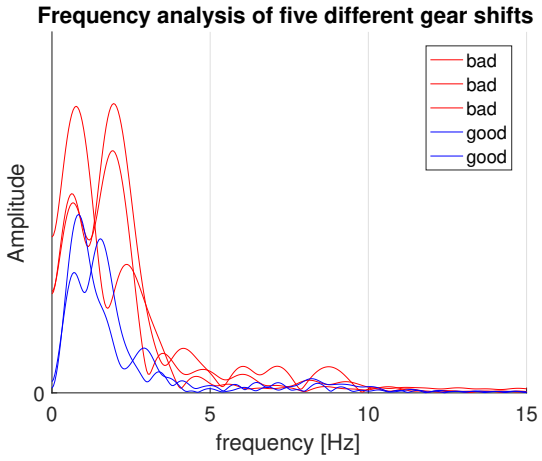

(b) Three good and two bad gear shifts.

Figure 4.7: Frequency analysis of good and bad gear shifts in z-direction. The red represents bad gear shifts and the blue represents good gear shifts. The energy in the bad gear shifts were higher at about 1 or 2 Hz.

The general difference between good and bad gear shifts was that there were more energy in the bad gear shifts than in the good ones. In x-direction the bad gear shifts affected the frequencies over 1 Hz. But there was no specific frequency of the bad gear shifts. It can be noted that in [10] the frequencies of 1 and 2 Hz in the horizontal plane were considered bad. But since these frequencies were present in both measurements the conclusion was that it should not affect the comfort.

In z-direction the energy at about 1 Hz was higher. In [10] the frequencies of 4 to 8 Hz were seen as bad. They were present in the measurement but the interesting part was that the general energy in the bad gear shifts was higher.

Thesis comfort definition

For this thesis the goal was to create more comfortable gear shifts. With respect to the data the conclusion was that to improve the comfort the cab acceleration and jerk should be minimized. An absolute limit between a good and a bad gear shift could not be drawn. This meant that given an acceleration the verdict of it being a good or bad gear shift was not possible. But when comparing measurements of gear shifts to each other the one with the lower acceleration and jerk was in the general case the better one.

With regards to the frequency there were no specific frequencies of interest. The bad gear shifts contained more energy than the good ones which meant that if the acceleration and jerk were minimized the energy of the frequencies present in gear shifts should be minimized.

4.2 Signal processing

The experiments meant lots of data collection and this data had to be processed to be used. Examples of the processing needed are to filter the signals to remove noise and to synchronize signals with different time vectors. Important functions developed are presented in Appendix A.

4.3 Models

To be able to control the cab movements by controlling the flywheel torque during the ramps of the gear shift it was necessary to develop models that described how the torque induced movements in the cab. The truck is a large vehicle containing many different parts. Figure 4.8 shows the different parts from demanded flywheel torque to the cab where each block was modelled individually. The input and output to each block is also described. As seen in the figure, the output from each model is the input to the next model in line. It was important to be accurate about how the models were connected in order to minimize the problems combining all the models into one big system.

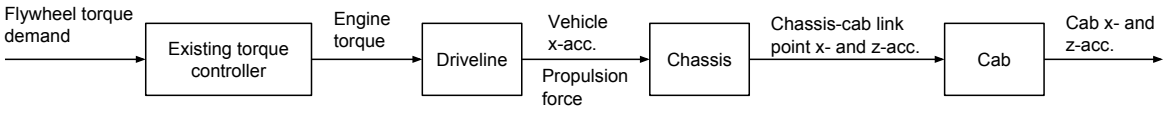

Figure 4.8: A block diagram of the vehicle components and through which signals they were connected.

This part of the chapter describes how the components in Figure 4.8 were modelled. The driveline model depends on the driving resistance of the vehicle which is also described in this section.

For the models to work, some states had to be initialized. If nothing is stated, the states were initialized using measurements.

4.3.1 Existing torque controller

The existing controller had the goal to control the flywheel torque to a reference value without inducing oscillations in the drivline. This controller is located before the driveline in the model diagram in Figure 4.8. The controller was non-linear since it saturated the error of the feedback and reference. A model of this

controller had to be developed in order to recreate the vehicle behavior. The input to the controller was demanded flywheel torque and the output was engine torque applied to the flywheel.

4.3.2 Driving resistance

To calculate the vehicle acceleration and the propulsion force Newton's second law was applied on the truck which generated (4.1).

$$m_{\text{tot}} a_{\text{vehicle,x}} = F_{\text{p}} - F_{\text{DR}} \tag{4.1}$$

The equation shows that the driving resistance, F_{DR}, of the truck had to be calculated. The equations of the driving resistances are displayed in (4.2)-(4.5) which are described in [2].

$$F_{\text{DR}} = F_{\text{r}} + F_{\text{a}} + F_{\text{g}} \tag{4.2}$$
$$F_{\text{r}} = mg(f_0 + f_{\text{S}} v) \tag{4.3}$$
$$F_{\text{a}} = \frac{A}{2} \rho d v^2 \tag{4.4}$$
$$F_{\text{g}} = mgsin(\theta_{\text{slope}}) \tag{4.5}$$

In order to use this model the constant rolling resistance coefficient, f_0, the speed dependent rolling resistance coefficient, f_{S}, and the air coefficient, d, of the specific truck had to be found. The front area of the truck, A, was known. The air density, ρ, was calculated using a method defined in [10]. Since the chassis model needed the decelerating force from the trailer the rolling resistance had to be split into different parts according to (4.6).

$$\begin{aligned} F_{\text{r}} =& m_{\text{trailer}} g(f_{0,\text{trailer}} + f_{\text{S,trailer}} v) + \\ & m_{\text{tractor}} g(f_{0,\text{tractor}} + f_{\text{S,tractor}} v) \end{aligned} \tag{4.6}$$

To calculate the driving resistance the vehicle was decoupled at 40 and 80 km/h, only letting the driving resistance decelerate the vehicle, waiting for it to stop. In this case the road slope was zero so the F_{g} term was removed. (4.1) was used in combination with (4.2)-(4.5) and the least squares method to calculate the constants needed for the model. The calculation was split into two parts with the trailer attached and detached to the tractor in order to obtain the parameters for the trailer and the tractor separately.

4.3.3 Powertrain model

The goal of the powertrain model was to generate the x-acceleration of the vehicle and the propulsion force given an engine torque. This section shows the two approaches used to model the powertrain, namely through a rigid and a flexible model. (4.7) and (4.8) shows how the acceleration and propulsion force were calculated for both models and the expressions are derived in [2]. The equations does not consider slip.

$$a_{\text{vehicle,x}} = r_{\text{w}} \ddot{\theta}_{\text{w}} \tag{4.7}$$
$$m_{\text{tot}} a_{\text{vehicle,x}} = F_{\text{p}} - F_{\text{DR}} \tag{4.8}$$

Rigid powertrain model

The most basic model investigated was the rigid powertrain model. In this model the driveline was considered stiff and no torsions were considered. This model was simple but it could be sufficient since the model only needed to catch the acceleration and propulsion force generated given a torque from the engine. The equation needed for this model is presented in (4.9) and is derived in [2].

$$(J_{\mathrm{w}} + mr_{\mathrm{w}}^2 + i_{\mathrm{t}}^2 i_{\mathrm{f}}^2)\ddot{\theta}_{\mathrm{w}} = i_{\mathrm{t}} i_{\mathrm{f}} M_{\mathrm{e}} - r_w F_{\mathrm{DR}} \tag{4.9}$$

The only parameter needed for this model was the wheel inertia, J_{w}. It was estimated using the least squares method.

The problem with this model was that the way to get a reasonable behaviour of the vehicle acceleration the flywheel torque had to be used. In order to calculate the flywheel torque the engine speed had to be known as well as the engine torque. This led to the conclusion that another model was needed to be able to control the model.

Flexible powertrain model

An alternative way was to model some parts of the driveline as flexible. In this case, the flexibilities were lumped into the driveshaft. (4.10) and (4.11) are the relevant equations of this model and are modified versions of the equations derived in [2]. The torsion, engine speed and wheel speed are the states of this model. The equations are true when the clutch is engaged.

$$J_{\mathrm{e}}\ddot{\theta}_{\mathrm{e}} = M_{\mathrm{e}} - b_{\mathrm{e}}\dot{\theta}_{\mathrm{e}} - k_{\mathrm{d}}(\frac{\theta_{\mathrm{e}}}{i_{\mathrm{t}} i_{\mathrm{f}}} - \theta_{\mathrm{w}})/(i_{\mathrm{t}} i_{\mathrm{f}}) - c_{\mathrm{d}}(\frac{\dot{\theta}_{\mathrm{e}}}{i_{\mathrm{t}} i_{\mathrm{f}}} - \dot{\theta}_{\mathrm{w}})/(i_{\mathrm{t}} i_{\mathrm{f}}) \tag{4.10}$$

$$mr_{\mathrm{w}}^2\ddot{\theta}_{\mathrm{w}} = k_{\mathrm{d}}(\frac{\theta_{\mathrm{e}}}{i_{\mathrm{t}} i_{\mathrm{f}}} - \theta_{\mathrm{w}}) + c_{\mathrm{d}}(\frac{\dot{\theta}_{\mathrm{e}}}{i_{\mathrm{t}} i_{\mathrm{f}}} - \dot{\theta}_{\mathrm{w}}) - b_{\mathrm{w}}\dot{\theta}_{\mathrm{w}} - r_{\mathrm{w}} F_{\mathrm{DR}} \tag{4.11}$$

Here, the engine inertia was assumed to be much greater than the transmission and final drive inertia, which therefore were neglected. The losses on the engine side of the driveshaft were lumped into one parameter, b_{e}. The wheel inertia was smaller than the vehicle mass times the squared wheel radius, and was therefore neglected.

The starting point when estimating the parameters for this model was the spring constant of the driveshaft which was provided by Scania. The other parameters were estimated using the least squares method with the constraint that they had to be larger or equal to zero. When estimating the parameters the driveshaft torsion was estimated using the Trapezoidal method in combination with the measured engine and wheel speeds. When the parameters had been obtained the behaviour of the different parts of the powertrain were analyzed and parameters were altered from their initial values to fit the measured data better.

In order to use this model the driveshaft torsion had to be initialized. By looking at the steady state of (4.11) the following expression for the initial torsion could be derived.

$$torsion = (-c_{\mathrm{d}}(\frac{\dot{\theta}_{\mathrm{e}}}{i_{\mathrm{t}} i_{\mathrm{f}}} - \dot{\theta}_{\mathrm{w}}) + b_{\mathrm{w}}\dot{\theta}_{\mathrm{w}} + r_{\mathrm{w}} F_{\mathrm{DR}})/k_{\mathrm{d}} \tag{4.12}$$

This was used when the wheel speed was higher than zero and if the vehicle was not moving at the beginning of the simulation the torsion was set to zero.

Decoupled model

When the clutch was disengaged the powertrain model shifted to (4.13) and (4.14). The equations are modified versions of the decoupled model derived in [2].

$$J_{\mathrm{t}}\ddot{\theta}_{\mathrm{t}} = -b_{\mathrm{t}}\dot{\theta}_{\mathrm{t}} - k_{\mathrm{d}}(\frac{\theta_{\mathrm{t}}}{i_{\mathrm{f}}} - \theta_{\mathrm{w}})/i_{\mathrm{f}} - c_{\mathrm{d}}(\frac{\dot{\theta}_{\mathrm{t}}}{i_{\mathrm{f}}} - \dot{\theta}_{\mathrm{w}})/i_{\mathrm{f}} \tag{4.13}$$

$$(J_{\mathrm{w}} + mr_{\mathrm{w}}^2)\ddot{\theta}_{\mathrm{w}} = k_{\mathrm{d}}(\frac{\theta_{\mathrm{t}}}{i_{\mathrm{f}}} - \theta_{\mathrm{w}}) + c_{\mathrm{d}}(\frac{\dot{\theta}_{\mathrm{t}}}{i_{\mathrm{f}}} - \dot{\theta}_{\mathrm{w}}) - b_{\mathrm{w}}\dot{\theta}_{\mathrm{w}} - r_{\mathrm{w}}F_{\mathrm{DR}} \tag{4.14}$$

The model was not continuous when shifting between the coupled and decoupled model. When the clutch was engaged the torsion and the derivative of the torsion should be transferred between the models. (4.15) shows how the states shifted when the clutch was engaged and disengaged.

$$(\frac{\dot{\theta}_{\mathrm{e}}}{i_{\mathrm{t}}i_{\mathrm{f}}} - \dot{\theta}_{\mathrm{w}}) = (\frac{\dot{\theta}_{\mathrm{t}}}{i_{\mathrm{f}}} - \dot{\theta}_{\mathrm{w}}) \rightarrow \begin{cases} \dot{\theta}_{\mathrm{p}} = \frac{\dot{\theta}_{\mathrm{e}}}{i_{\mathrm{t}}}, & \text{clutch disengaged} \\ \dot{\theta}_{\mathrm{e}} = \dot{\theta}_{\mathrm{t}}i_{\mathrm{t}}, & \text{clutch engaged} \end{cases} \tag{4.15}$$

To estimate the parameters b_{t} and J_{t}, the simulations were analyzed and altered according to the behaviour of the model.

4.3.4 Chassis model

The goal with the chassis model was to capture how the propulsion force, F_{p}, and vehicle x-acceleration affected the chassis movements. The vehicle x-acceleration, $a_{\mathrm{vehicle,x}}$ was seen as the chassis x-acceleration, $a_{\mathrm{ch,x}}$. Chassis models of different complexity were investigated in the thesis. One model considered only movements in x-direction, one included up and down movements also, and another was extended with chassis rotation. Data from the experiments were used to analyze the movements and to estimate parameters needed to achieve a desired behaviour. The investigated chassis models are introduced below.

Chassis moving only in x-direction

The chassis model including only movements in x-direction is shown in Figure 4.9. This model was considered under the assumption that the z-accelerations would be significantly smaller than the x-acceleration and therefore could be neglected.

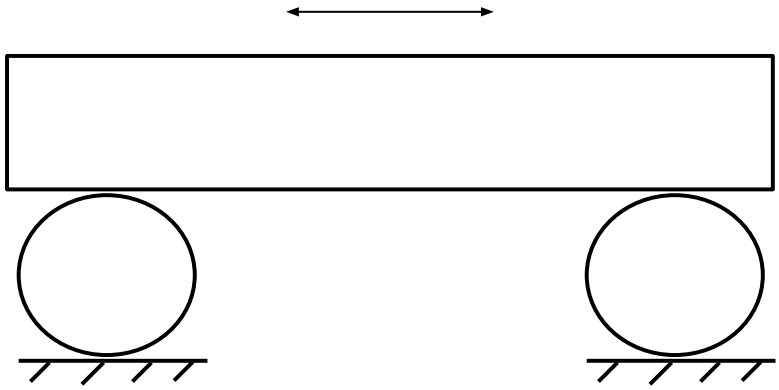

Figure 4.9: A sketch of the simplest chassis model investigated. The model only included chassis movements in x-direction.

The movements of this model is described by (4.16),

$$m_{\text{ch}} a_{\text{ch,x}} = F_{\text{p}} - F_{\text{DR}} - F_{\text{tr,x}} - F_{\text{link,x}} \tag{4.16}$$

where $F_{\text{tr,x}}$ is the force induced by the trailer in x-direction and is calculated using Newton's second law in (4.17). $F_{\text{link,x}}$ is the force in x-direction from the cab and was approximated as (4.18).

$$F_{\text{tr,x}} = m_{\text{tr}} a_{\text{ch,x}} + F_{\text{r,trailer}} + m_{\text{tr}} g sin(\theta_{\text{slope}}) \tag{4.17}$$

$$F_{\text{link,x}} = m_c g sin(\theta_{\text{slope}}) \tag{4.18}$$

As stated above, this model was considered under the assumption that z-accelerations in the chassis could be neglected. The results from the experiment with the driving situation accelerating from 0 m/s^2 showed that the x- and z-accelerations were in the same size. Therefore a model including movements in z-direction was needed.

Model extended with up and down movements

The model considering movements in both x- and z-directions is shown in Figure 4.10.

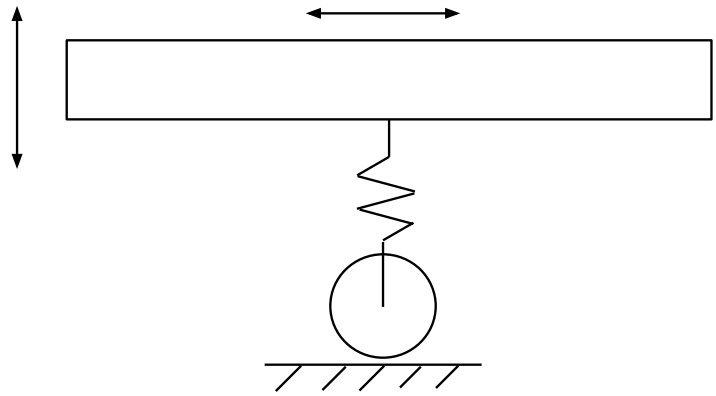

Figure 4.10: Chassis model including movements in both x- and z-direction, but no rotation.

The equations describing the movements are shown in (4.19),

$$\begin{aligned} m_{\text{ch}} a_{\text{ch,x}} &= F_{\text{p}} - F_{\text{DR}} - F_{\text{tr,x}} - F_{\text{link,x}} \\ m_{\text{ch}} a_{\text{ch,z}} &= -m_{\text{ch}} g - F_{\text{s,front}} - F_{\text{tr,z}} - F_{\text{link,z}} \end{aligned} \tag{4.19}$$

where $F_{\text{tr,x}}$ is calculated as (4.17), $F_{\text{link,x}}$ as (4.18), $F_{\text{link,z}}$ as the force in z-direction from the cab, calculated as (4.20), and $F_{\text{tr,z}}$ is the force induced by the trailer in z-direction. $F_{\text{tr,z}}$ was seen as a constant force calculated using the difference between the weights of the tractor with and without trailer attached, see (4.21).

$$F_{\text{link,z}} = m_{\text{c}} g cos(\theta_{\text{slope}}) \tag{4.20}$$

$$F_{\text{tr,z}} = (m_{\text{tractor with trailer}} - m_{\text{tractor without trailer}}) g \tag{4.21}$$

This model had the possibilities to capture movements and accelerations in the xz-plane. The problem with this model was that the movements in z-directions would be induced by the road or the cab. Bumps and sudden slopes would make the chassis move up and down. However in this thesis the movements induced by the propulsion force were investigated. In this model, the propulsion force only affected the chassis in x-direction. Figure 4.11 shows how similar the z-acceleration in the chassis and seat were. Therefore it was important to capture how the chassis z-acceleration was affected by the propulsion force, and this model was therefore not sufficient.

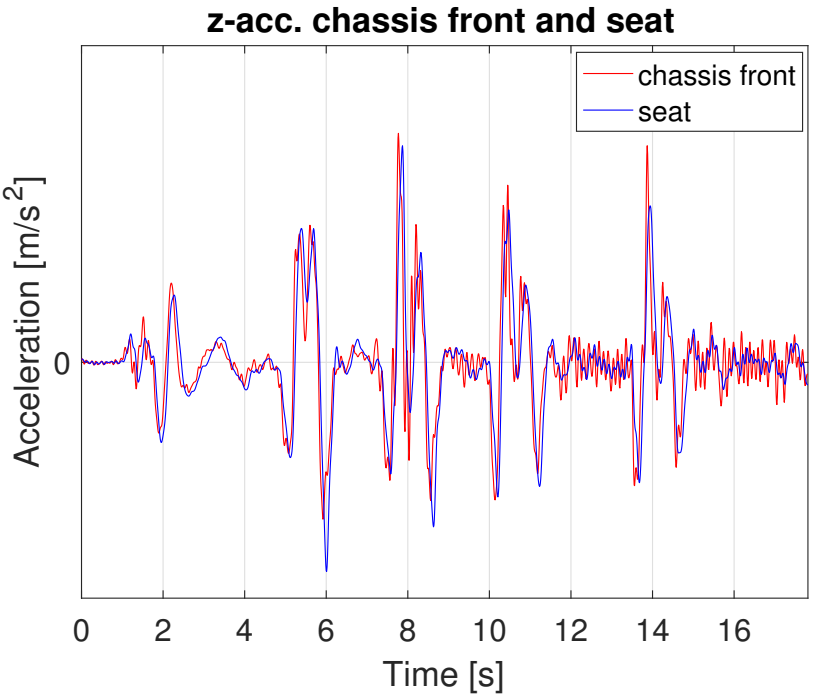

Figure 4.11: z-accelerations in the chassis front and seat.

Model extended with chassis rotation

Keeping in mind the importance, mentioned above, to capture how the propulsion force affected the movements in z-direction. Adding information from Figure 4.12, where the z-acceleration in the chassis front and rear is seen. It is obvious that the acceleration was larger in the chassis front than the chassis rear. Analyzing this information, a model including chassis rotations around the chassis rear induced by the propulsion force should be investigated.

In this model, the chassis rear acceleration was approximated as the vehicle x-acceleration from the driveline.

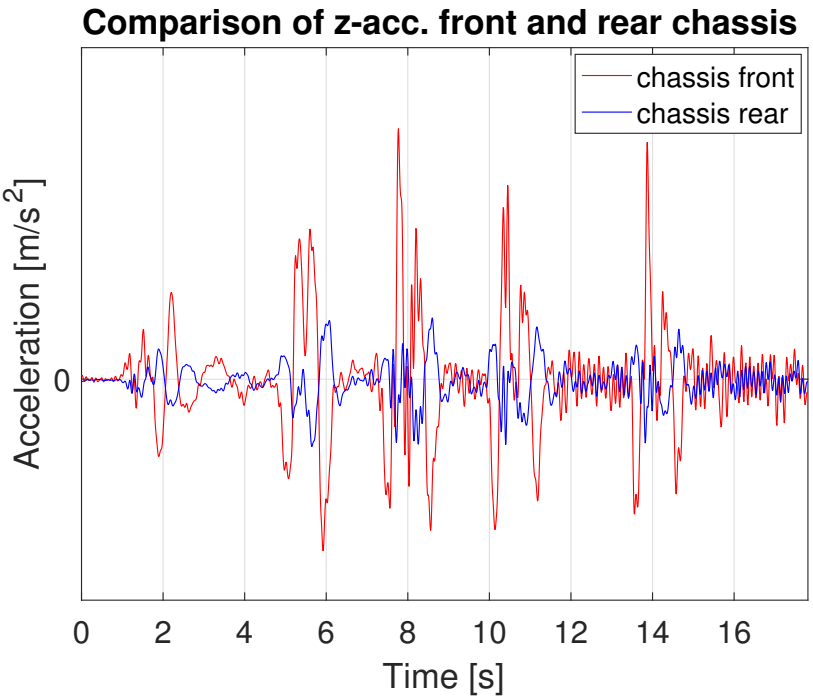

Figure 4.12: z-accelerations in the chassis front and rear.

In Figure 4.13, two plots where the cab z-acceleration are plotted with the z-accelerations in the chassis front and rear respectively are seen. The accelerations in the chassis front and cab were much more alike than the chassis rear and cab. Therefore, the rear axle and wheel were modelled stiff, while the front axle were modelled as a spring-damper configuration.

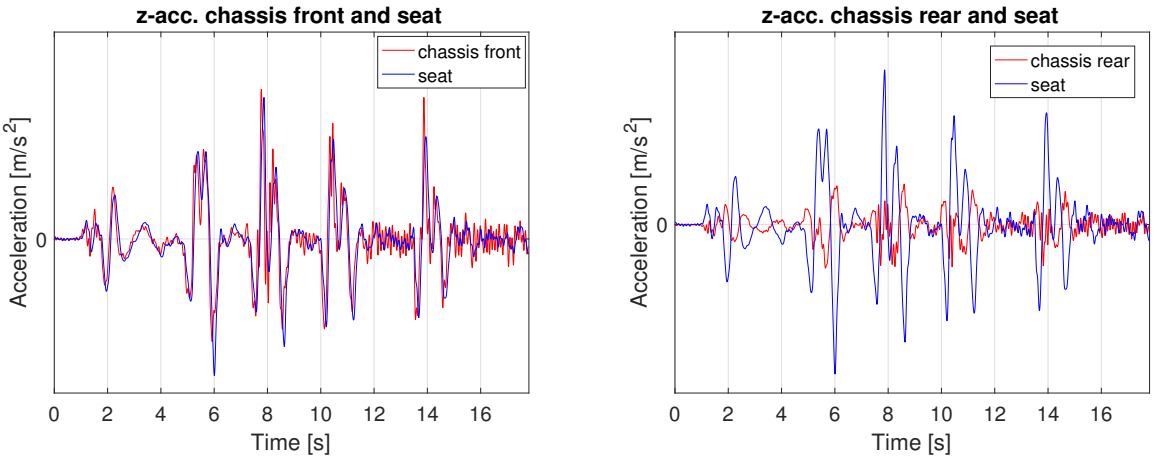

(a) Chassis front and seat z-accelerations.

(b) Chassis rear and seat z-accelerations.

Figure 4.13: The two plots show the difference in how the chassis front and rear are connected to the seat z-accelerations.

Figure 4.14b shows a sketch of the chassis model and the forces acting on different points of the chassis. The lengths and heights in the chassis are defined in Figure 4.14a.

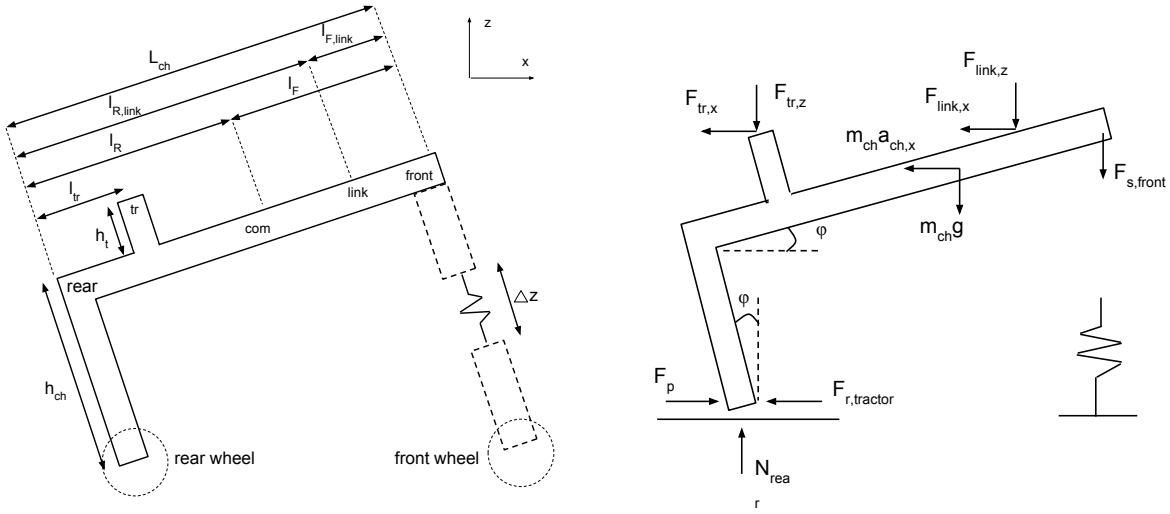

(a) Chassis lengths and heights.

(b) Angle definition and the forces acting on the chassis.

Figure 4.14: Chassis definitions and forces acting on the chassis.

The inputs to the chassis model were the propulsion force and vehicle acceleration in x-direction. The purpose with the chassis model was to calculate the x- and z-accelerations in the link point of the chassis and cab seen in Figure 4.14a. This was done by using the rigid body acceleration movement rule in two dimensions, derived in [16] and seen in (4.22).

$$\begin{aligned}\mathbf{a}_{\text{ch,link}} =& \mathbf{a}_{\text{ch,rear}} + \alpha \times \mathbf{r}_{\text{rear to link}} - \dot{\omega}^2 \mathbf{r}_{\text{rear to link}} \\ =& \begin{pmatrix} a_{\text{ch rear,x}} \\ 0 \\ 0 \end{pmatrix} + \begin{pmatrix} 0 \\ -\ddot{\phi} \\ 0 \end{pmatrix} \times \begin{pmatrix} l_{\text{R,link}} \\ 0 \\ 0 \end{pmatrix} - \dot{\phi}^2 \begin{pmatrix} l_{\text{R,link}} \\ 0 \\ 0 \end{pmatrix}\end{aligned} \tag{4.22}$$

Note that $a_{\text{ch rear,z}}$ is zero since the rear axis was considered stiff. The vector $\mathbf{r}_{\text{rear to link}}$ was approximated as constant since the chassis movements in z-direction were small even if the z-accelerations sometimes were large for a short time. The resulting accelerations in the link point are expressed by (4.23).

$$\begin{aligned}a_{\text{ch link,x}} =& a_{\text{ch rear,x}} - \dot{\phi}^2 l_{\text{R,link}} \\ a_{\text{ch link,z}} =& \ddot{\phi} l_{\text{R,link}}\end{aligned} \tag{4.23}$$

In order to calculate the accelerations in the linking point, the chassis angular acceleration and angular velocity were needed. [17] derives an expression of how torque is induced by forces, see (4.24). This expression was used to derive an expression of the chassis angular acceleration. The expression is described in (4.25), with the rear end of the chassis used as the momentum point, the chassis angle, ϕ, and the chassis angular velocity, $\dot{\phi}$, are states.

$$\mathbf{M} = \mathbf{F} \times \mathbf{r} \tag{4.24}$$

$$\begin{aligned}J_{\text{rear}}\ddot{\phi} =& (F_{\text{p}} - F_{\text{r,tractor}})h_{\text{ch}} - F_{\text{tr,z}} l_{\text{tr}} - F_{\text{link,z}} l_{\text{R,link}} \\ & - F_{\text{s,front}} L_{\text{ch}} - m_{\text{ch}} g L_{\text{R}} cos(\theta_{\text{slope}})\end{aligned} \tag{4.25}$$

$F_{\text{s,front}}$ is calculated as (4.26),

$$F_{\text{s,front}} = k_{\text{front}}(\Delta z - l_0) + c_{\text{front}}\Delta\dot{z} \tag{4.26}$$

where Δz is the difference in chassis front position from the starting position, l_0 is a constant contribution to keep the right equilibrium position, and $\Delta\dot{z}$ is the time derivative of the chassis front position. k_{front} and c_{front} are the spring and damper constants.

Estimating chassis parameters

The parameters that were used to tune the model were k_{front}, c_{front} and l_0 in the spring-damper force, $F_{\text{s,front}}$, and the chassis inertia, J_{rear}. A chassis inertia was provided by Scania. This inertia was valid for moment around the center of mass. Since the moment around the chassis rear was used for the estimations, also the inertia J_{rear} was estimated. Measurements from the driving situations standing still on horizontal ground and driving with constant velocity on a horizontal road were used to estimate the parameters l_0 and k_{front}. This choice was made since the chassis would get into an equilibrium position affected by constant forces. Since the chassis would be in a constant angle, the damper part of F_s would not affect the force since $\Delta\dot{z} = 0$. This would give two different expressions using (4.25) with two unknown parameters, k_{front} and l_0, which could be solved for. With values on l_0 and k_{front}, measurements from when the vehicle was accelerating from 0 m/s^2 in a slope were used. c_{front} and J_{rear} were estimated by solving (4.25) for c_{front} and J_{rear} and then using least squares.

However, this way of calculating the parameters did not result in a model evaluated to be good enough. One problem with using different driving situations to estimate the parameters could be that the dampers were non-linear. The pressure in the dampers could be altered when driving with constant velocity compared to when standing still. This would result in different chassis movements and accelerations compared to another pressure.

This was solved using a 2-dimensional grid search over a number of k_{front} and l_0 solving (4.25) for c_{front} and J_{rear} using least squares, see Algorithm 1. By starting with grid searches with large steps, smaller steps could be taken when the right range was found by the large stepped grid search.

Algorithm 1 Estimating chassis parameters using grid search

```
Initialize cost.
for Number of values of l_0 do
    Set a length l_0
    for Number of values of k_front do
        Set a spring constant k_front
        Estimate J_rear and c_front with least squares method.
        Simulate cab using current parameters
        Calculate cost of simulation compared with measured.
        if Current cost < cost then
            cost=current cost
            save parameters
        end if
    end for
end for
```

4.3.5 Cab model

A cab model had to be derived in order to catch the behaviour by the seat. In this section two different models considered in the project are presented. The first one is an inverted pendulum and the second one is

a suspended model.

Inverted pendulum

Data was analyzed to pick a model that would follow the behaviour and still be a simple cab model. In Figure 4.15a and Figure 4.15b plots of the x- and z-acceleration by the seat compared to the acceleration in the chassis front are displayed.

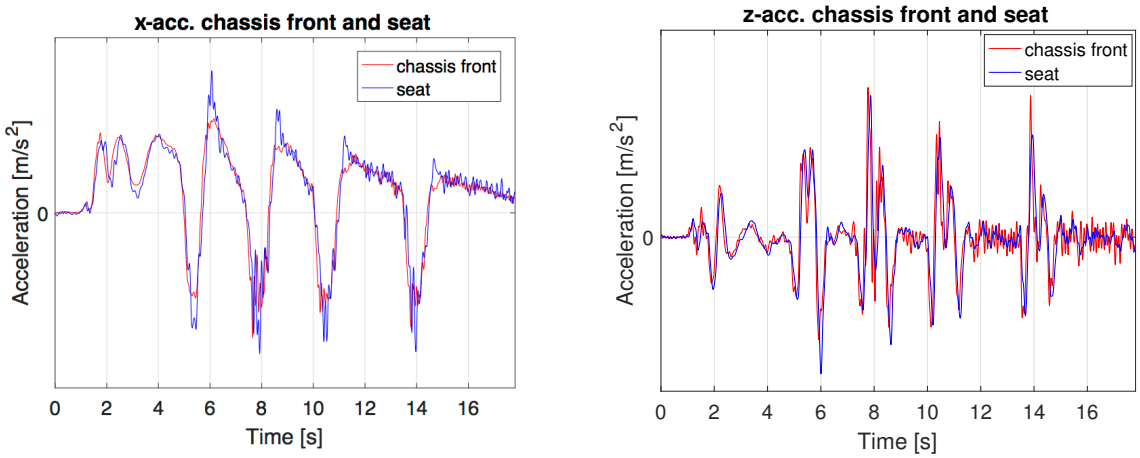

(a) Measured acceleration in x-direction

(b) Measured acceleration in z-direction

Figure 4.15: Difference between the measured acceleration by the seat and the acceleration at the chassis front.

The figures show that the accelerations in z-direction were almost identical while the accelerations in x-direction differed. With this in mind the inverted pendulum, displayed in Figure 4.16 was chosen as a possible cab model. It should be more similar in the z-direction than the x-direction and was a simple model to implement.

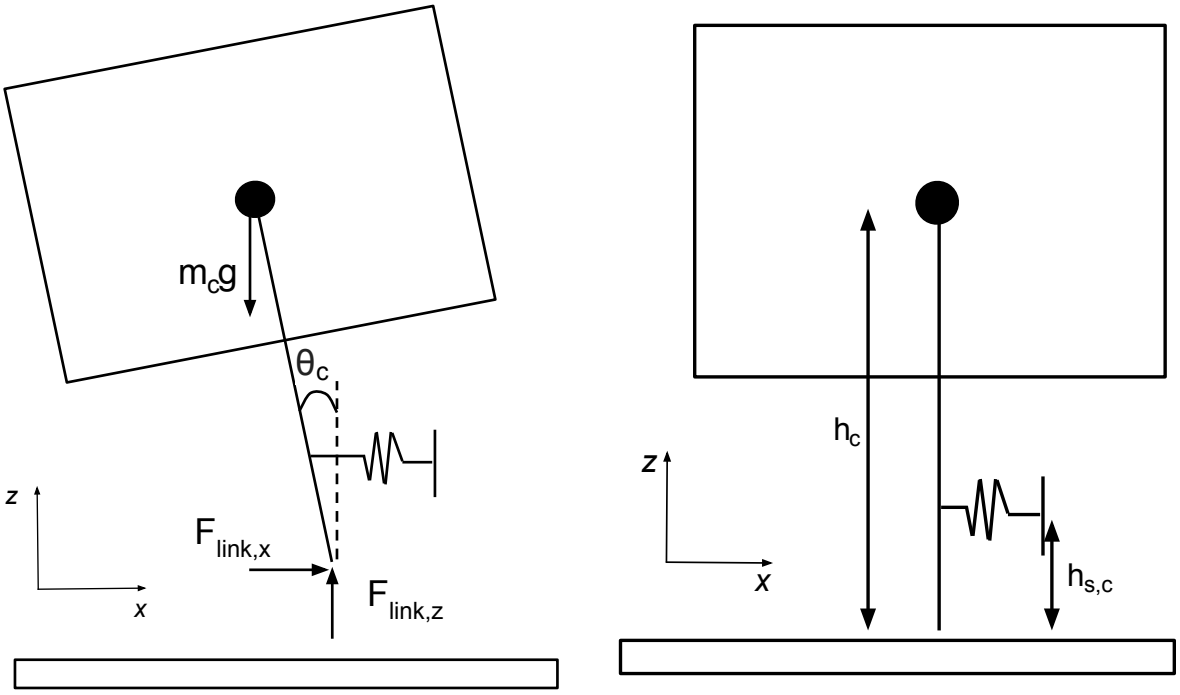

(a) Inverted pendulum forces.

(b) Inverted pendulum lengths.

Figure 4.16: Lengths and forces defining the inverted pendulum model.

The cab inertia and mass were provided by Scania. The parameters that had to be found in this model were the following:

- h_{c}: Height of pendulum arm.
- $h_{\mathrm{s,c}}$: Position of spring position.
- k_{c}: Spring constant.
- c_{c}: Damper constant.

The equations that defined the cab movements are displayed in (4.27) - (4.30). (4.27) was expressed using (4.24), (4.28) and (4.29) were expressed using Newton's second law.

$$\ddot{\theta}_{\mathrm{c}} J_{\mathrm{c}} = h_{\mathrm{c}} F_{\mathrm{link,x}} cos(\theta_{\mathrm{c}}) + (h_{\mathrm{c}} - h_{\mathrm{s,c}}) F_{\mathrm{s,c}} cos(\theta_{\mathrm{c}}) + h_{\mathrm{c}} F_{\mathrm{link,z}} sin(\theta_{\mathrm{c}}) \tag{4.27}$$

$$a_{c,x} m = F_{\mathrm{link,x}} + F_{\mathrm{s,c}} - m_{\mathrm{c}} g sin(\theta_{\mathrm{slope}} + \phi) \tag{4.28}$$

$$a_{c,z} m = F_{\mathrm{link,z}} - m_{\mathrm{c}} g cos(\theta_{\mathrm{slope}} + \phi) \tag{4.29}$$

$$F_{\mathrm{s,c}} = k_c \Delta x + c_c \Delta \dot{x} = k_c h_{\mathrm{s,c}} sin(\theta_{\mathrm{c}}) + c_c h_{\mathrm{s,c}} \dot{\theta}_{\mathrm{c}} cos(\theta_{\mathrm{c}}) \tag{4.30}$$

It can be noted that the spring force only affects the cab in x-direction. This simplification was motivated by the small angles of the cab.

(4.31) shows how the acceleration in the cab can be expressed using the acceleration in the chassis and the acceleration movement rule in (4.22).

$$\begin{pmatrix} a_{c,x} \\ 0 \\ a_{c,,z} \end{pmatrix} = \begin{pmatrix} a_{\text{link,x}} \\ 0 \\ a_{\text{link,z}} \end{pmatrix} + \begin{pmatrix} 0 \\ -\ddot{\theta}_{\text{c}} \\ 0 \end{pmatrix} \times \begin{pmatrix} -h_{\text{c}} sin(\theta_{\text{c}}) \\ 0 \\ h_{\text{c}} cos(\theta_{\text{c}}) \end{pmatrix} - \dot{\theta}_{\text{c}}^2 \begin{pmatrix} -h_{\text{c}} sin(\theta_{\text{c}}) \\ 0 \\ h_{\text{c}} cos(\theta_{\text{c}}) \end{pmatrix} =$$
$$\begin{pmatrix} a_{\text{link,x}} \\ 0 \\ a_{\text{link,z}} \end{pmatrix} + \begin{pmatrix} -h_{\text{c}} \ddot{\theta}_{\text{c}} cos(\theta_{\text{c}}) \\ 0 \\ -h_{\text{c}} \ddot{\theta}_{\text{c}} sin(\theta_{\text{c}}) \end{pmatrix} + \begin{pmatrix} h_{\text{c}} \dot{\theta}_{\text{c}}^2 sin(\theta_{\text{c}}) \\ 0 \\ -h_{\text{c}} \dot{\theta}_{\text{c}}^2 cos(\theta_{\text{c}}) \end{pmatrix} \tag{4.31}$$

By combining (4.27) - (4.31) the angular acceleration of the cab shown in (4.32) could be derived.

$$\begin{aligned} \ddot{\theta}_{\text{c}}(J_{\text{c}} + h_{\text{c}}^2 m_{\text{c}}) = h_{\text{c}} m_{\text{c}} a_{\text{link,x}} cos(\theta_c) - h_{\text{c,s}} F_{\text{s,c}} cos(\theta_{\text{c}}) + \\ + m_{\text{c}} g h_{\text{c}} sin(\theta_{\text{c}} + \theta_{\text{slope}} + \phi) + h_{\text{c}} m_{\text{c}} a_{\text{link,z}} sin(\theta_{\text{c}}) \end{aligned} \tag{4.32}$$

The states in this model were the angular velocity, $\dot{\theta}_{\text{c}}$, and the cab angle, θ_{c}.

In order to estimate the parameters needed for the model a combination of the least squares method and a grid search was used. This was done since some parameters depended on the others, for example the spring and damper constants would depend on the position of the spring. Even though the inertia of the cab was provided by Scania it might not suit the chosen model. This led to two different estimations where the inertia was seen as known and unknown.

(4.30) and (4.32) were used for the least squares estimation. The cab angle was calculated using the position sensors that measured the difference between the chassis and the cab positions. The derivatives of the angle was calculated using the *Finite difference method forward*.

Algorithm 2 displays how the parameters were estimated. Two different measurements were used, one for estimating the spring and damper constants and one for the simulation. Both measurements were accelerating in slope at low speed since this was the situation where the model was supposed to work.

Algorithm 2 Estimating cab parameters using grid search

```
Initialize cost.
for Number of pendulum lengths, h_c do
    Set a length h_c
    for Number of spring positions, h_s,c do
        Set a spring position h_s,c
        Estimate spring and damper constant with least squares method.
        Simulate cab using current parameters
        Calculate cost of simulation compared with measured.
        if Current cost<cost then
            cost=current cost
            save parameters
        end if
    end for
end for
```

The heights for which the pendulum was tested were between one and five meters in which there were 30 steps. The spring was tested for ten positions for each height of the arm. From one tenth to the top of the arm.

Suspended cab model

The suspended cab model described the reality in a more real way than the inverted pendulum mentioned above. Figure 4.17 shows a sketch of the model. The cab was attached to the chassis through three spring-damper pairs. The horizontal spring-damper was attached to the chassis through a raised point called the *tower*.

There were some problems developing this model leading to the conclusion that the inverted pendulum would be a better choice. The measurement system explained in 4.1.1 did not include measurements of the movements in the x-direction. Without the position measurement in the x-direction the spring-damper in the x-direction was difficult to model since the position and the angle of the cab was needed. The model would also mean more states, apart from the rotation the positions and velocities in the x- and z-direction would also be needed. It was of interest to keep the complexity of the model down. Therefore, the inverted pendulum model, with two states, was a better choice in this point of view.

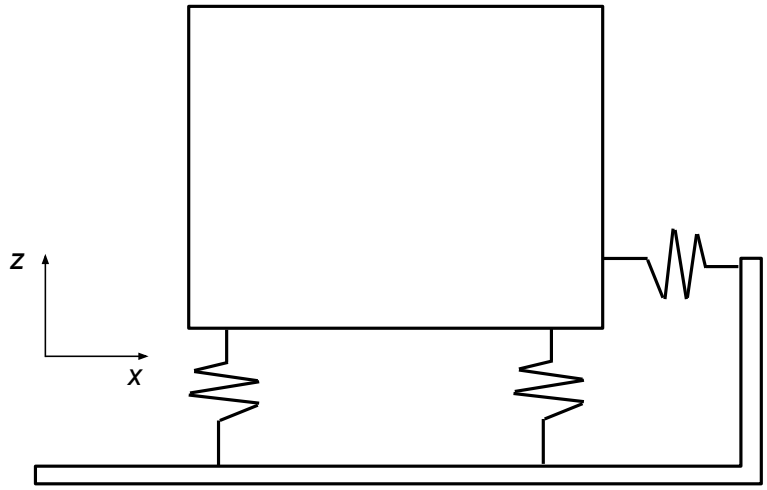

Figure 4.17: The suspended model with three spring-damper pairs.

4.4 Control

The purpose of the controller was to improve the cab comfort. Comfort was, in 4.1.3, defined as low accelerations and jerk. The jerk is the time derivative of the acceleration and is kept low if the acceleration does not change abruptly. By making sure the acceleration was kept low without abrupt changes, the comfort would be improved.

To improve the cab movements during the gear shift the focus has been to change the shape of the offramp and onramp shown in Figure 2.3. It is important to steer the flywheel torque down to zero before disengaging the clutch in order to minimize the risk of inducing jerk or brake components in the powertrain. Scania's work in developing the gear shift functionality at this point, has had the focus on good behaviour in the powertrain during the gear shift. In this thesis, the focus has instead been to investigate the chassis and cab behaviour during the gear shift.

The controller was only active during the offramp and onramp. A signal was sent to the controller to trig and tell the controller whether it was an onramp or offramp.

This part of the section describes the different controllers developed and the motivation behind them.

4.4.1 Existing torque controller

The existing torque controller, from now on referred to as ETC, was located between the powertrain and the controller that was developed. Therefore the developed controller had to calculate control signals making the torque controller deliver the desired flywheel torque. ETC could be controlled by three variables, reference torque, saturation limits and settling time. The reference torque is the reference for the flywheel torque, the saturation limits saturates the error in ETC and the settling time is used to scale the error to make it less sensitive to changes. How they were used in each controller is described below.

4.4.2 Open loop control

An open loop controller is a cheap (with respect to computer calculations and there is no need for additional sensors), simple controller that might work well for a specific task for which it is tuned for. Risks with open loop control are that the constructed control signals might not have the same effect on the real vehicle as on the models. Two different open loop control algorithms were investigated. One was to low pass filter the reference signal and saturations in ETC which always had the shape of a step during the gear shift, and the other was to take smaller steps ramping up or down the flywheel torque.

The complete vehicle model and the driving situation accelerating in slope were used to design the open loop controllers. This was also the driving situation used when validading the controller.

Figure 4.18 shows the flywheel torque reference, actual flywheel torque and engine torque during a gear shift only using ETC. In order to design an open loop controller it was important to have a good system understanding about which changes would give the desired cab behaviour. The investigated open loop controllers are presented below.

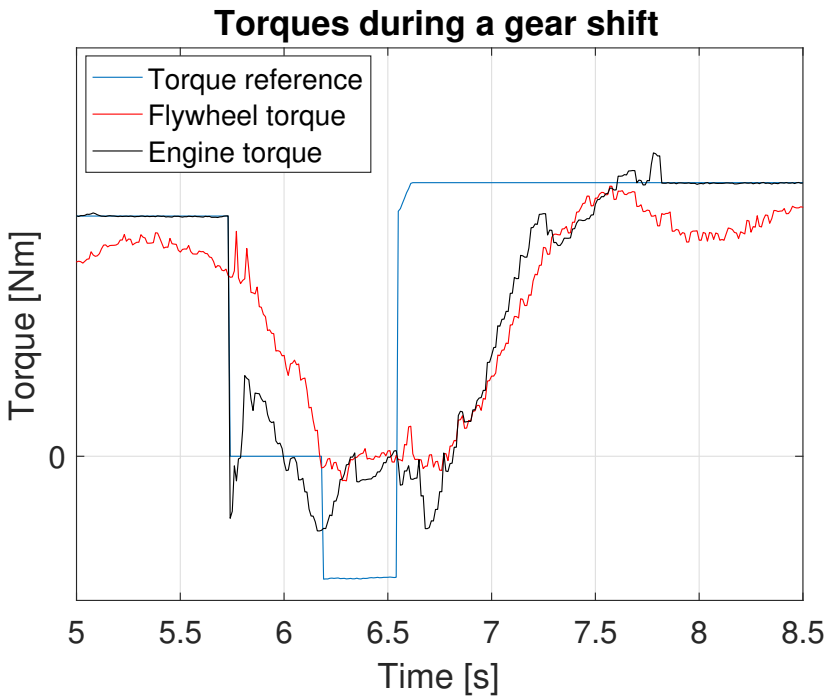

Figure 4.18: Flywheel torque reference, engine torque and actual flywheel torque as it was controlled by the time of this thesis.

Stair shaped ramps

One alternative for an open loop controller was to shape the ramp as steps. The thought about the shape was to, initially, take a small step in order to trigger the cab movements in a small scale and then control in counter phase to the trigged movement by taking another larger step. By looking at the downramp in Figure 4.18, it is seen that there were possibilities and time to pause the downramp if it was controlled down faster than in the figure.

The results from trying to create a step in flywheel torque is seen in Figure 4.19. The controller was applying as large and low engine torque as possible to create a step shaped downramp in flywheel torque. Due to limitations in ETC this was not possible. Probably because a step in flywheel torque would induce oscillations and jerk in the driveline. The stair shaped ramp controller was therefore not further investigated.

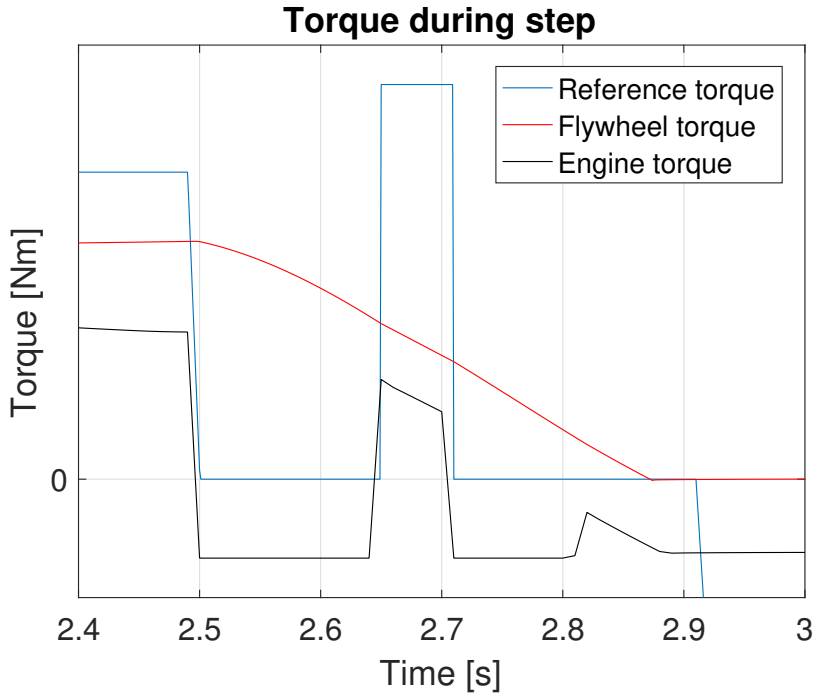

Figure 4.19: Torques during offramp step.

Low pass filtering control signals

In Figure 4.18 it is seen that the reference of the flywheel torque is a step. The engine torque therefore also takes a step. By abruptly changing the engine torque there would be a quick change in acceleration. This change in acceleration would affect the cab. By changing the acceleration in a smooth way the behaviour of the cab could be improved as well as minimizing the jerk in the system. A simple way of making a signal smoother is by using a low pass filter.

When designing a low pass filter there are some parameters to consider. The shape of the low pass filter is influenced by the order of the filter. The orders that were tested was a second and a sixth order filter. The reason that these orders were used was based on the behaviour of the filters displayed in Figure 4.20.

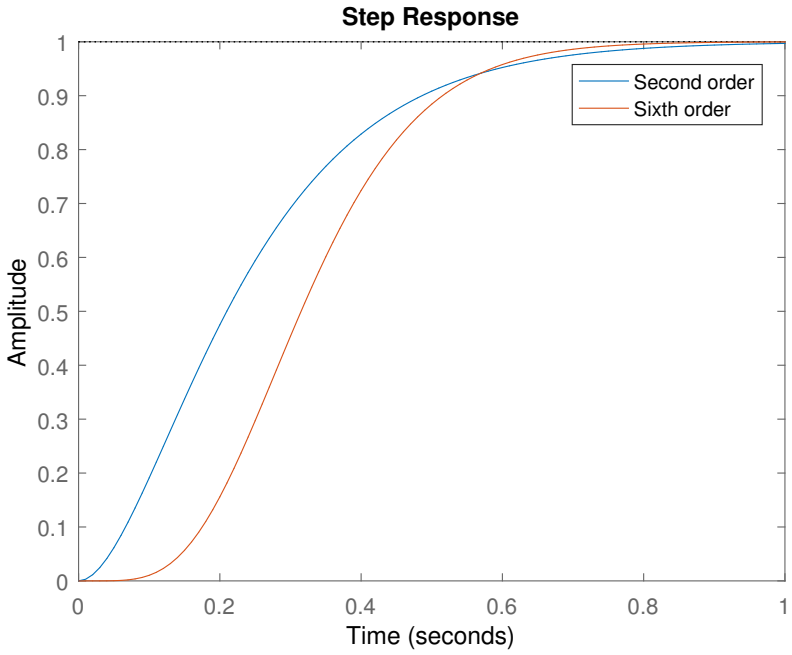

Figure 4.20: Step responses of a second and a sixth order low pass filter. The filter constants were chosen to have about the same time to converge to one.

The second order filter was chosen since it was smoother than the original signal but still had the form of the step. The sixth order filter was chosen since it was smoother in the beginning.

The time constant of the filter is affected by the choice of filter constant. The filter constant was chosen to not increase the times of the offramp nor the onramp.

The low pass filter was developed as a continuous time filter and then discretized. The time continuous low pass filter is shown in (4.33),

$$Y(s) = \frac{1}{(1+s\tau)^n} U(s) \tag{4.33}$$

where $Y(s)$ is the output, $U(s)$ is the the input, τ is the filter constant, n is the filter order and s is a Laplace variable.

The low pass filter was discretized using Tustin's formula, described in [18]. Tustin's formula was used since there is equivalency between a stable time continuous transfer function and the discretized transfer function when using Tustin's formula. The discretized low pass filter had the shape of (4.34). It was implemented by storing old values of the input and the output from the filter. The output was calculated solving (4.34) for $y[k]$.

$$Y[z] = \frac{a_0 + a_1 z^{-1} + ... + a_n z^{-n}}{b_0 + b_1 z^{-1} + ... + b_n z^{-n}} U[z] \tag{4.34}$$

To improve the cab comfort using open loop control two approaches were used. One low pass filtered the reference flywheel torque which ETC worked towards. This filter was initialized by the current flywheel torque and had the goal of reaching the reference. The second approach was to low pass filter the saturation of the input to ETC. It started by saturating the signal and then increasing the allowed signal.

4.4.3 Feedback controller

When analyzing the model, it was discovered that the z-acceleration was sensitive to large, abrupt changes in engine torque. Therefore the z-acceleration was used as feedback in the controller to calculate the error, e, between the feedback and a reference acceleration. The controller was going to control ETC without changing it. Therefore a somewhat unconventional controller was developed. A saturation in Scania torque controller saturated the error between the reference torque and the feedback. These saturation limits were used to control ETC. A block diagram of the controller in the system is shown in Figure 4.21.

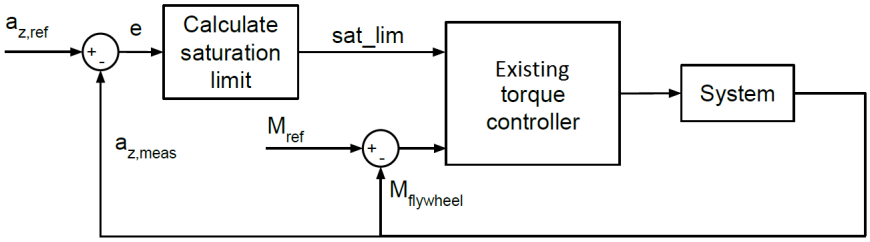

Figure 4.21: Block diagram of the feedback controller and its connection to the system.

The idea of the controller was to use the saturation limits in ETC to allow it to apply a larger engine torque as long as the cab z-acceleration was not considered uncomfortable. The chassis front and cab z-accelerations were closely connected. The z-acceleration in the chassis front was used as feedback since it was more directly connected to the propulsion force than the cab. The dynamics in z-direction between the chassis front and cab were thus neglected. The settling time was kept constant and the reference torque was kept as the original reference (step). The offramp and and onramp were designed in different ways and are described below.

Offramp

A z-acceleration reference was set to a value that was considered comfortable with experience from 4.1.3. e was calculated at each iteration of the controller. If it was negative it meant that a larger engine torque could be applied to the flywheel and the saturation limits were increased. If e was positive, it meant that the z-acceleration had reached the reference. Then the saturation was kept at the same level until e was negative again.

The tuning parameters of the offramp controller were:

- The z-acceleration reference value.
- The constant value added to the saturation limits in case e was negative.

The offramp controller is described in detail in Algorithm 3.

Algorithm 3 Offramp controller

```
while Offramp active do
    Set a_{z,ref}
    Calculate the error, e
    if e ≤ 0 then
        Set saturation limits = saturation limits + constant
    else
        Set saturation limits = saturation limits
    end if
end while
```

Onramp

Just like in the offramp, a z-acceleration reference was set and e was calculated at each iteration. When e was positive it meant that a larger engine torque could be applied to the flywheel and the saturations were increased.

The tuning parameters of the onramp controller were:

- The z-acceleration reference value.
- The constant value added to the saturation limits in case e was positive.

The onramp controller is described in detail in Algorithm 4.

Algorithm 4 Onramp controller

```
while Offramp active do
    Set a_{z,ref}
    Calculate the error, e
    if e ≥ 0 then
        Set saturation limits = saturation limits + constant
    else
        Set saturation limits = saturation limits
    end if
end while
```

4.4.4 Other controllers

A control structure that was considered is called *Linear quadratic controller*, LQ. The LQ-controller minimizes a quadratic criterion of the control error and the control signal. LQ-control is based on linear systems which the system in this thesis is not. The system would therefore have to be linearized around a stationary point. Linearizing around a stationary point is described in [19]. If the system is described by non-linear differential equations it can be expressed on non-linear state space form, (4.35),

$$\begin{aligned} \dot{x} &= f(x,u) \\ y &= h(x,u) \end{aligned} \tag{4.35}$$

where x are the states and u the input. A stationary point is a point where f in (4.35) evaluated in the stationary point is equal to zero. The system contained several states and nonlinear differential equations. Finding a stationary point for this system was problematic. The calculations would also become demanding since the *Jacobians* of f and h in (4.35) would have to be calculated and evaluated in the stationary point in order to find the matrices of the system expressed on state-space form. Since time was a limitation and it was of interest to begin with an easy controller LQ-control was not investigated further.

5. Results

This section presents the results obtained in this thesis. First, the results of the driving resistance modelling are presented. The driving resistance was estimated both with and without trailer to be able to separate the driving resistances applied to the truck and the trailer respectively. Further on, the performances of the rigid powertrain model and the flexible powertrain model are presented and compared in order to decide which model to use in the combined model connecting models of every component. The same process is made with chassis and cab, leading to a combined model. The last part of the section presents the results of the controllers.

5.1 Models

The performances of the models are presented below.

5.1.1 Driving resistance

The models described in 4.3.2 were used to estimate the driving resistance parameters. The first parameters that were estimated were the resistance parameters of the tractor only. This was done by removing the trailer which led to the following expression.

$$m_{\text{tractor}} a_{\text{tractor,x}} = -m_{\text{tractor}} g(f_{0,\text{tractor}} + f_{\text{S,tractor}} v) - \frac{A}{2} \rho d_{\text{without trailer}} v^2 \tag{5.1}$$

Using this equation, the measurements without the trailer and the least squares method, the following parameters were obtained.

Table 5.1: Obtained driving resistance parameters without trailer.

Parameter	Result
$f_{0,\text{tractor}}$	0.0055
$f_{\text{S,tractor}}$ (s/m)	$3.7759 \cdot 10^{-4}$
$d_{\text{without trailer}}$	0.5580

With the parameters in Table 5.1, (5.2) could be used to estimate the rolling resistance parameters for the trailer.

$$\begin{aligned} m_{\text{tot}} a_{\text{vehicle,x}} = &- m_{\text{tractor}} g(f_{0,\text{tractor}} + f_{\text{S,tractor}} v) - \frac{A}{2} \rho d_{\text{with trailer}} v^2 \\ &- m_{\text{trailer}} g(f_{0,\text{trailer}} + f_{\text{S,trailer}} v) \end{aligned} \tag{5.2}$$

Note that $m_{tractor}$ differs from the earlier expression since the weight on the wheels of the tractor is different when the trailer is attached. Using the least square method with the measurements the parameters in the Table 5.2 were obtained.

Table 5.2: Obtained driving resistance parameters with trailer.

Parameter	Result
$f_{0,\text{tractor}}$	0.0055
$f_{\text{S,tractor}}$ (s/m)	$3.7759 \cdot 10^{-4}$
$f_{0,\text{trailer}}$	0.0052
$f_{\text{S,trailer}}$ (s/m)	$1.4325 \cdot 10^{-4}$
$d_{\text{with trailer}}$	0.4218

The air drag coefficient was smaller with the trailer attached than without it. This might be due to different reasons. The test track did not have exactly zero road slope and the added trailer weight might affect the truck acceleration if the road was not flat. Another reason might have been that the model did not consider effects on the sides of the truck since the model only takes the front area into account.

The obtained parameters were used in Figure 5.1 where the driving resistance is compared to vehicle speed and the different components of the driving resistance are displayed. The measurement used as input was

performed in 8 % slope at low speed to represent the case that was of interest for this thesis. The figure shows that the driving resistance model has an expected behaviour. Since the truck was driving in a slope, there was a large contribution from the gravitational force. The shape of the driving resistance follows the shape of the velocity.

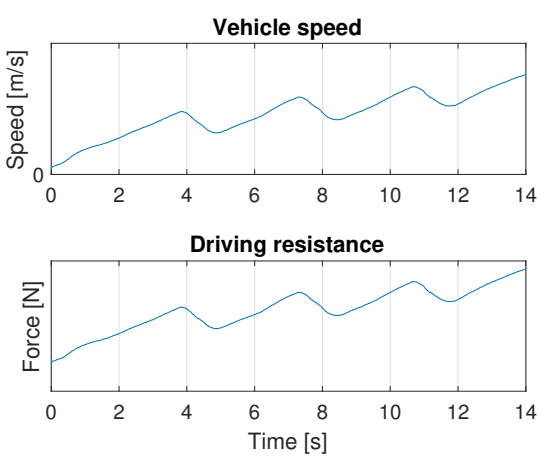

(a) Vehicle speed (above) and driving resistance (below).

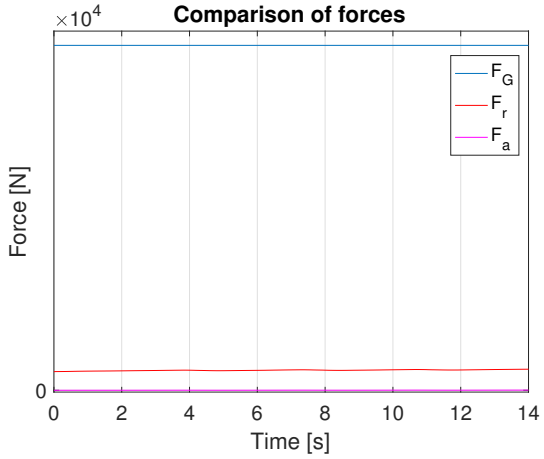

(b) Forces contributing to the driving resistance.

Figure 5.1: The figures show the result of the estimated parameters.

As seen in the figure the aerodynamic force on the vehicle was small compared to the other forces. This led to the conclusion that the aerodynamic force on the vehicle could be neglected and the driving resistance was calculated as (5.3).

$$F_{\text{DR}} = m_{\text{tractor}} g(f_{0,\text{tractor}} + f_{\text{S,tractor}} v) + m_{\text{trailer}} g(f_{0,\text{trailer}} + f_{\text{S,trailer}} v) + mgsin(\theta_{\text{slope}}) \tag{5.3}$$

5.1.2 Rigid powertrain model

For the model to work the wheel inertia was estimated using the least squares method. The obtained parameter is presented in Table 5.3.

Table 5.3: Obtained parameter of the rigid powertrain model.

Parameter	Value
J_{w} (kgm^2/rad)	129.6601

The obtained value was high but it was a simple model and this might have led to parameters with odd values since they had to compensate for model errors.

Using the estimated wheel inertia and the flywheel torque Figure 5.2 was obtained.

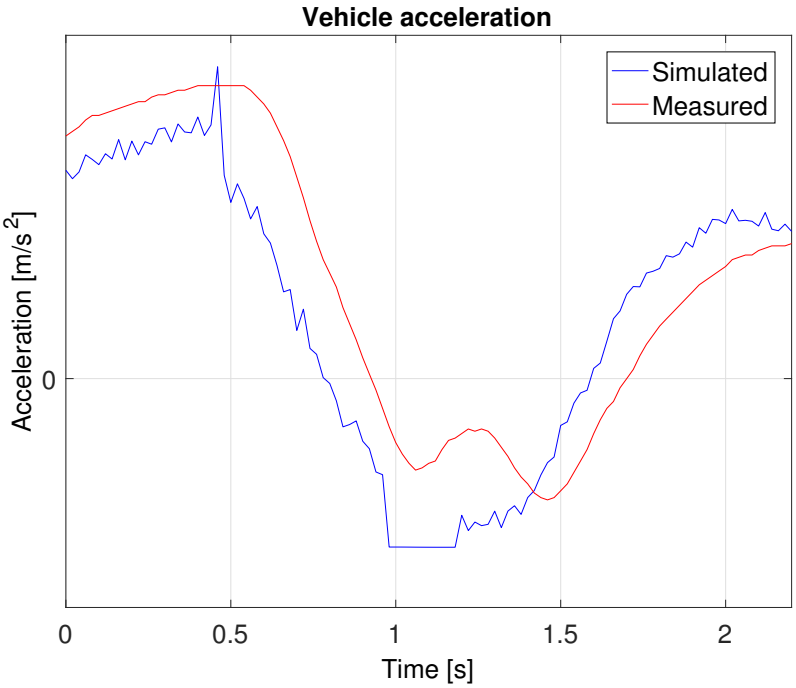

Figure 5.2: Vehicle x-acceleration generated by the powertrain. The model has the same shape as the real measurement with an offset. Note that between about 1 s to about 1.25 s the model is not valid since the powertrain is decoupled.

The model generated an acceleration which represented the measured acceleration quite well. The input to the rigid powertrain model was flywheel torque and Figure 5.3 shows the resemblance between the input torque and the acceleration. This was expected since the wheel acceleration was a scaled version of the torque with some added resistances.

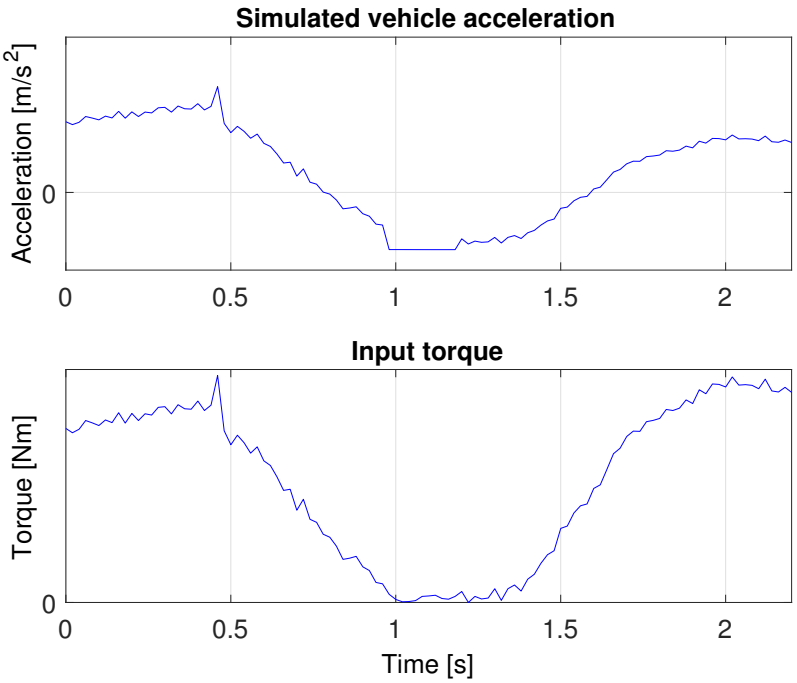

Figure 5.3: Vehicle acceleration and input torque to the model. It is obvious that the flywheel torque directly affects the acceleration for this model.

With this figure in mind the problem of the rigid powertrain model was that it used the flywheel torque as input. The flywheel torque depended on the engine speed and acceleration. The real input to the system should be the engine torque to be able to control it at the end of the project. In Figure 5.4 the difference between the engine torque and the flywheel torque is shown.

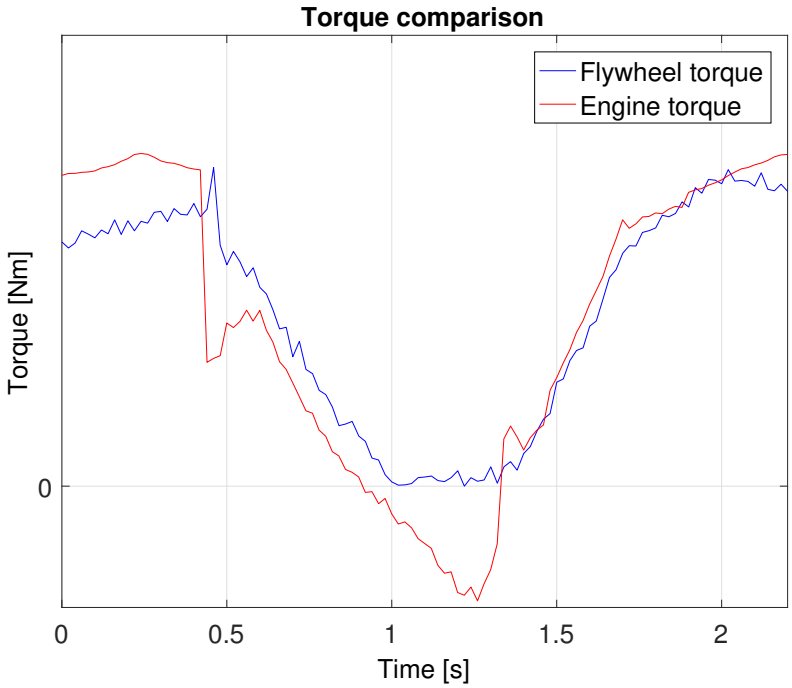

Figure 5.4: Comparison of the flywheel torque and the engine torque.

The figure shows the difference in torque and motivates why the stiff model could not be used in combination with the engine torque since it would translate into an acceleration which resembles the engine torque. This meant that another model had to be used.

5.1.3 Flexible powertrain model

The parameters were estimated using the least squares method with the constraint that they had to be larger than or equal to zero. The estimated parameters are listed in Table 5.4.

Table 5.4: Estimated parameters for the flexible powertrain model.

Parameter	Result
$k_{\mathrm{d}}(Nm/rad)$	–
$c_{\mathrm{d}}(Nms/rad)$	$9.7357 \cdot 10^3$
b_{e} (Nms/rad)	2.3381
$b_{\mathrm{w}}(Nms/rad)$	0

The obtained damper constant of the driveshaft was high but could work for this model. With these parameters the results in Figure 5.5 and Figure 5.6 were obtained.

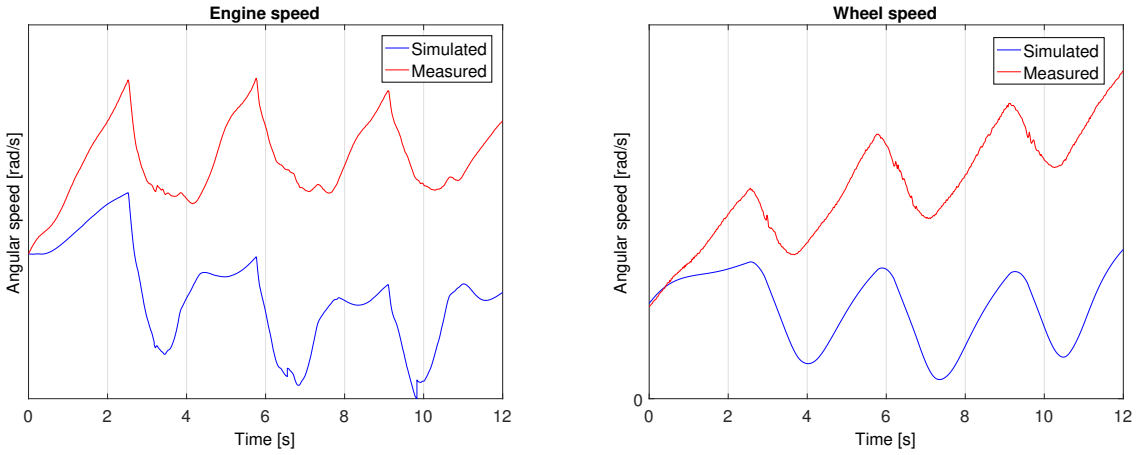

(a) Simulated and measured engine speed.

(b) Simulated and measured wheel speed.

Figure 5.5: Simulated and measured engine and wheel speeds.

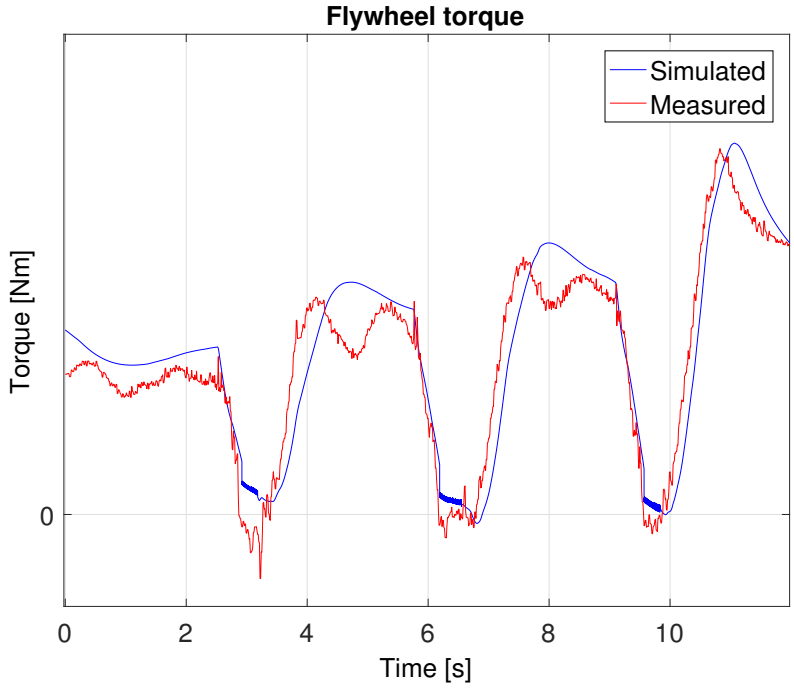

Figure 5.6: Simulated and measured flywheel torque.

As the figures show the parameters obtained using the least squares method did not follow the measurement well. By analyzing the figures the parameters could be changed. For example by looking at Figure 5.5a it was clear that the loss b_e was to high and should be altered. In Appendix B the complete sequence of altering and adapting the parameters is shown.

The final parameters of the powertrain are displayed in Table 5.5.

Table 5.5: Tuned parameters for the flexible powertrain model.

Parameter	Result
$k_{\mathrm{d}}(Nm/rad)$	$1.0755 \cdot 10^5$
$c_{\mathrm{d}}(Nms/rad)$	2000
$b_{\mathrm{e}}(Nms/rad)$	0
$b_{\mathrm{w}}(Nms/rad)$	75

Using the parameters in Table 5.5 the results in Figure 5.7 and Figure 5.8 were obtained.

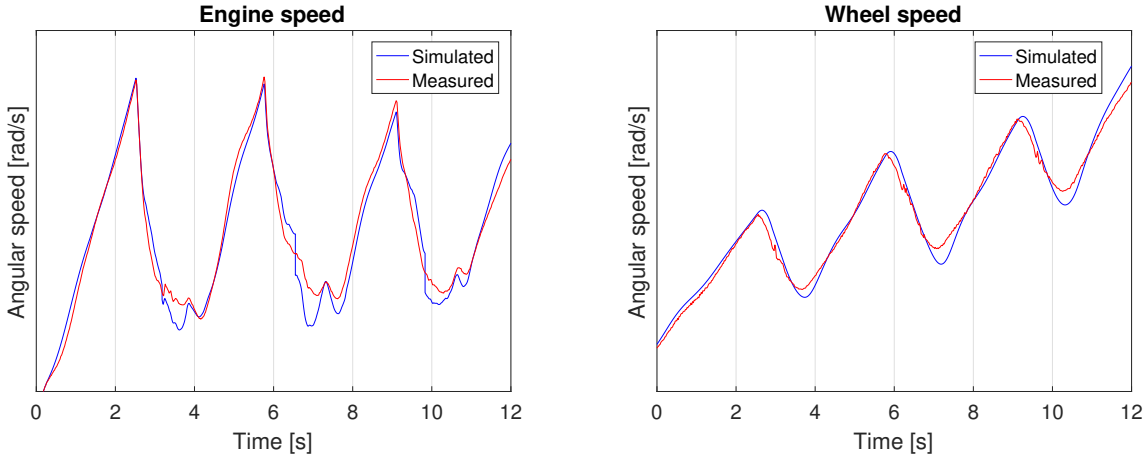

(a) Simulated and measured engine speed.

(b) Simulated and measured wheel speed.

Figure 5.7: Simulated and measured engine and wheel speeds.

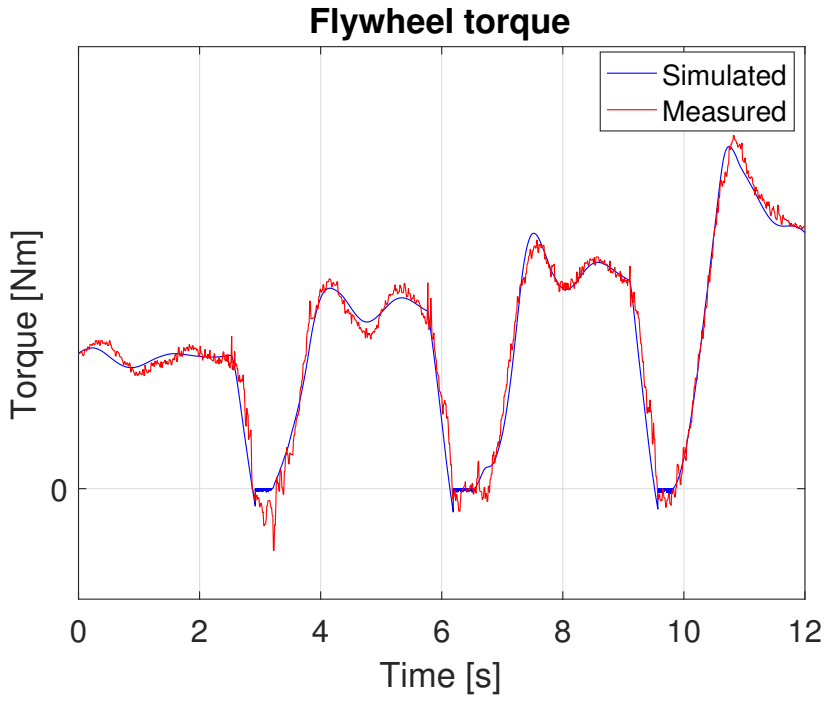

Figure 5.8: Simulated and measured flywheel torque.

In Figure 5.7a it is seen that the simulated engine speed followed the measured engine speed well. When the clutch was disengaged at about 4 s, 7 s and 10 s the engine speed did not follow the measurement. This was not of importance to the model since it was supposed to capture the wheel speed and acceleration which were not affected by the engine speed at these moments in the simulation. The wheel speed in Figure 5.7b was captured well. The simulated flywheel torque in Figure 5.8 followed the measurement well. When the model was decoupled the model did not catch the flywheel torque which was expected since it was the wheel side that was of interest.

5.1.4 Decoupled flexible powertrain model

With the engine side of the transmission modelled the parameters of the decoupled model had to be found. By using the initial guess stated in Table 5.6, Figure 5.9 was obtained. The initial guess of the inertia was based on that the transmission and propeller shaft inertia should be smaller than the engine inertia. The initial guess of the mechanical loss was based on that the loss should be small.

Table 5.6: Parameters for the decoupled powertrain model.

Parameter	Result
$J_t(kgm^2/rad)$	0.1
$b_t(Nms/rad)$	0

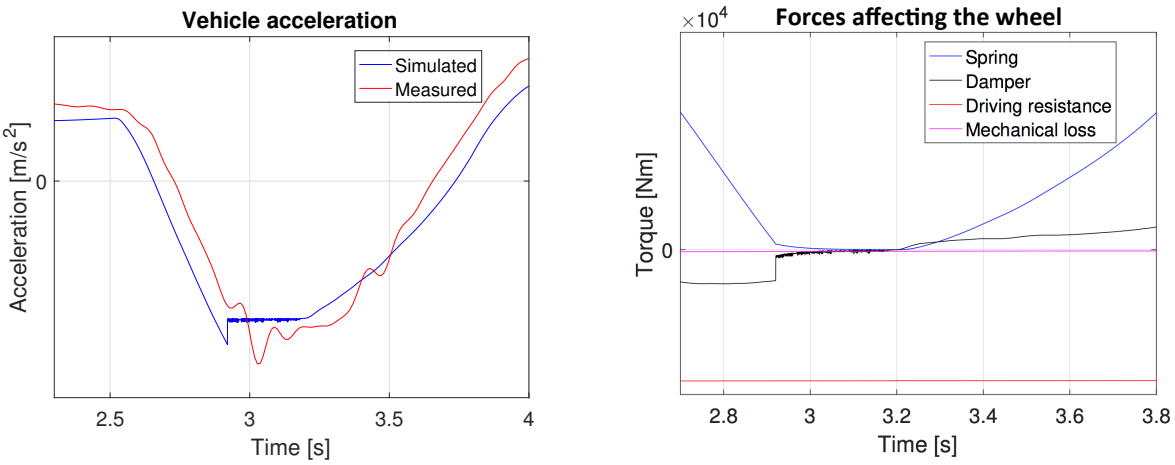

(a) Simulated vehicle acceleration.

(b) Simulated torque applied on the wheel.

Figure 5.9: Simulation of the decoupled model.

The transition between the coupled and decoupled model, at about 2.9 s shown in Figure 5.9a, was not good. The reason for this was that the model did not take into account when zero transmitted torque had been reached. Instead it worked with the measured time the controller was active. This fault would be removed by switching between the models when zero transmitted torque had been achieved. In Figure 5.9b the torque applied to the wheel is shown. As expected by the model the main torque on the wheel when decoupled was the driving resistance.

The model worked as expected but one thing that was removed was the oscillating behaviour when decoupled. This was done by altering the inertia. By altering it to 1 the results in Figure 5.10 and Figure 5.11 were obtained.

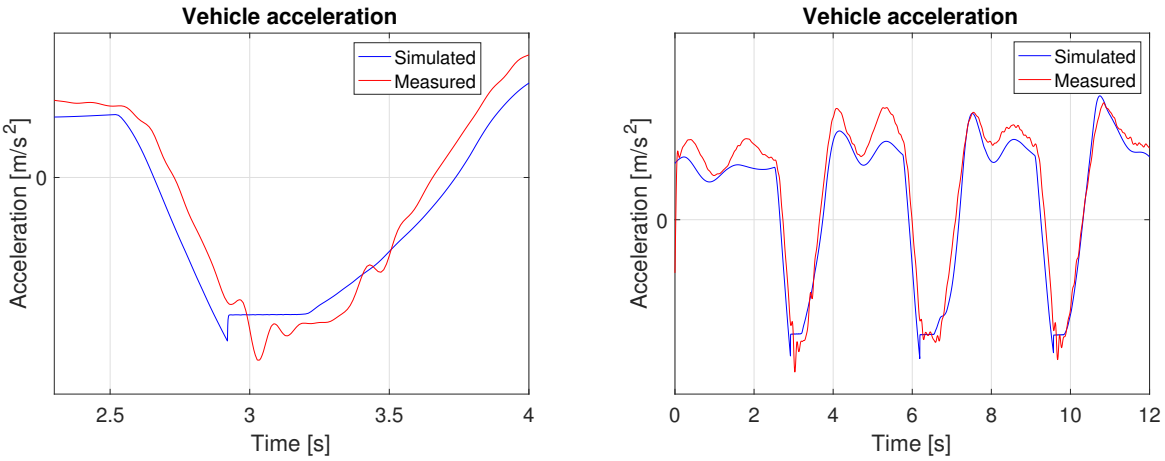

(a) Zoomed simulated vehicle acceleration.

(b) Simulated vehicle acceleration.

Figure 5.10: Simulated vehicle acceleration. The first plot is the first gear shift of the second plot.

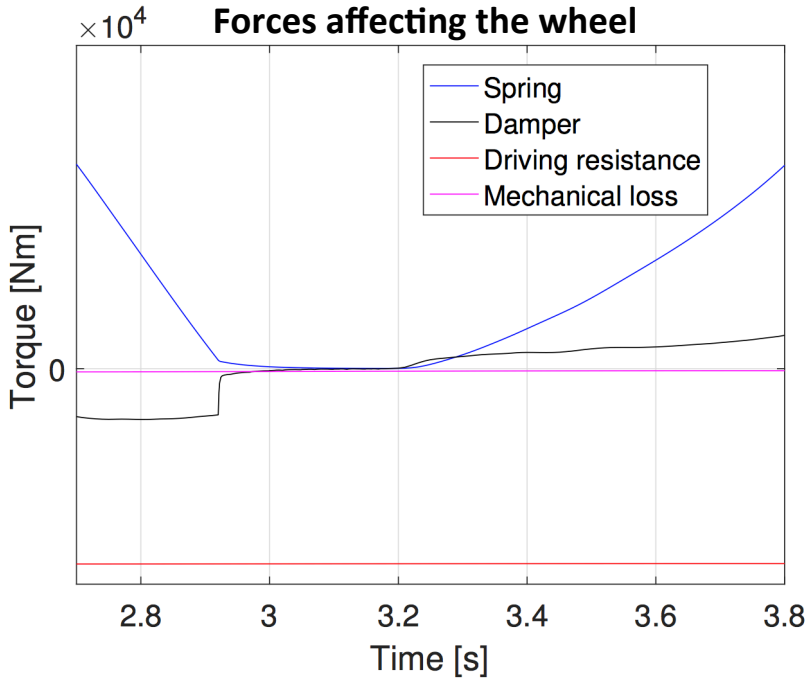

Figure 5.11: Simulated torque applied on the wheel.

The figures show that the oscillations were removed when decoupled. Figure 5.10a could have been a reason for increasing the mechanical loss since the measured acceleration was smaller. Figure 5.10b contradicts this since it shows that the acceleration was correct for another gear shift. Another reason that the loss could have been increased was that in Figure 5.11 it is seen that the spring provides the wheel with a positive force while it should be negative in the decoupled case. But there was no measure of the transmission speed and the effect was small compared to the driving resistance. Therefore the loss was not altered.

In Figure 5.12 the wheel and transmission speeds are displayed.

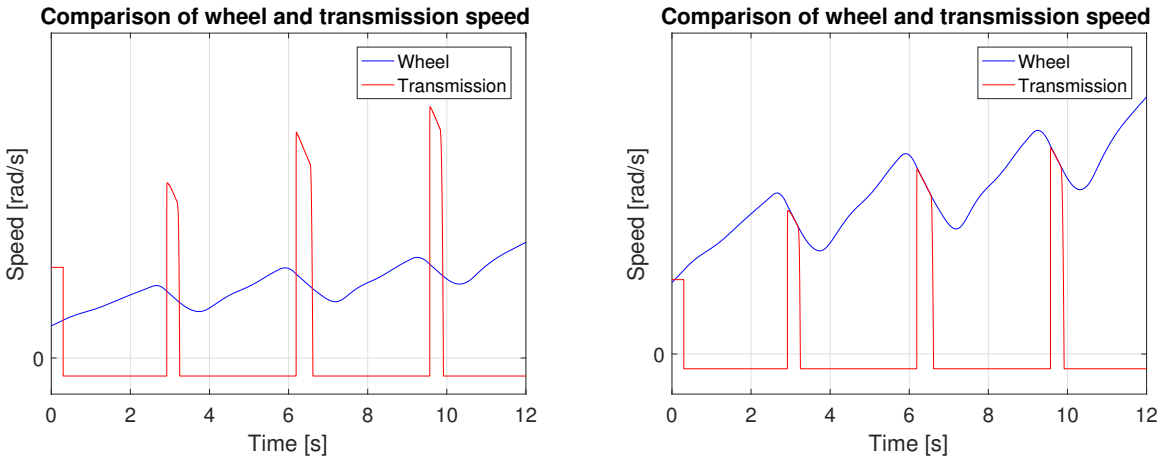

(a) Simulated wheel and transmission speed.

(b) Simulated wheel and scaled transmission speed.

Figure 5.12: Comparison of the wheel and transmission speed. The initial value of the transmission speed was set to initialize the powertrain correctly. Since the transmission model only was of interest when decoupled a default value was set when not active. The default value was negative since the model was adapted for forward movements.

The figures show that the transmission speed got to a scaled value of the wheel speed. This was expected by the model since the transmission should follow the wheel speed when decoupled.

5.1.5 ETC model

ETC was implemented and adapted for the model specific for this thesis. Figure 5.13 shows the result of the model where the input to the system was demanded flywheel torque.

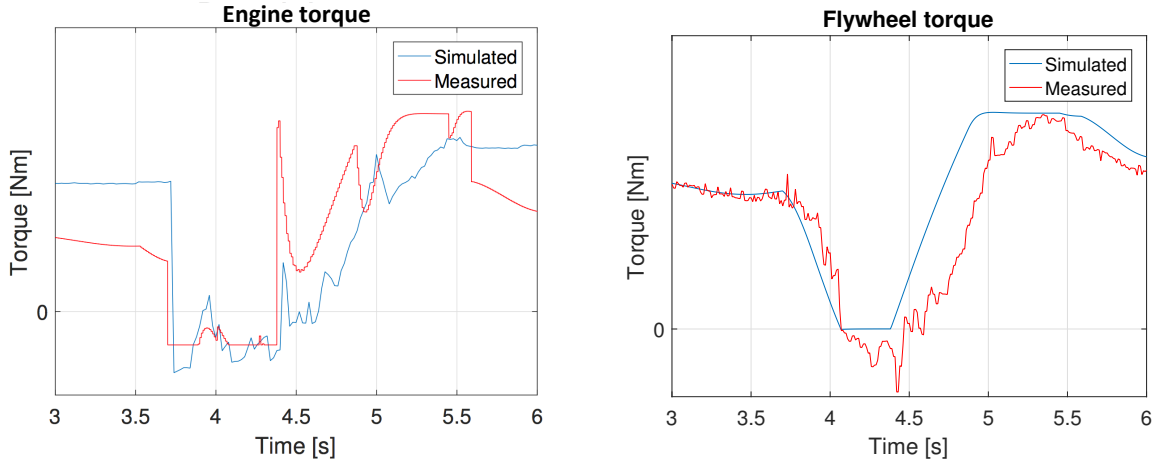

(a) Engine torque.

(b) Flywheel torque.

Figure 5.13: The figures show the performance of the ETC model. The left figure shows the engine torque generated by the ETC model. The right figure shows the measured and simulated flywheel torque.

The model generated the expected behaviour based on the model acquired in 5.1.3. The demanded engine torque before the initial output at about 3.75 s and after 5.6 s could be neglected. The reason it could be neglected was that the controller was only active during the gear shift. When the controller was not active

the measured engine torque was selected as input to the powertrain model. It is clear in the figure that the simulated flywheel torque increased faster than the measurement. This effect could be explained by the fact that the powertrain model did not consider the synchronization of the transmission and the backlash between gears.

One of the effects of the model being faster than the real system was that the controller was done faster. Even though it was done it still tried to follow the reference which meant that it would hold the reference torque. At the offramp the model could be switched when the goal of the ramp was achieved. This could not be done in the onramp since between gear shifts the measured engine torque applied on the flywheel was used as input to the powertrain model. The effects of the bad transition between models could be neglected since the goal was to reach the reference torque in a more comfortable way and what happened after that was not important for this thesis.

5.1.6 Performance of chassis model

As mentioned in 4.3.4, there were two different approaches to calculate the spring-damper constants modelling the front axle.

Using three different driving situations

The results from where three different driving situations were used to isolate and estimate the parameters of the spring-damper and chassis inertia are presented below. Table 5.7 contains the values of the parameters, and Figure 5.14 and Figure 5.15 contains real measurements plotted together with the simulation.

Table 5.7: Parameter values estimated by using three different driving situations.

Parameter	Value
l_0 (m)	0.1085
k_{front} (N/m)	$5.4601 \cdot 10^5$
c_{front} $(Ns/m$ $)$	$5.4931 \cdot 10^5$
J_{rear} $(kgm^2$ $)$	$1.3819 \cdot 10^4$

It is obvious that this model captured the chassis front x-accelerations in an impeccable way since it is more or less exactly the same, see Figure 5.14a. Figure 5.14b however, shows that the model did not capture the chassis front z- acceleration. This is explained by Figure 5.15b together with (4.23). The figure shows that the angular acceleration is too low compared to the angular acceleration needed to capture the chassis front z- acceleration. The equation shows that the model expression for the chassis front z- acceleration depended only on the angular acceleration and a length parameter. Since the angular acceleration was too low and had the wrong shape, also the acceleration had the wrong amplitude and shape. This model was not considered to be good enough since both x- and z-accelerations were taken into consideration when looking at the comfort.

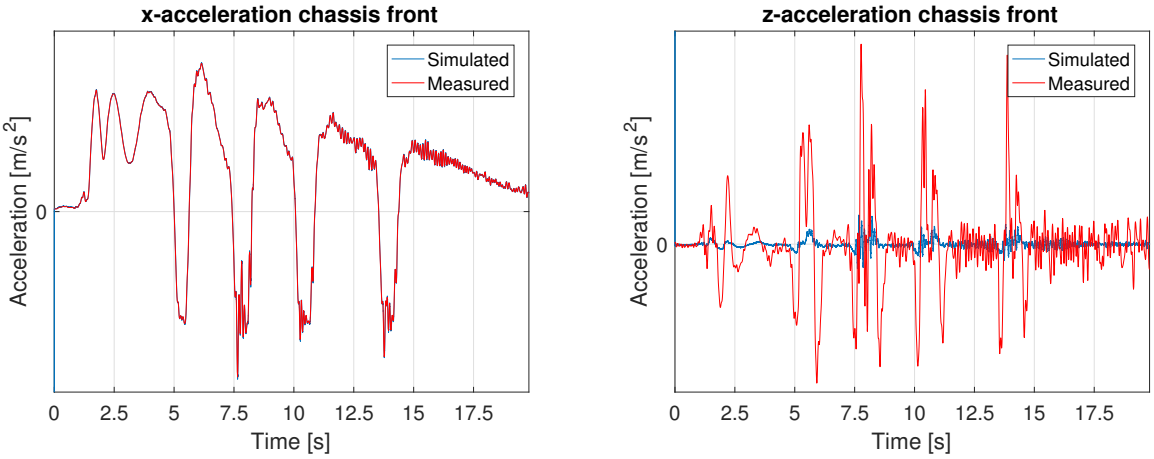

(a) x-acceleration. (b) z-acceleration.

Figure 5.14: Comparison between simulated and measured acceleration in the chassis front. The parameters in the model were estimated using three different driving situations.

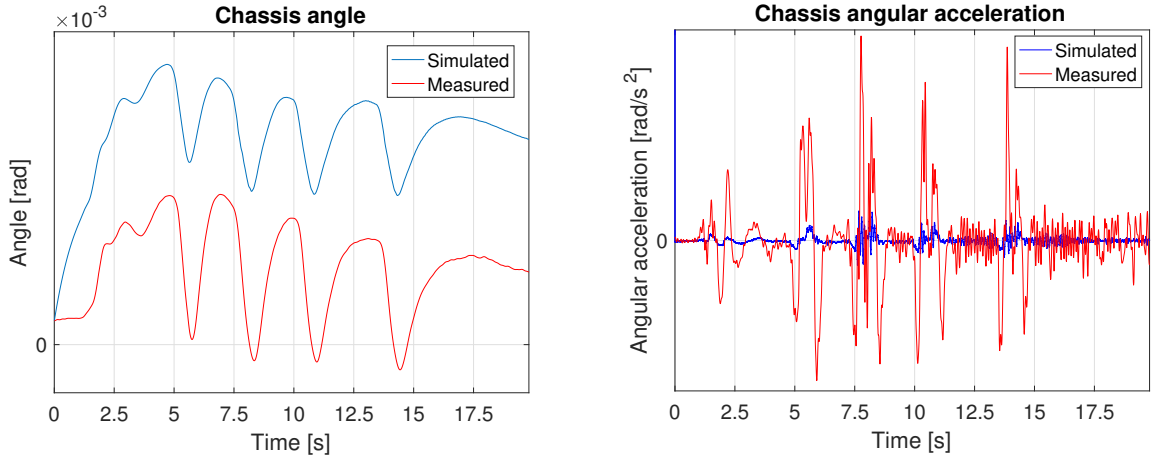

(a) Chassis angle ϕ. (b) Chassis angular acceleration $\ddot{\phi}$.

Figure 5.15: Comparison between simulated and measured chassis angle, ϕ, and angular acceleration, $\ddot{\phi}$. The parameters in the model were estimated using three different driving situations.

Grid search

The grid search with parameter estimation resulted in a chassis angle that had a good behaviour but an offset. To get rid of the offset the constant part, l_0, of the spring-damper was tuned. The values of the parameters after tuning are shown in Table 5.8.

Table 5.8: Parameter values after tuning the constant part of the spring-damper force.

Parameter	Value
l_0 (m)	0.15
k_{front} (N/m)	$3.6 \cdot 10^5$
c_{front} (Ns/m)	$4.3658 \cdot 10^4$
J_{rear} $(kgm2)$	$3.9475 \cdot 10^4$

Figure 5.16 shows the measured and simulated chassis front x- and z- accelerations. This model was able to capture both accelerations in a good way. Looking at the angular acceleration in Figure 5.17b, it is obvious that this model captured the angular acceleration in a better way than the previous model, therefore the chassis front z- acceleration could also be captured. The chassis angle is seen in Figure 5.17a. The angle has a correct mean value and a correct behavior. The amplitude of the movements is smaller, but the angle is relatively small, the difference is small, and this was not considered to be a problem.This model was considered to be good enough since it captured both accelerations, which were the output, together with the chassis angle, from the chassis model used as inputs to the cab model.

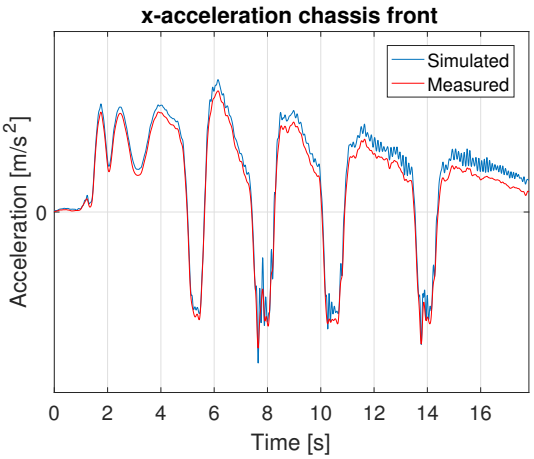

(a) x-acceleration.

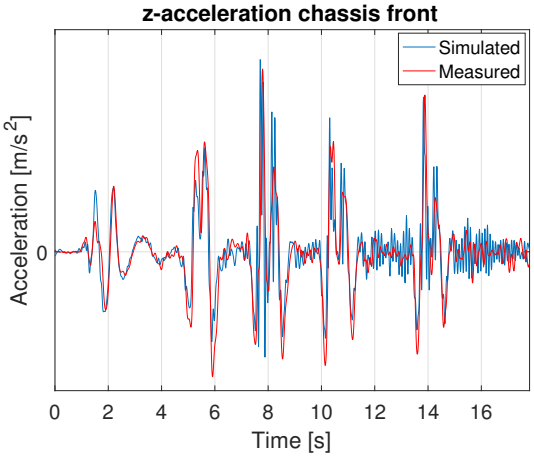

(b) Chassis angular acceleration, $\ddot{\phi}$.

Figure 5.16: Comparison between simulated and measured acceleration in the chassis front. The parameters in the model were estimated using grid search.

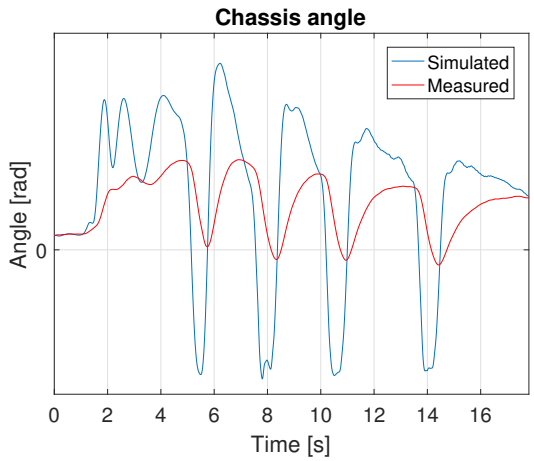

(a) Chassis angle, ϕ.

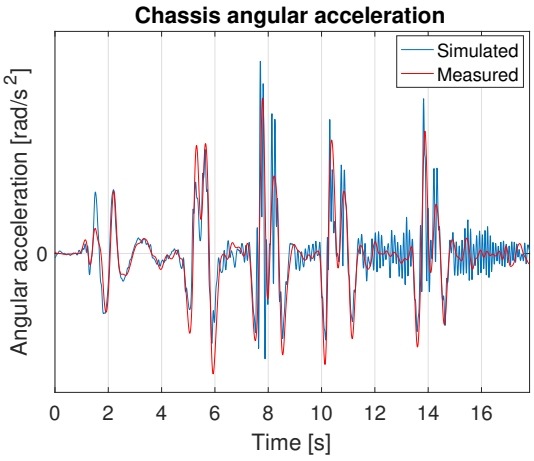

(b) Chassis angular acceleration, $\ddot{\phi}$.

Figure 5.17: Comparison between simulated and measured chassis angle, ϕ, and angular acceleration, $\ddot{\phi}$. The parameters in the model were estimated using grid search.

5.1.7 Cab model

In Table 5.9 the obtained parameters using Algorithm 2 are presented.

Table 5.9: Obtained cab parameters using the provided inertia and an estimated inertia.

Parameter	Case: Known J_c	Case: Estimated J_c
Inertia J_c (kgm^2)	–	795.3003
Height $h_c(m)$	4.7241	1
Position $h_{c,s}$ (m)	2.3621	0.3000
Constant k_c (N/m)	1.3711e+05	1.6257e+06
Constant c_c (Ns/m)	7.8015e+03	1.0761e+05

Using these parameters, Figure 5.18 - Figure 5.20, containing measurements plotted together with simulations, were obtained. The inputs for the simulation were the chassis angle, the road slope and the accelerations in x- and z-direction in the front of the chassis.

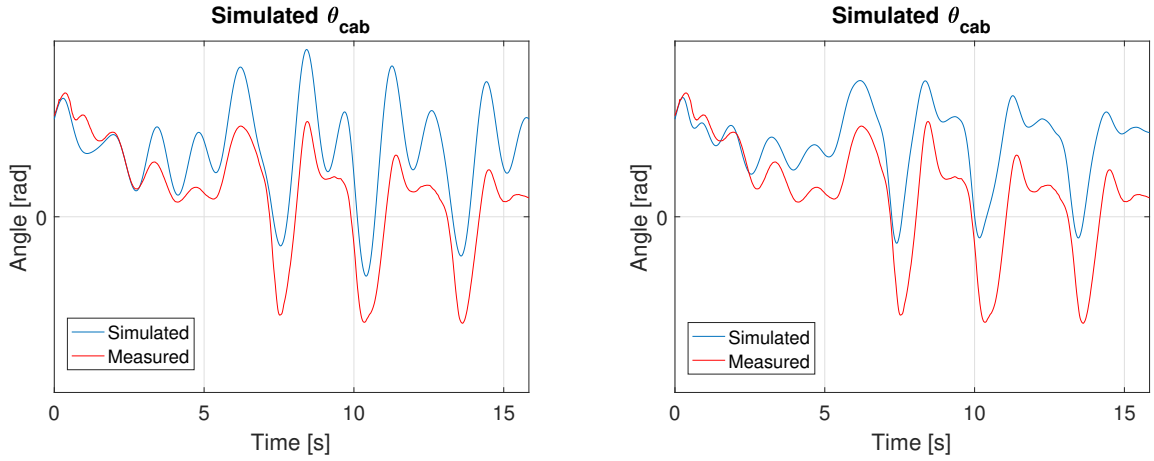

(a) Simulation with provided J_c.

(b) Simulation with estimated J_c.

Figure 5.18: Simulated cab angle compared to measurements. The simulation was better when estimating the inertia of the cab.

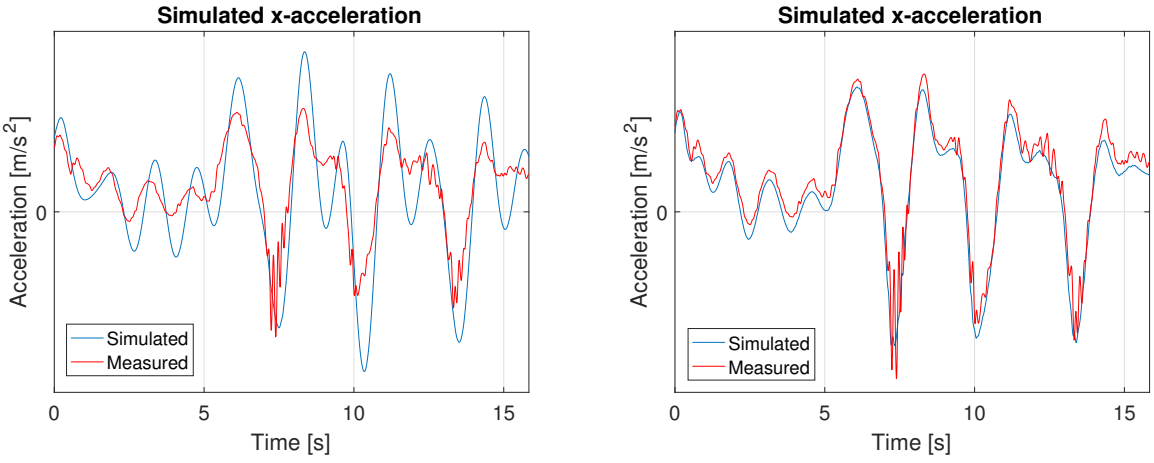

(a) Simulation with provided J_c.

(b) Simulation with estimated J_c.

Figure 5.19: Simulated cab x-acceleration. The model with the estimated inertia follows the acceleration better.

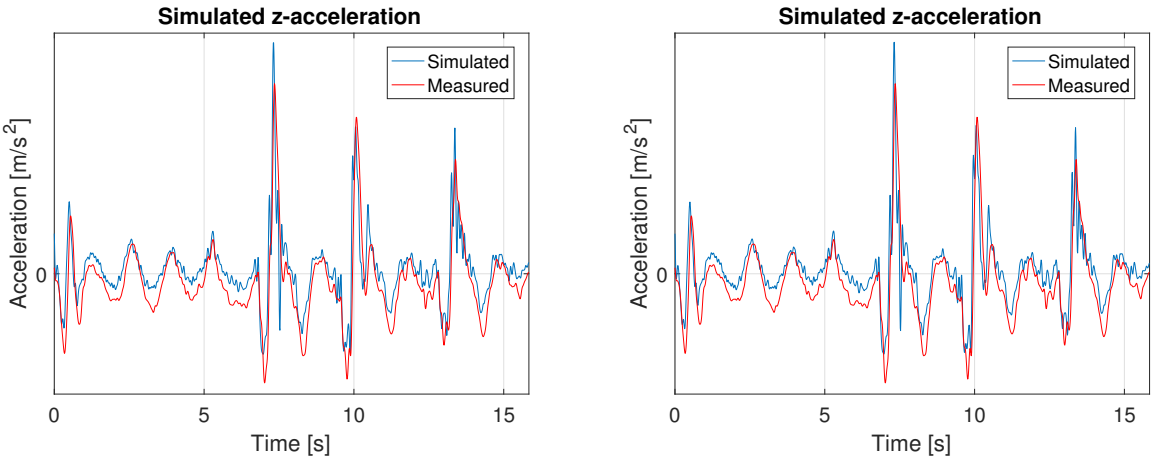

(a) Simulation with provided J_c.

(b) Simulation with estimated J_c.

Figure 5.20: Simulated cab z-acceleration. The simulated acceleration did not differ too much in the z-direction.

The simulation shows that the model using the estimated inertia followed the measurements better than the model with known inertia. The simulations in z-direction did not differ much between the two approaches. When looking at the angle and the x-acceleration the parameters with the estimated inertia were better. This led to the conclusion that the parameters with the estimated inertia should be used.

When analyzing how the model performed with the estimated inertia it followed the measurement quite well. The angle of the cab drifted from the mean but the general motion was good. In x-direction the general shape was captured by the model. Figure 5.21a is a zoomed version of Figure 5.19b. The figure shows that when comparing the gear shifts, with respect to the results in 4.1.3, the correct ranking of the gear shifts were possible. That is that the amplitude of the second gear shift was the smallest and the first one was the largest. In the ideal case the difference between the acceleration would have been bigger. The oscillations in x-direction were not captured by the model. In z-direction the general acceleration was captured and the amplitudes, displayed in Figure 5.21b, were correct when ranking the comfort.

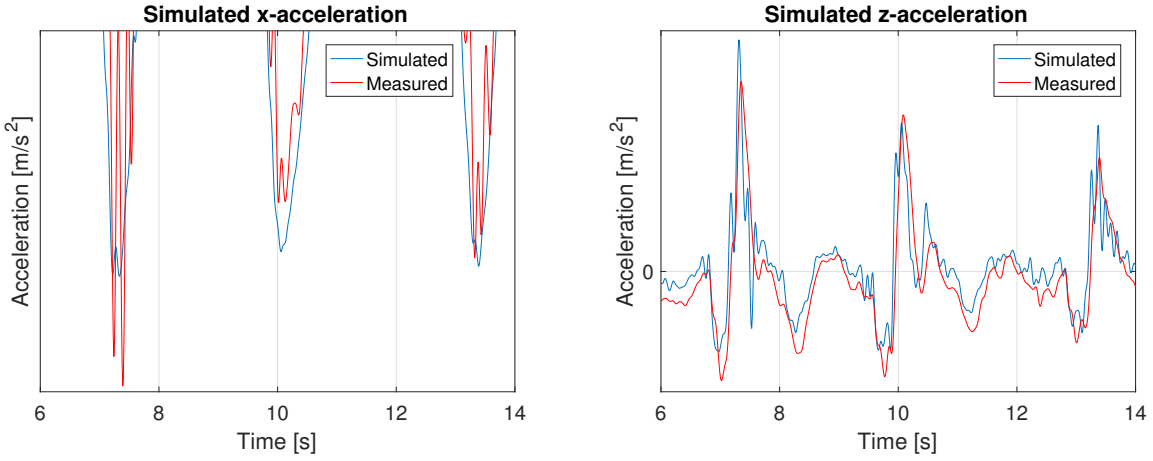

(a) Simulated x-acceleration with estimated J_c.

(b) Simulated z-acceleration with estimated J_c.

Figure 5.21: Simulated x- and z-acceleration. The figures are zoomed to be able to compare the amplitude of the acceleration.

5.1.8 Complete vehicle model

The models were combined and this section displays the results. The powertrain model was supposed to generate the propulsion force and the acceleration of the vehicle given the torque produced by the engine. Figure 5.22a and Figure 5.22b shows the propulsion force and the acceleration of the vehicle respectively.

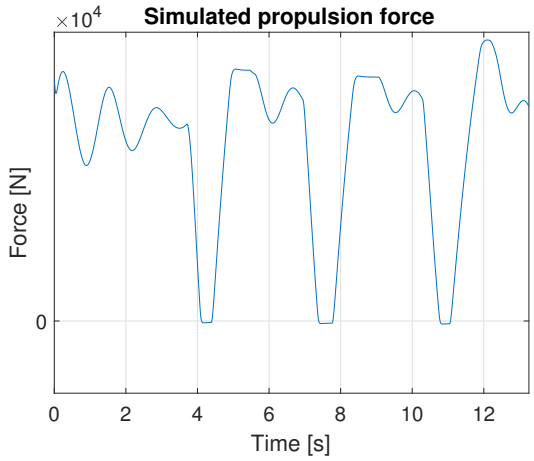

(a) Propulsion force generated by the powertrain.

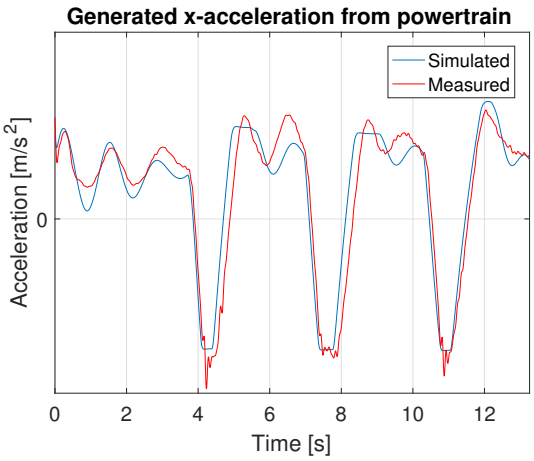

(b) Vehicle acceleration.

Figure 5.22: Generated vehicle acceleration and propulsion force by the powertrain.

The model catched the general shape of the acceleration during the gear shift. When comparing the three gear shifts it was clear that they all ended up at the same acceleration, this was a problem which would become clear in the cab simulation. There was no real difference compared to the result shown in 5.1.3 which was expected since it was the first model in the chain. These two signals were inputs to the chassis model and Figure 5.23 and Figure 5.24 shows the results of the chassis model.

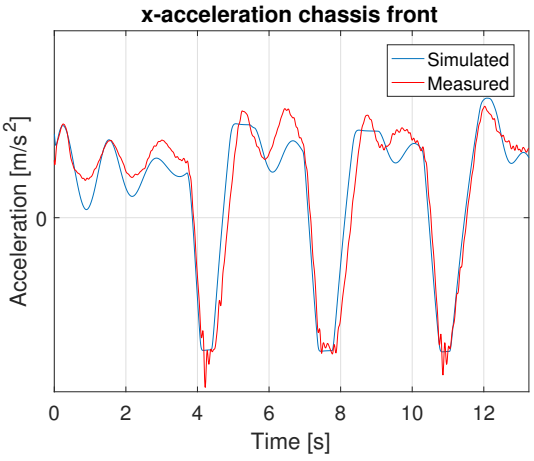

(a) Chassis front x-acceleration.

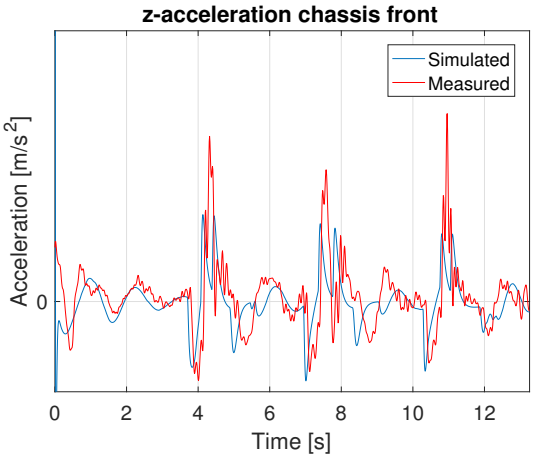

(b) Chassis front z-acceleration.

Figure 5.23: Chassis front accelerations.

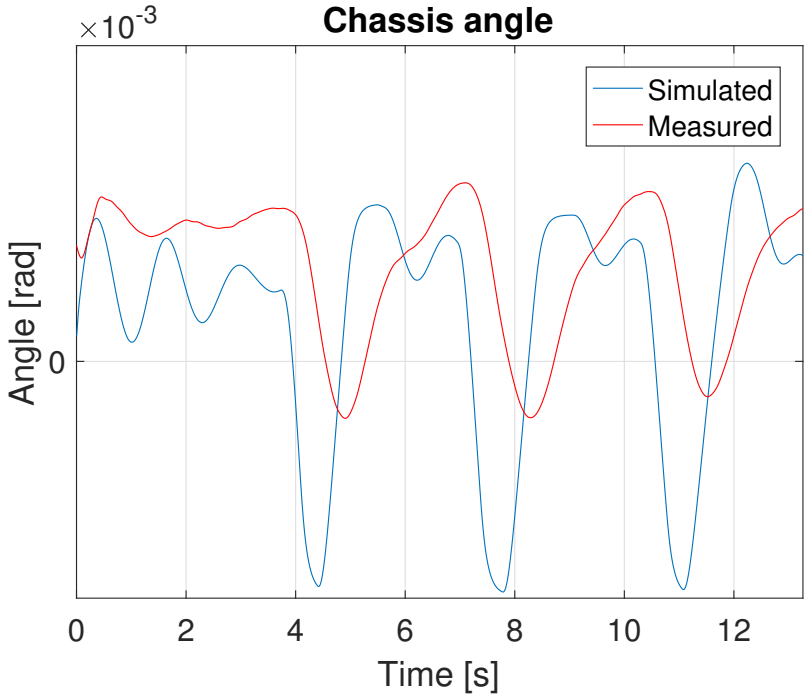

Figure 5.24: Simulated chassis angle.

The x-acceleration in Figure 5.23a had the same shape as the acceleration which the powertrain generated. This was expected of the model. The z-acceleration in Figure 5.23b followed the general shape of the real acceleration. When decoupled the positive peaks of z-acceleration had a deviating behaviour. The chassis angle in Figure 5.24 was somewhat captured by the model.

The last model in the chain was the cab model with the results displayed in the Figure 5.25 and 5.26.

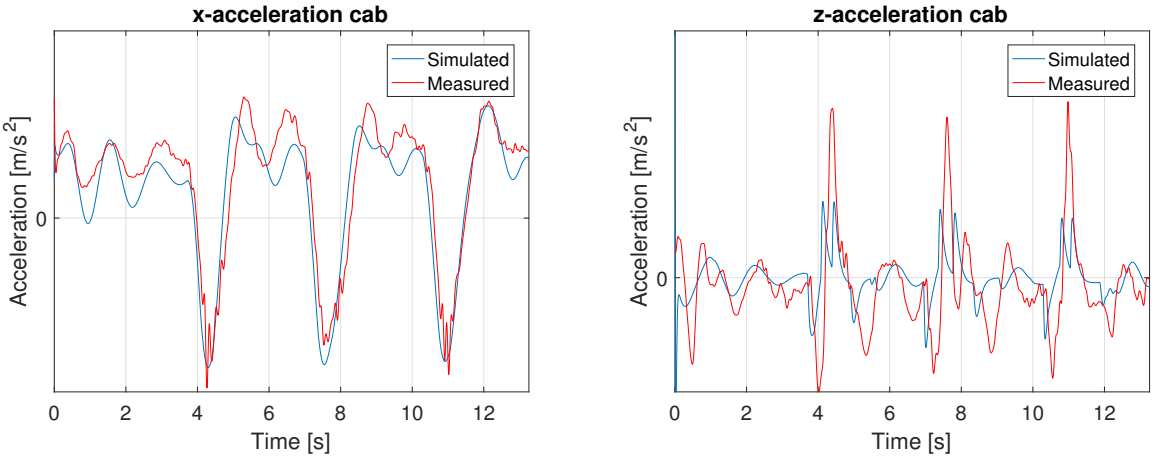

(a) Cab x-acceleration.

(b) Cab z-acceleration.

Figure 5.25: Cab accelerations.

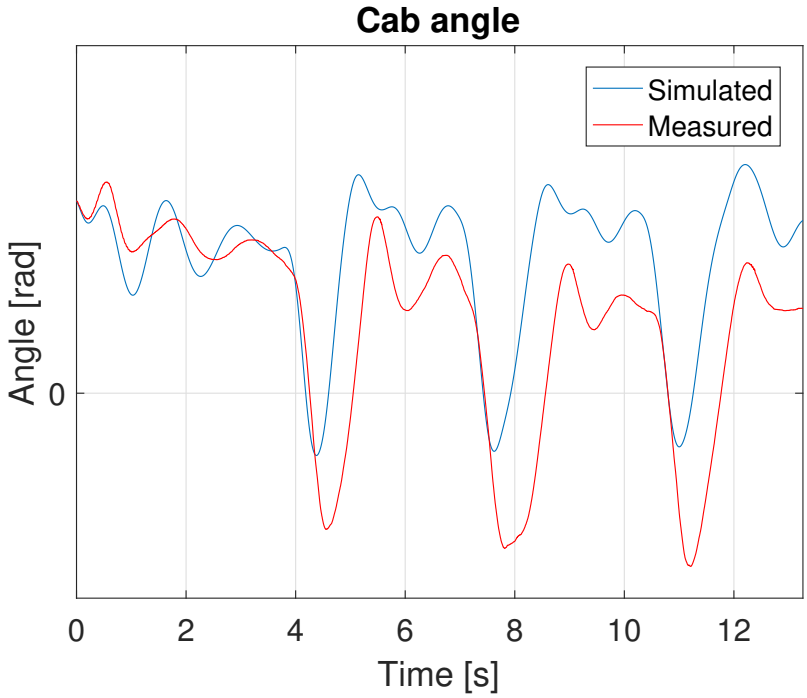

Figure 5.26: Simulated cab angle.

The x-acceleration displayed in Figure 5.25a had the same shape as the measured acceleration. The z-acceleration displayed in Figure 5.25b shows that the simulated acceleration was smaller than the measured one but it had the same general shape. The cab angle was drifting away from the real angle but it had the same shape.

To evaluate the result Figure 5.27 which is a zoomed version of Figure 5.25a was produced.

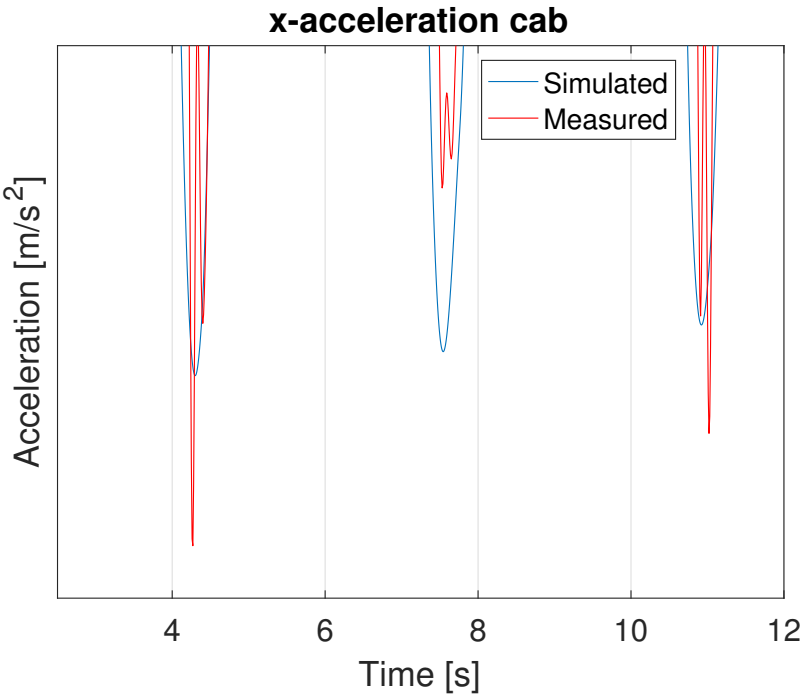

Figure 5.27: Zoomed simulated cab x-acceleration.

The second gear shift in Figure 5.25a shows a problem with the model. When comparing the gear shifts section 4.1.3 stated that the goal was to minimize the acceleration to improve the comfort in the cab. The second gear shift should according to measurements be a more comfortable gear shift than the others. According to the simulation the second gear shift was not the most comfortable gear shift. This problem originated from the generated acceleration of the powertrain shown in Figure 5.22b. The same could be said in the z-direction which is displayed in Figure 5.25b. The third gear shift should be a more uncomfortable gear shift than the second one but it did not show in the model.

Figure 5.28 shows the calculated jerk in the cab.

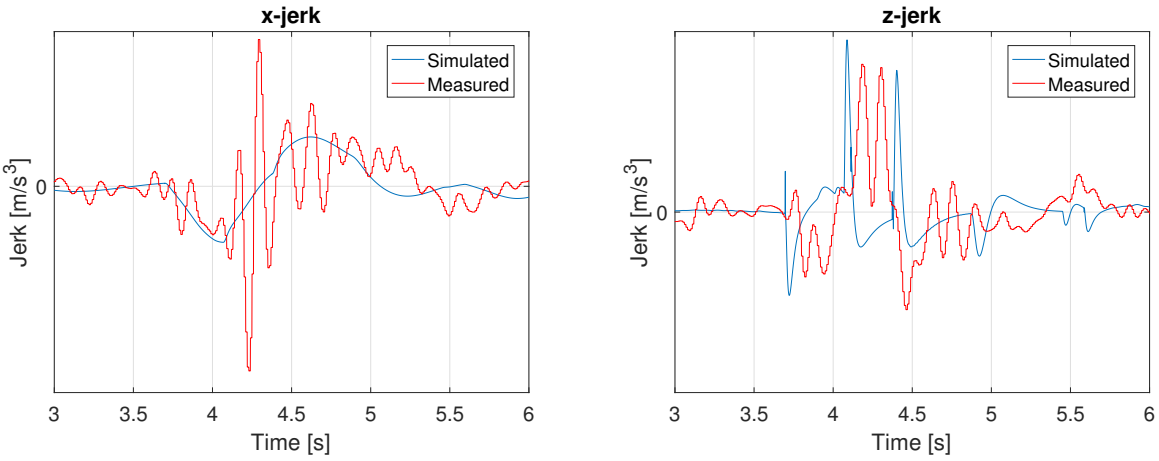

(a) Cab x-jerk.

(b) Cab z-jerk.

Figure 5.28: Calculated cab jerk.

Figure 5.28a shows the cab x-jerk. The cab jerk was not captured by the model. The model followed the general movement but the interesting changes were not captured. In 5.28b the cab z-jerk is shown. The peaks in the jerk originates from the transition between the coupled and the decoupled model. With these figures in mind the conclusion was that it would not be possible to analyze the cab jerk since the models did not capture the behaviour good enough.

5.2 Controller

The performances of the investigated controllers are presented. The validation was done in simulation environment.

5.2.1 Low pass filtering control signals

This section shows the result of the low pass filtered signals. Table 5.10 shows the different filter constants for the chosen filters. The time of the onramp was longer than the offramp which meant that the filter constants had to be different for the ramps.

Table 5.10: Filter constants for the different filters.

Filter	**Offramp constant**	**Onramp constant**
Second order, reference	22	16
Sixth order, reference	40	25
Second order, Saturation	30	16
Sixth order, Saturation	60	25

Figure 5.29 shows the difference between the reference signal and the sixth order low pass filtered reference signal.

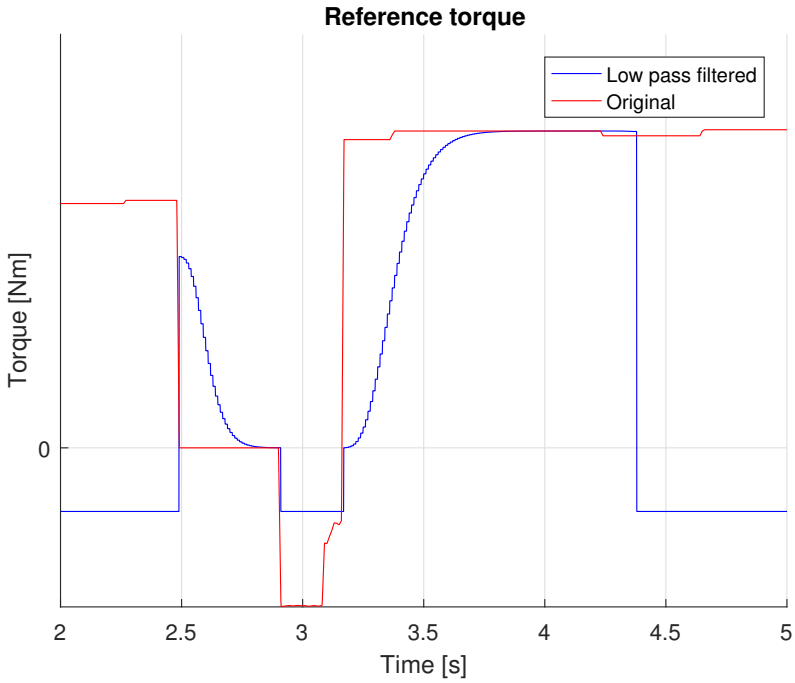

Figure 5.29: Comparison of the low pass filtered reference torque and the original reference torque. The reason the starting point was lower for the filtered signal than the original signal was that the filter was initialized with the current flywheel torque.

In Figure 5.30 the cab accelerations in x- and z-direction are displayed.

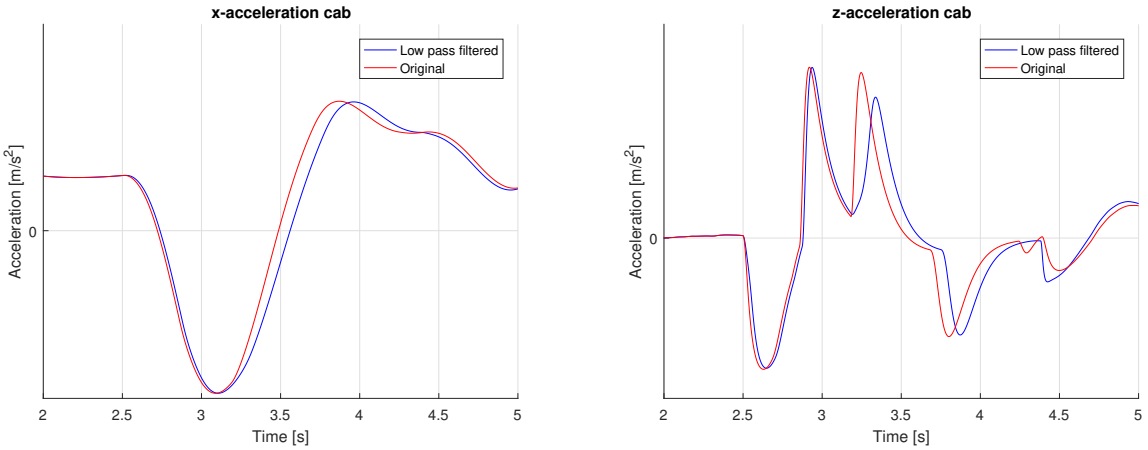

(a) Cab x-accelerations.

(b) Cab z-acceleration.

Figure 5.30: Cab accelerations. The original signal is the simulation without the low pass filtered reference.

The figure shows that the comfort was better with the low pass filtered signal. But the figure is misleading which Figure 5.31 shows.

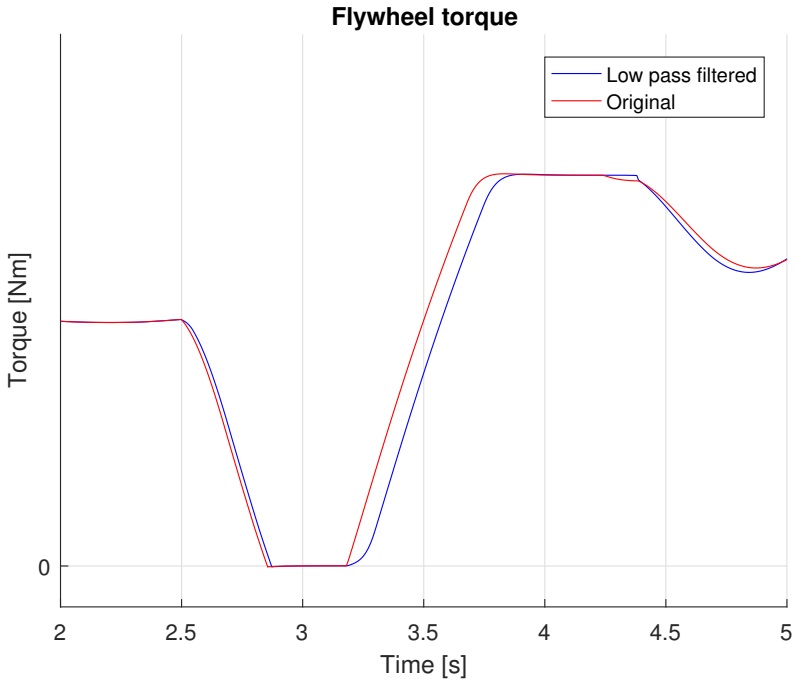

Figure 5.31: Comparison of flywheel torques.

The figure shows that both ramps, especially the onramp, are slower than the original simulation. This would be an unfair comparison since it of course is easier to perform a more comfortable gear shift if the time is longer. In order to change the behaviour the derivative of the ramps were altered such that the ramps had the same time to be completed.

The filters were implemented in two ways, filtering the reference and filtering the saturation. For both implementations there were one filter of order two and one with order six. This generated four different cases which were compared. Figure 5.32 shows the simulated z-acceleration for the different cases.

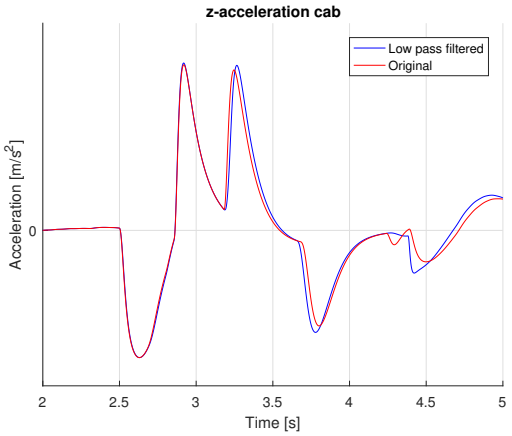

(a) Second order filtered reference signal.

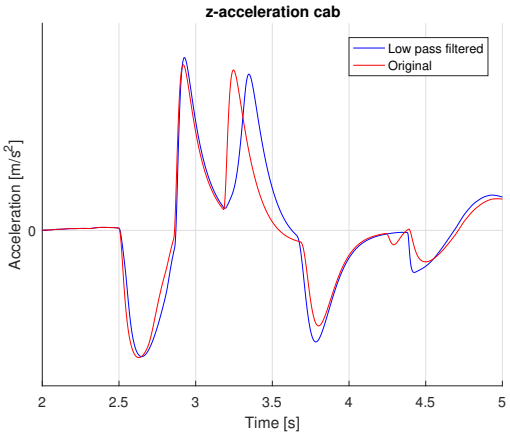

(b) Sixth order filtered reference signal.

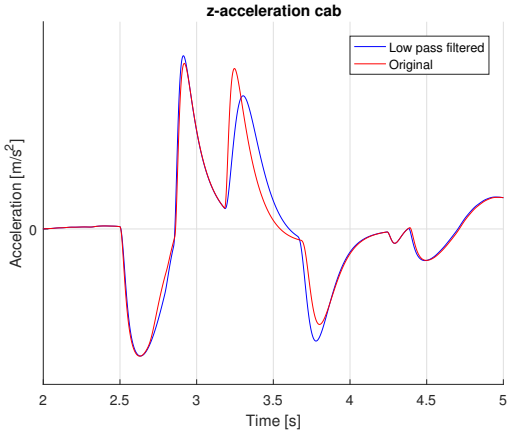

(c) Second order filtered saturation.

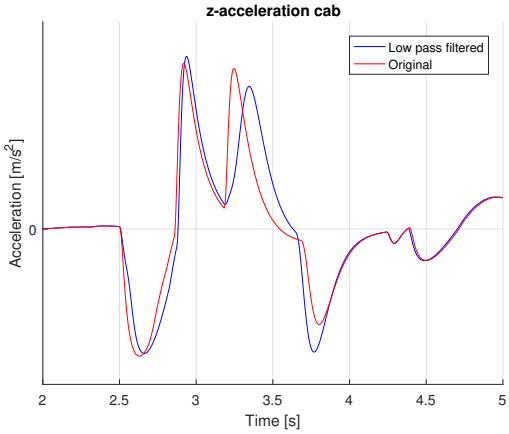

(d) Sixth order filtered saturation.

Figure 5.32: Simulated acceleration in z-direction. The "original" signal is a simulation without the low pass filtered signals.

The figure shows the z-acceleration of the different cases. Figure 5.32a and Figure 5.32c show that when filtering with order two the offramp did not change in acceleration. This was due to the engine torque, generated by ETC, not changing. What could be said for all of the figures apart from Figure 5.32a was that the onramp had a better acceleration curve in the beginning. But the acceleration at the end of the onramp was increased instead. This was due to the engine torque having to compensate for the slower reaction when low pass filtering the signal.

An interesting thing was to compare the results in Figure 5.32c and Figure 5.32d. Both of them had the same onramp shape but the second order filtered signal produced a negative acceleration that was smaller compared to the sixth ordered one.

The conclusion from these figures was that if this was to work the second order filtered saturation should be investigated for the onramp. It could be possible to investigate a first order filter to see if the negative acceleration at the end could be improved. In the offramp a filter with order six should be investigated since it was the only one that had a resonable effect.

Figure 5.33 shows the behaviour in x-direction.

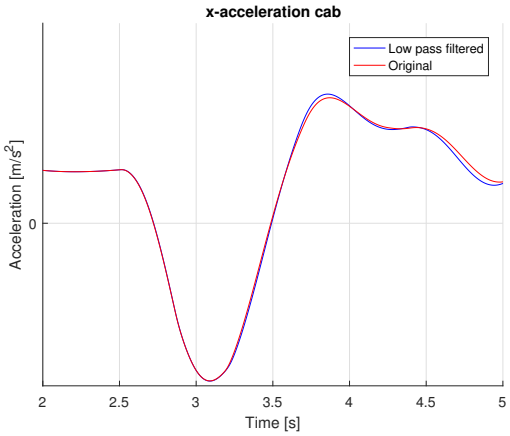

(a) Second order filtered reference signal.

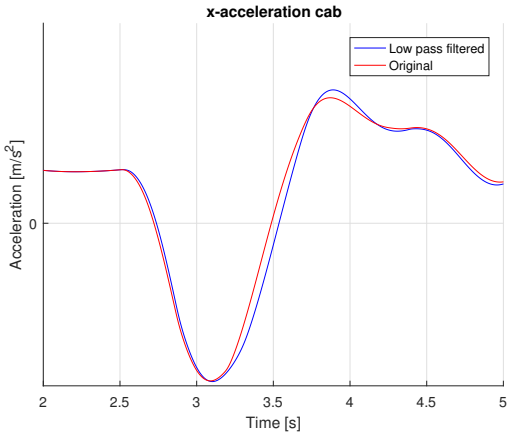

(b) Sixth order filtered reference signal.

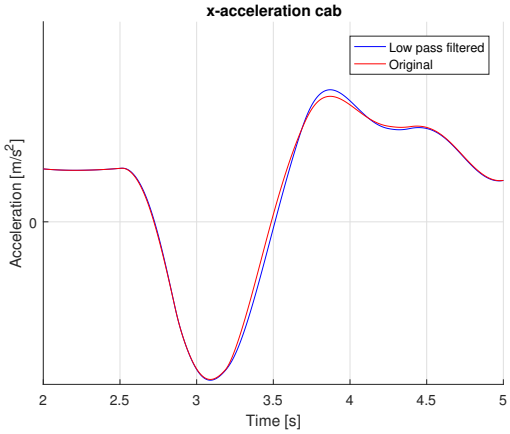

(c) Second order filtered saturation.

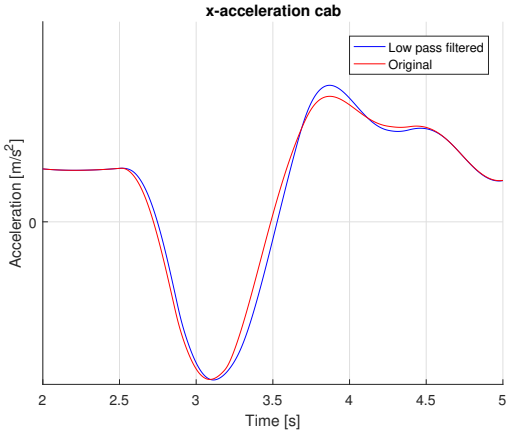

(d) Sixth order filtered saturation.

Figure 5.33: Simulated acceleration in x-direction. The "original" signal is a simulation without the low pass filtered signals.

The figures show that the effect in the x-direction was not as obvious as in the z-direction. The lower order filters had a better behaviour than the higher order ones in the onramp.

With the figures showing the acceleration in the x- and the z-direction the conclusion was that the best performing controller was the second order filtered saturation. Figure 5.34 show the saturated input to the model and the engine torque. In Figure 5.35 the wheel speed and the flywheel torque are displayed.

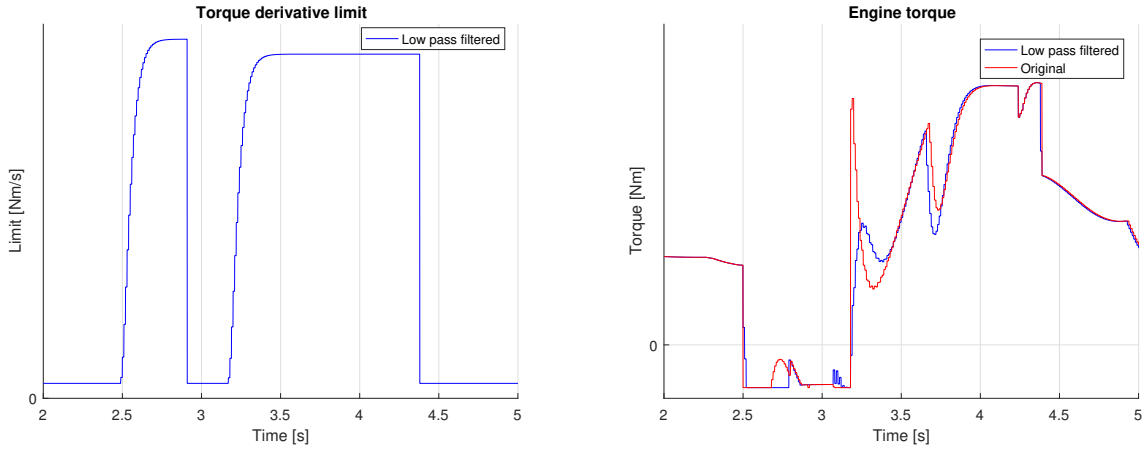

(a) Filtered saturation limit.

(b) Comparison of the engine torque.

Figure 5.34: Results from low pass filtering the saturations with filter order 2.

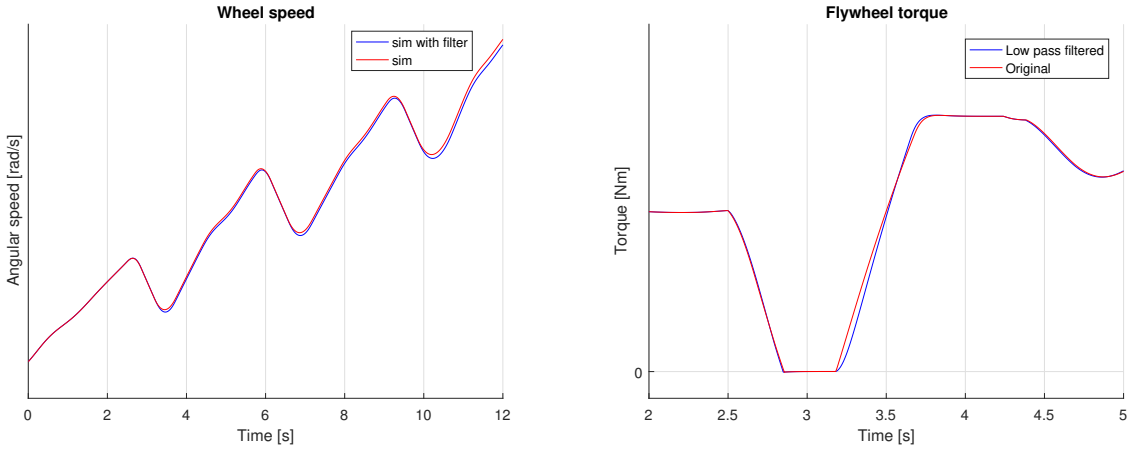

(a) Simulated wheel speed.

(b) Simulated flywheel torque.

Figure 5.35: Comparison of wheel speed and flywheel torque with and without the low pass filter.

Figure 5.35 shows that the wheel speed and the flywheel torque was not altered substantially. This could be used as an indication that the gear shift would be executable if implemented in a truck.

The improved behaviour in the onramp seemed to have a connection with the smaller peak in engine torque at 3.2 s in Figure 5.34b. By not generating as much engine torque the behaviour of the acceleration was improved. The dip in acceleration at about 3.75 s in Figure 5.32c was related to the change in engine torque shown in Figure 5.34b. This would not be affected by the low pass filter and another method has to be used to improve it.

The conclusion of the filter performance was that low pass filtering the saturation with a low order filter was the best way to improve the comfort in the onramp. The gain in some parts led to losses in other parts. But if the the dip in engine torque at the end of the onramp could be changed this method could be promising. For the offramp the sixth order filtered saturation was the best performing filter.

5.2.2 Feedback controller

The performance of the feedback controller is shown in several plots. Only the performance of the first gear shift is presented since this was the one with the worst comfort in most of the measurements presented in 4.1.3. Figure 5.36 shows a comparison between the cab accelerations with and without the developed controller. Figure 5.37 shows the engine torque calculated by ETC and the actual flywheel torque with and without the developed controller.

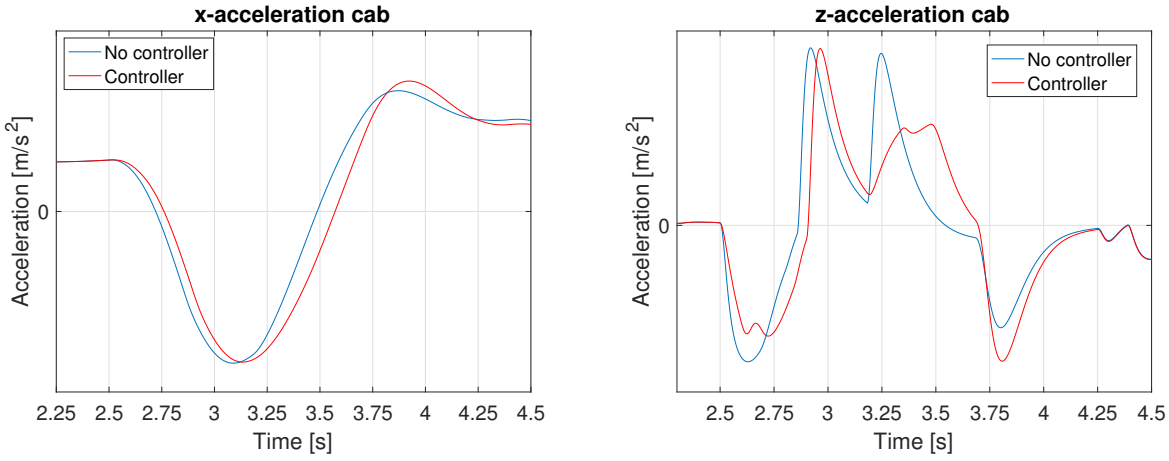

(a) x-acceleration.

(b) z-acceleration.

Figure 5.36: Cab accelerations with and without the developed controller.

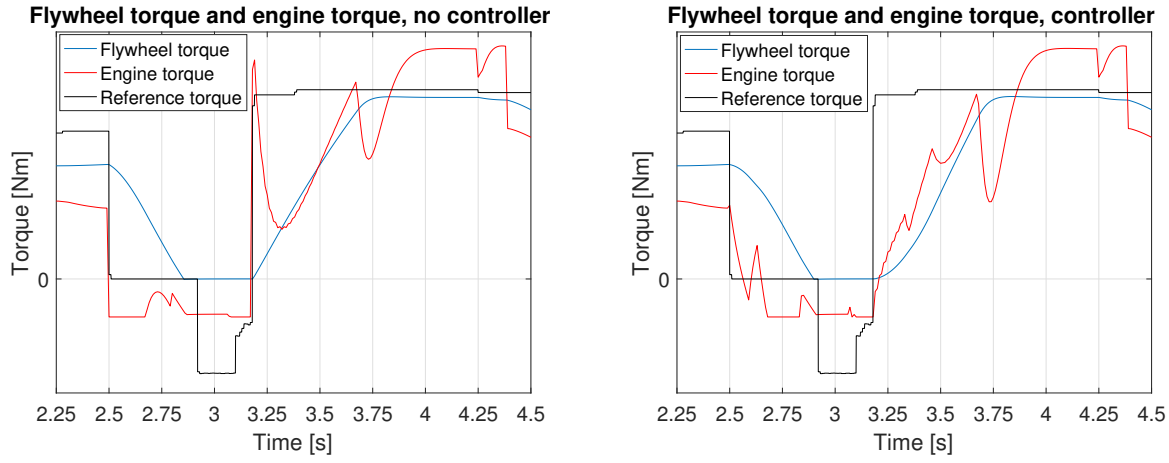

(a) Torques, no controller.

(b) Torques with controller.

Figure 5.37: Engine torque and flywheel torque with and without the developed controller.

The controller is described by Algorithm 3 and Algorithm 4. The control signal was calculated in order to keep the z-acceleration at a desired level, and it did not consider the x-acceleration. The offramp was active between 2.5 s and 2.9 s and the onramp was active between 3.2 s and 4.4 s.

Offramp

Looking at the z-acceleration during the offramp in Figure 5.36b, the controller has lowered the acceleration. Figure 5.36a shows that the controller did not change the amplitude of the x-acceleration but the offramp has a smoother start, which would indicate lower jerk. Figure 5.37a and Figure 5.37b shows the engine torque with and without the developed controller. There was a significant difference between the engine torques. Instead of applying as low engine torque as possible to push down the flywheel torque, the controller was raising the engine torque when the z-acceleration was lower than the reference.

Onramp

Looking at the z-acceleration during the onramp in Figure 5.36b, the controller has lowered the acceleration. The dip at around 3.75 s was due to ETC trying to shape the flywheel torque. This could possibly be improved by altering the settling time. A higher settling time was investigated but resulted in a slower gear shift. It was also investigated to change the value of the settling time from a low to a high value during the onramp. This resulted in a bad behaviour since the settling time is a scaling factor of the error in ETC. Changing it continuously might give a better performance and was not investigated due to time limitations. Another attempt to prevent the dip was to control the acceleration to zero before the dip, as seen in Figure 5.38 around 3.4 s.

Figure 5.36a shows that the x-acceleration has a slightly greater overshoot with the controller. Just like in the offramp, the engine torque, seen in Figure 5.37b, was controlled up in a way to keep the acceleration at reference level.

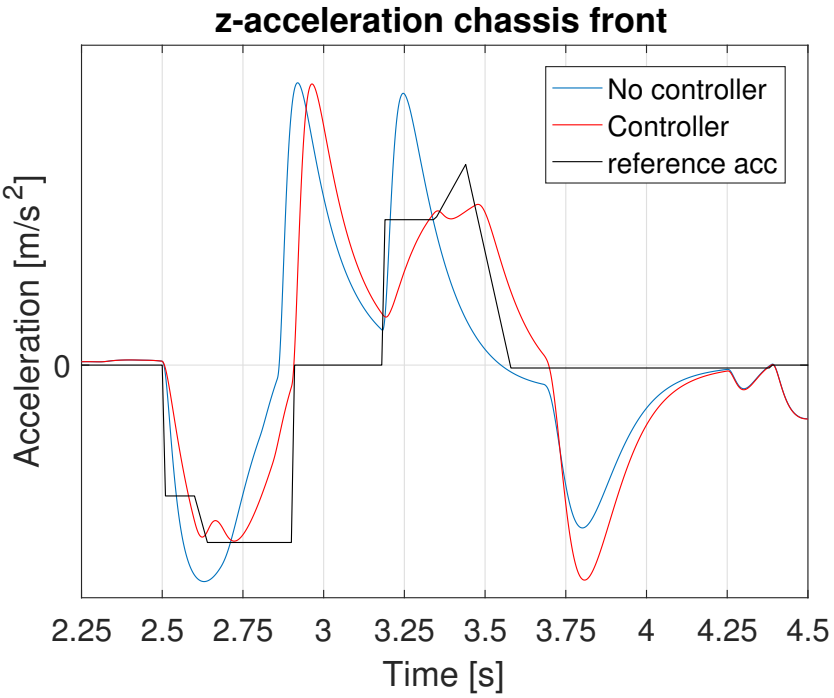

Figure 5.38: z-accelerations in the chassis front together with the reference.

As a measure of if the gear shift was executable two conditions were validated. The first condition was that the flywheel torque was supposed reach the reference value using the developed controller in the same time as without it. Looking at Figure 5.37 the flywheel torque reached the final value in the same amount of time both in the offramp and onramp.

The second condition was to look at the wheel speed with and without the developed controller to see how the gear shift affected the velocity. Figure 5.39 shows that the wheel speed was unaffected over time.

By fulfilling these two conditions it was concluded that the gear shift was executable.

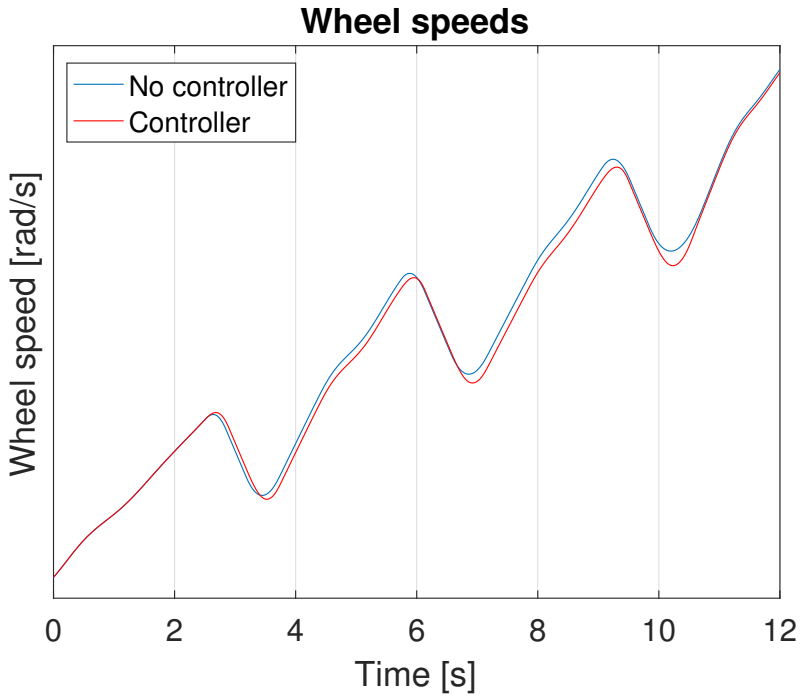

Figure 5.39: Wheel speed comparison between a simulation with and without the developed controller.

6. Discussion and conclusions

The first part of this section contains a discussion about the work in this thesis. The experiments, models and controllers are all discussed with the performance and possible improvements as topics. This section also contains a part about future work. This part includes the improvements of the product developed that the authors find most important and would give the most improvements. Finally, a conclusion about the thesis is given. The objectives of the thesis is commented whether they have been fulfilled or not.

6.1 Discussion

This thesis included a wide variation of problems that had to be solved. These problems had to be solved in a confined time window of 20 weeks. In order to develop all the models, measurements and controllers simple models were implemented and then improved in order to reach the goals. The models and controllers are not at their final states but a foundation for further investigation has been laid.

6.1.1 Experiments

Comments about the performance and possible improvements of the measurement system and comfort investigations are presented below.

Measurement system

In general, the data needed to analyze the truck behaviour and to develop the models were received. There was however one sensor that would have completed the measurement system. A position sensor, measuring the distance in x-direction between the chassis tower and its connection point at the cab lower front. This would have made it possible to also investigate the free movement cab model in 4.3.5 since the parametrization would have been easier.

Another comment is that the position sensors measuring the distance between the wheel axles and chassis were placed diagonally and the accelerometers in the chassis front and rear were placed on the left side. In the approximations where frame twisting is not considered, this would not be a problem since both sides would move similarly. But since frame twisting is a truck behaviour in reality, this might mean that the position sensor and accelerometer placed on different sides in the front were not coordinated. This was not further investigated but might have influenced the model parametrization.

Comfort

The comfort measurement had some flaws. The first flaw was that it could not draw an absolute limit between good and bad gear shifts which would be the ideal case. The second flaw was that only one person had the say about which gear shifts were bad or good. It would have been good if multiple drivers would have given their verdict on the cab behaviour to get a more qualitative measure of comfort. With this said the measure of comfort was seen as a good enough measure for this thesis.

6.1.2 Models

The models developed are discussed below where performance and possible improvements are brought up.

Powertrain model

The powertrain model used in this thesis performed in a decent way. It captured the general acceleration behaviour, flywheel torque, wheel speed and engine speed. With this said, there are room for improvements. The spring and damper constants were large which resulted in a very reactive model. The parameters might be tuned in a better way to improve the powertrain behaviour by making it less reactive.

The jerk and oscillations in the powertrain were not captured at all by the model. A way to improve the model behaviour would be to introduce more states to keep track of the backlash for example. The model in this thesis did not consider backlash which meant that some dynamics were removed from the system.

If a more advanced powertrain model, containing more states, would be introduced it could be of interest to improve the decoupled model as well. With more states describing speeds on the wheel side of the clutch, it would be possible to improve the powertrain behaviour when decoupled. This would probably include jerk and oscillations when decoupled which are not captured with the current model.

Chassis model

The chassis model included some approximations and did not describe reality in an exact way. The model would better reflect reality if, for example, the rear axle would be modelled as a spring-damper configuration. To be as real as possible is however not always the purpose of a model. In this case, it was necessary to capture the main behaviour in the chassis front since that was where the cab was connected to the chassis. The chassis model captured this behaviour in a satisfying way.

One further development would be to consider frame twisting. Frame twisting is a phenomenon that can occur at large engine torques. The torque makes one side of the chassis raise more than the other, forcing the frame to twist. This means that the z-acceleration is larger on one side than on the other which could have an impact on the cab movements not investigated in this thesis.

The model has been tuned using measurements from the driving situation when the truck was accelerating in a slope. It has not been investigated how the model fits other driving situations. However, due to the non linear dampers modelled as linear dampers, it is likely the model does not show the same performance as when accelerating in a slope. Therefore another improvement of the chassis model would have been to use a non linear damper model.

The force on the chassis generated by the cab was modelled as constant to be able to develop the chassis and cab model at the same time. The model could be improved by letting the cab behaviour affect the chassis.

Cab model

When looking at the cab model it is clear that the oscillating movements of the cab were not captured. To estimate the spring and damper constants the least squares method was used. This method might not be the best method when there are oscillations in the real system. An alternative could be to try to find the natural frequencies of the cab and estimate the parameters using them. A measurement was not performed where the natural frequencies of the cab were found.

When combining the models the lack of oscillations in the cab model was not a big problem since the powertrain did not capture the oscillations in the acceleration of the vehicle.

The suspended cab model should be able to capture the true cab movements in a better way. To be able to use this model a measurement of the position in x-direction is needed.

ETC

The ETC model was developed in order to recreate the vehicle behaviour with the same input as in reality, the demanded torque. Instead of developing a new controller to control ETC with respect to the acceleration, it might be a good idea to develop one controller containing the goals of both ETC and the new controller.

6.1.3 Controller

Comments about the developed controllers are brought up in this part of the section. The performance, problems and possible improvements are discussed.

Open loop control

The approach of filtering different inputs to the system was tested and compared to the current method. It showed promise when low pass filtering the saturation in ETC. This simple method improved the acceleration in some parts of the onramp. This method was not perfect since it introduced larger accelerations at other parts of the onramp instead. But when analyzing the measurements the effect were generated by the torque controller. In the offramp there was no significant effect when using the lower order filters.

One of the main reasons for investigating this method was the hypothesis that the jerk could be minimized. Since the model which the controller was tested on did not capture the jerk of the system no conclusions could be drawn.

If this method was to be improved a filter of low order should be investigated and used on the saturation according to the tests in this thesis. The behaviour of the torque controller could be further investigated to remove the poor behaviour when considering comfort.

Feedback controller

The performance of the feedback controller was good. The amplitude of the acceleration was minimized in both the offramp and onramp. There is a dip in the z-acceleration around 3.75 s in Figure 5.36b which is due to the characteristics of ETC.

The feedback controller has been tuned for one specific driving situation. It was tuned by the choice of the reference acceleration. The reference acceleration is the limit for when ETC can apply a larger engine torque or not. The limit has to be large enough to avoid extending the duration of the gear shift but still be small enough to be considered comfortable. The controller might work well for other driving situations as well but a lot of tuning would have to be performed. Then a look-up-table could be used containing tuning parameters for different driving situations.

Another solution would be to fuse the functionalities of ETC and the feedback controller into one controller. This might lead to a controller better suited for every driving situation. A reference acceleration would however have to be developed.

6.2 Future work

There are several ways the models and controllers developed in this thesis could be improved. In the powertrain the focus should be on capturing the powertrain behaviour during a gear shift in a better way. This could be done by introducing more states and model more components as flexible. By doing this for example backlash could be captured by the model.

To improve the cab model it would be of importance to capture the jerk. This could be done by investigating the suspended model.

The controllers derived in this thesis were based on adapting the input to ETC which considered the powertrain behaviour. The long term solution of creating comfortable gear shifts should be by replacing the existing torque controller instead of controlling it. In this way the new controller could consider the powertrain behaviour as well as the cab comfort.

6.3 Conclusion

Models of the powertrain, chassis and cab have been developed and combined in order to capture how the cab is affected by the powertrain. It captured the general behaviour of the different parts of the model. The

combined model gave a good general knowledge of the system as well as the possibility to create a controller to improve the comfort according to simulations.

In order to improve the cab comfort a measure of comfort was defined. The variables affecting the cab comfort were jerk and acceleration. The derivation of the comfort measure took different approaches of comfort measurements into consideration and combined it with the experiments performed in this thesis.

The developed combined model were used to develop two different controller structures. One was based on open loop control and the other was a feedback controller. The derived open loop controller indicated that by using a low pass filter the cab acceleration for some parts of the gear shift could be improved. The feedback controller used the chassis front z-acceleration as feedback. The results were promising and the cab accelerations could be improved in most parts of the gear shift. The feedback controller shows that it is possible to improve the cab comfort and it would be a good idea to investigate this further. By fusing ETC and the developed controller into one controller there are possibilities to improve the comfort during a gear shift.

The controllers were not implemented on a Scania truck due to a combination of time limitations and vehicle problems.

The purpose of the thesis was to investigate whether it was possible to improve the comfort during gear shifts. Using the comfort definition stated in this thesis, it has been shown that it is possible to both affect and improve the cab comfort by altering the way the engine torque is applied to the flywheel during a gear shift.

A. Signal processing

This appendix includes the most relevant signal processing used in this thesis. First the synchronization of the measurement are described. After that the adaptation of the acceleration is shown.

A.1 $DEWEsoft$ and $Vision$ synchronization

When measuring, the person in the passenger seat had to take care of both measurement systems. Therefore it was decided that the best way to execute the measurements was to let $Vision$ record one long file containing several different measurements. $DEWEsoft$, on the other hand, recorded only one measurement on each file. Since both signals registered the engine speed, the engine speed was compared between the two measurement systems in order to synchronize the signals.

The way the signals were synchronized was to create a cost function of the squared difference between the signals letting the shorter signal travel across the long signal. At each step a part of the long signal was compared to the short signal. Then, the sample corresponding to the smallest cost indicated at which sample of the long signal the signals started to match. The cost function is described in (A.1),

$$cost = \sum_{k=1}^{N_{long}-N_{short}-1} (signal_{long}(k : N_{short} - 1) - signal_{short})^2 \tag{A.1}$$

where N_{long} and N_{short} are the number of samples of the long and short signal respectively. The k corresponding to the smallest *cost* was the first sample where the signals matched. The delay of the $DEWEsoft$ signals at 10-15 ms was adjusted by subtracting the number of samples corresponding to the delay from k.

One problem with the signals was that the signals of different sensors registered by $Vision$ did not have the same sample time. It differed between sample time 0.01 s, 0.02 s and 0.1 s. This was dealt with by upsampling the signals with higher sample time to the lower sample time at 0.01 s. The reason upsampling was chosen instead of decimation was that important information of the signal might be lost when decimating a signal. Upsampling of a signal was done as described in [20].

Another problem with $Vision$-signals was the time different sensors started register data. As shown in Figure A.1, one sensor started recording at time 0.31 s, while another started at 0.8 s. The figure also shows the large number of samples recorded by the red signal before the blue signal started recording. This meant that the time of sample k for one $Vision$-signal did not have to match the time of sample k for another $Vision$-signal. This meant that the indices matching one $Vision$-signal to the $DEWEsoft$-signal was not necessarily the same for another $Vision$-signal. This was solved by comparing the first and last times in the time vector of the signal that was already matched to the $DEWEsoft$-signal with the time vector of the new signal. The starting time and ending time gave two samples corresponding to the times most alike the starting time and ending time. By taking the samples between these times the correct signal was attained. The signal was now matched to the $DEWEsoft$-signal.

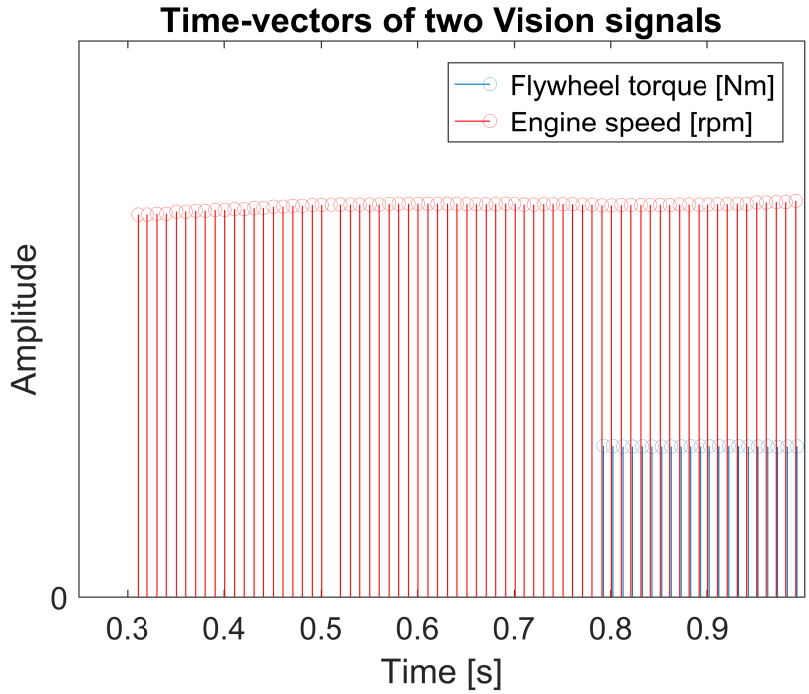

Figure A.1: Two sensors started recording at different times. One sensor registered many samples before the other sensor started, making it a problem synchronizing the signals since a sample k corresponded to different times for the two signals.

The last part of synchronizing the signals was to synchronize the accelerometer and position sensor signals to the $DEWEsoft$ engine speed. The engine speed was recorded with sample time 0.02 s and the other sensor signals were recorded with sample time 0.001 s. All sensors recorded with $DEWEsoft$ started recording at 0 s. Therefore the first and last sample number had to be multiplied by 20, since the accelerometer and position sensors had 20 times faster sample time than the engine speed in $DEWEsoft$. When the first and last sample number were achieved, all samples in between were extracted. These samples were matching the signal sampled with 0.001 s to the engine speed.

A.2 Processing of accelerometer signals

Figure A.2 shows an accelerometer signal in the time domain and the frequency domain. In this case the truck was standing still at 0 % road slope. The time domain shows how noisy the signal was, while the frequency domain shows in which frequencies the energy of the noise was.

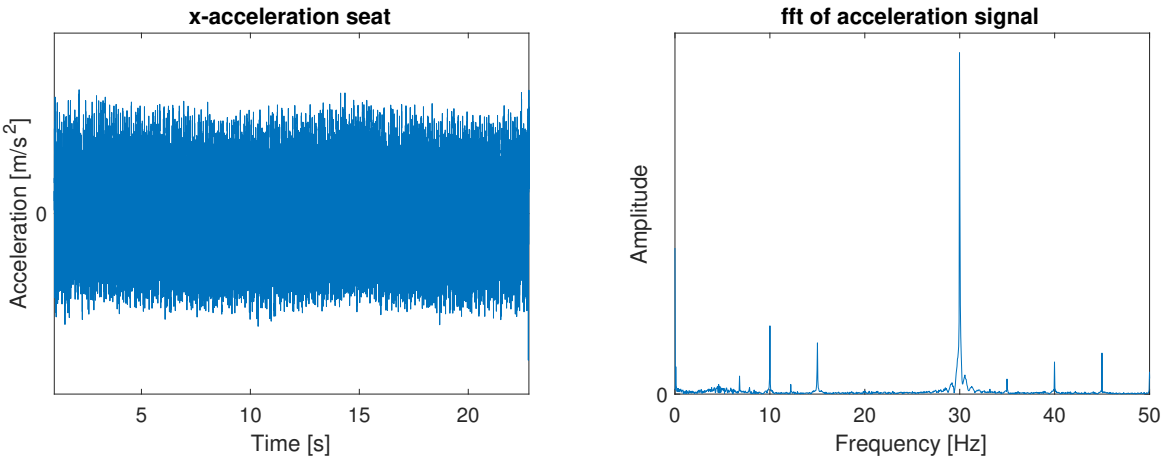

(a) Noise in the time domain.

(b) Noise in the frequency domain.

Figure A.2: Noise measurements in different domains. The figure shows the obvious presence of noise and in which frequencies the noise has its energy in.

The distinct peaks at 10 and 30 Hz were induced by engine speed at 600 rpm and ignition frequency respectively. The calculations are shown in (A.2).

$$\begin{aligned} \text{Engine speed frequency} = & 600\ rpm = \frac{10 \text{ revolutions}}{s} = 10\ Hz \\ \text{Ignition frequency} = & /\text{4-stroke engine}/ = \\ & \text{Engine speed frequency} \times 3 = 30\ Hz \end{aligned} \tag{A.2}$$

These disturbances would move to higher frequencies as the engine speed increased. One way to filter out these would be to use a band stop filter that adapts its cut-off frequencies depending on the engine speed. This solution would mean that all the information kept in other frequencies would be saved. However, the judgement was made that frequency components higher than 10 Hz would not be of interest since it would not be reasonable to control the cab movements with such frequencies due to large components with large intertias. Therefore, a low pass filter with cut-off frequency 10 Hz was used to filter out noise of the accelerometer signals.

The situation where the truck was standing still in 0 % road slope was used to zero the accelerometers. However, some of the experiments were performed in slope with a rotating cab and chassis. In this situation, the sensors were affected by a gravity component. This resulted in an incorrect acceleration relative to the ground. The accelerometer signals therefore had to be translated into accelerations in x- and z-directions with respect to the ground. This was done by using (A.3),

$$\begin{aligned} a_{c,x,real} &= a_{c,x,meas} - gsin(\theta_{slope} + \theta_c + \phi) \\ a_{c,z,real} &= a_{c,z,meas} + (g - gcos(\theta_{slope} + \theta_c + \phi) \\ a_{\text{ch front},x,real} &= a_{\text{ch front},x,meas} - gsin(\theta_{slope} + \phi) \\ a_{\text{ch front},z,real} &= a_{\text{ch front},z,meas} + (g - gcos(\theta_{slope} + \phi) \\ a_{\text{ch rear},x,real} &= a_{\text{ch rear},x,meas} - gsin(\theta_{slope} + \phi) \\ a_{\text{ch rear},z,real} &= a_{\text{ch rear},z,meas} + (g - gcos(\theta_{slope} + \phi) \end{aligned} \tag{A.3}$$

where the index "meas" refers to the measured sensor signal and "real" refers to the acceleration in x- or z-direction relative to the ground.

B. Powertrain parameters

This appendix shows the complete sequence of altering the parameters of the powertrain.

The initial obtained parameters are listed in Table B.1.

Table B.1: Powertrain parameters.

Parameter	Result
$k_{\mathrm{d}}(Nm/rad)$	–
$c_{\mathrm{d}}(Nms/rad)$	$9.7357 \cdot 10^3$
$b_{\mathrm{e}}(Nms/rad)$	2.3381
$b_{\mathrm{w}}(Nms/rad)$	0

The obtained damper constant of the driveshaft seemed high but it might work for this model. With these parameters the Figure B.4 and Figure B.2 were obtained.

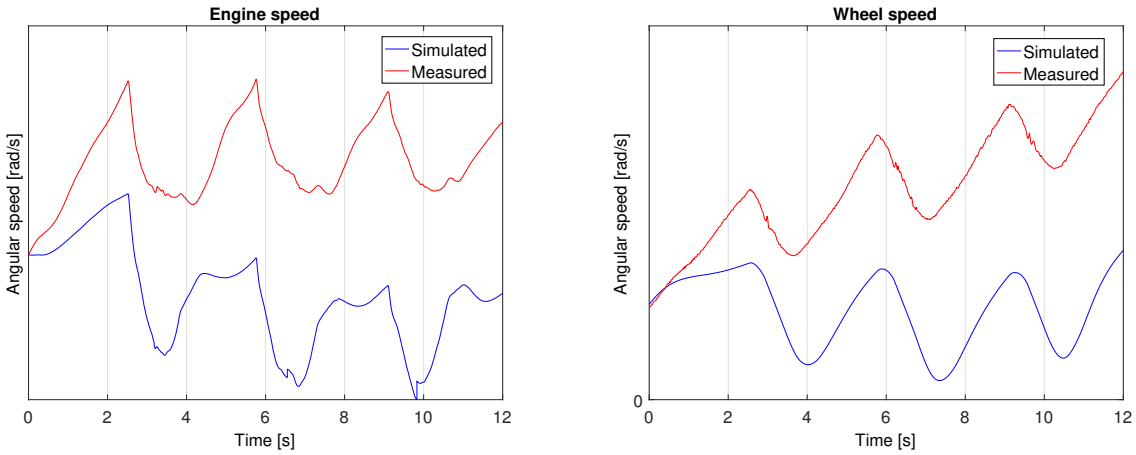

(a) Simulated and measured engine speed.

(b) Simulated and measured wheel speed.

Figure B.1: Simulated and measured speed of the engine and wheels.

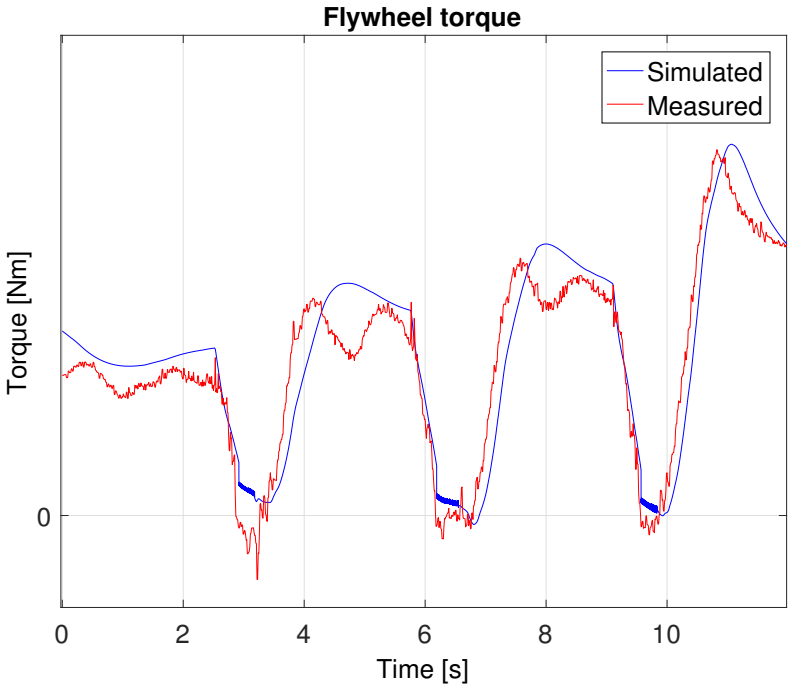

Figure B.2: Simulated and measured flywheel torque. The simulated torque followed the measured one quite good but would be improved.

The conclusion based on the figures was that the mechanical loss on the engine side should be lowered. It was set to zero which generated Figure B.3.

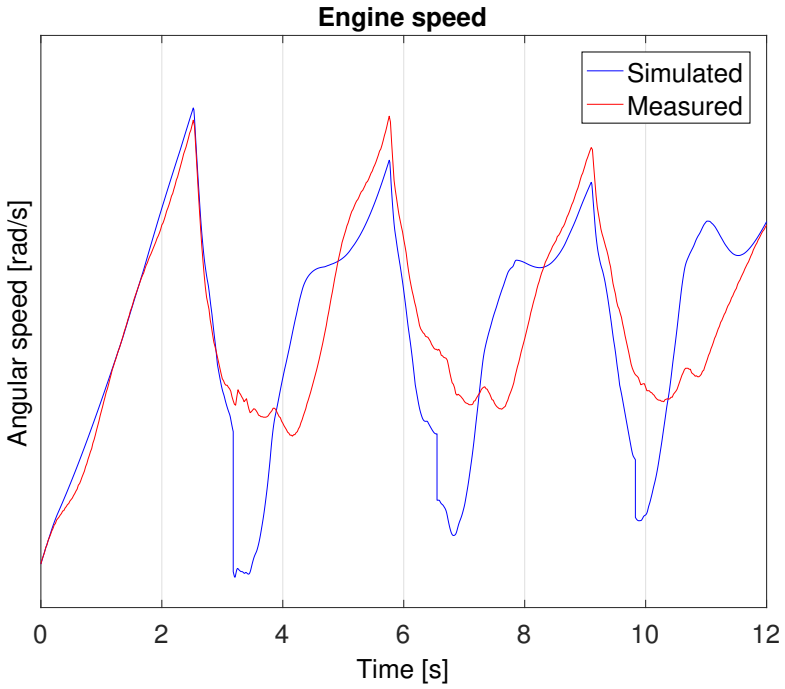

Figure B.3: Simulated and measured engine speed. The simulated engine speed was improved but the model with these parameters did not fully capture the real behaviour.

The simulated engine speed was better with the the new parameter but the other parameters had to be improved. Figure B.4a shows the flywheel torque given the new parameter. The figure shows that the torque on the flywheel did not react fast enough in the onramp. This led to the conclusion that the spring constant had to be increased for this model to work. By increasing the spring constant the simulated flywheel torque was as Figure B.4b shows.

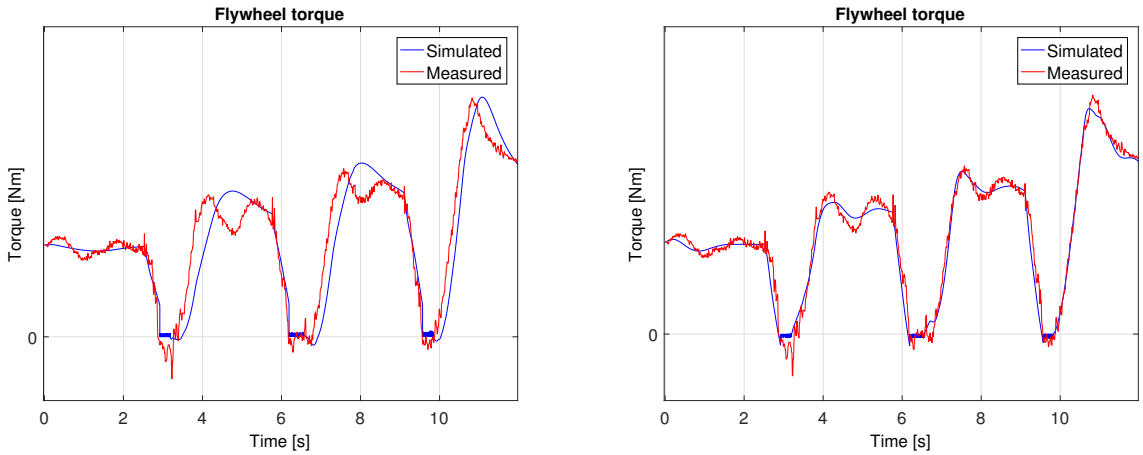

(a) Before alteration.

(b) After alteration.

Figure B.4: Simulated and measured flywheel torque.

The behaviour of the flywheel was improved. With the new spring constant the parameters were estimated once again using the least squares method. Table B.2 shows the new obtained parameters.

Table B.2: Powertrain parameters.

Parameter	**Result**
$k_{\mathrm{d}}(Nm/rad)$	$1.0755 \cdot 10^5$
$c_{\mathrm{d}}(Nms/rad)$	$9.6416 \cdot 10^3$
$b_{\mathrm{e}}(Nms/rad)$	0
$b_{\mathrm{w}}(Nms/rad)$	0

The Figures B.5 and Figure B.6 shows the poweertrain behaviour given the new parameters.

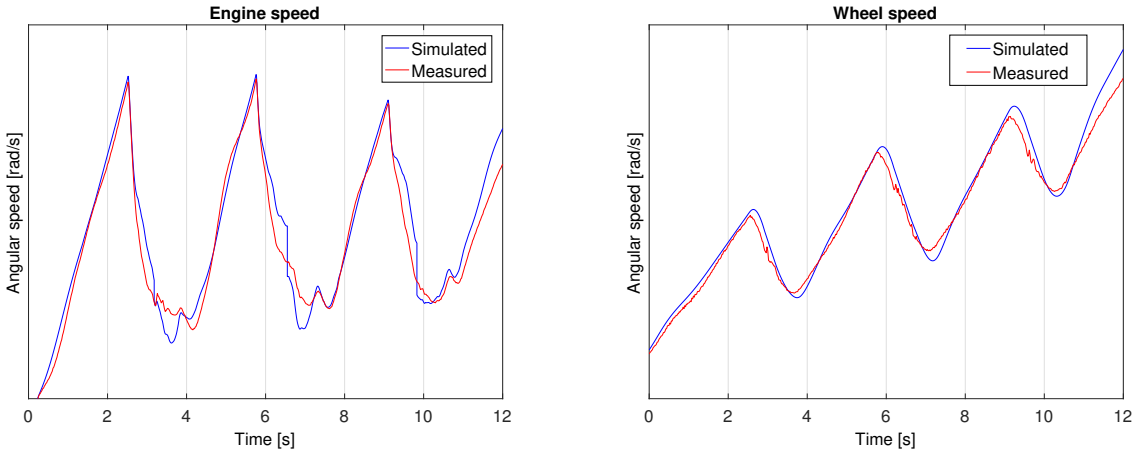

(a) Simulated and measured engine speed.

(b) Simulated and measured wheel speed.

Figure B.5: Simulated and measured engine and wheel speed.

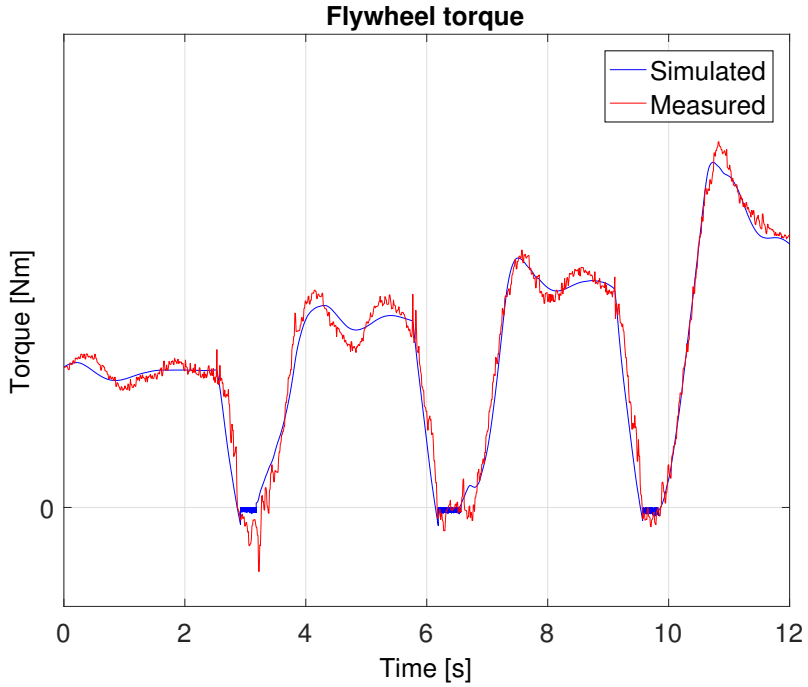

Figure B.6: Simulated and measured flywheel torque. The simulated torque follows the measure one quite well.

The parameter which could improve the behaviour of the model was the damper constant. The damper constant was altered to 2000 which generated the flywheel torque shown in Figure B.7.

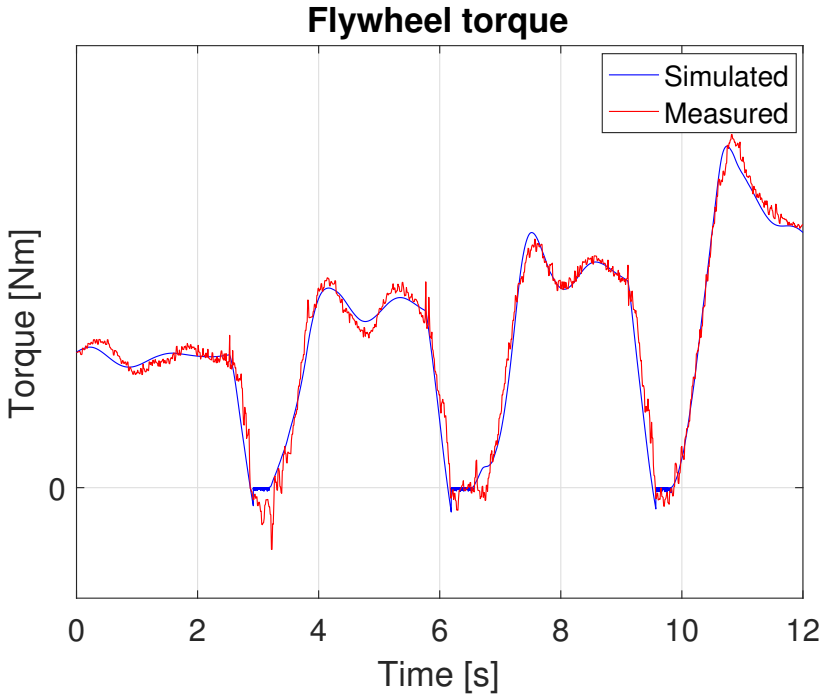

Figure B.7: Simulated and measured flywheel torque.

The new parameters generated a good simulated torque apart from when the clutch was disengaged. This was not of importance since it was the wheel side of the transmission that was of interest and the engine side did not effect it when the clutch was disengaged. Figure B.8 shows the wheel speed given the new parameters.

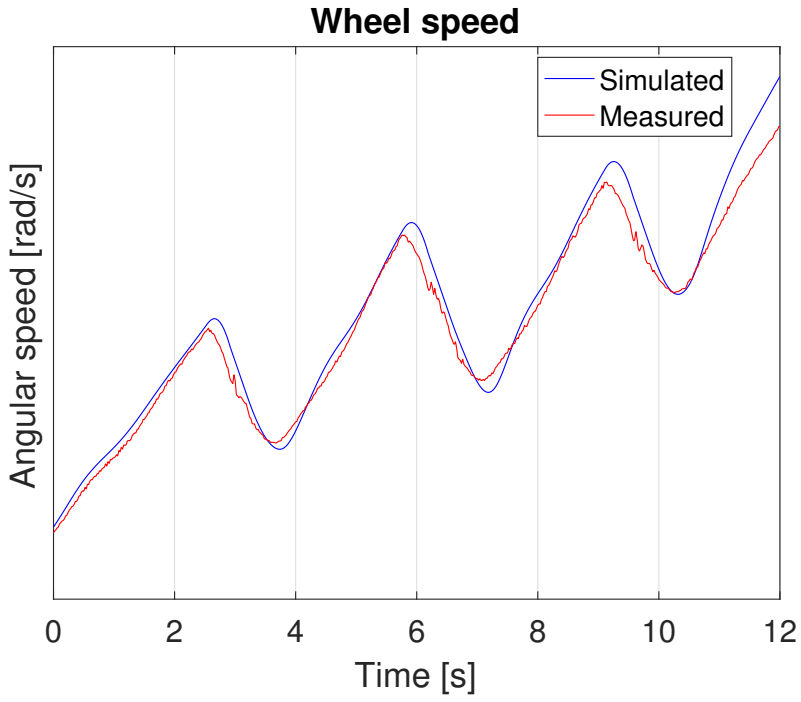

Figure B.8: Simulated and measured wheel speed. The speed seems a bit high with the current parameters.

In order to improve the models behaviour the losses of the wheel was increased to 75 which generated Figure B.9 and Figure B.10.

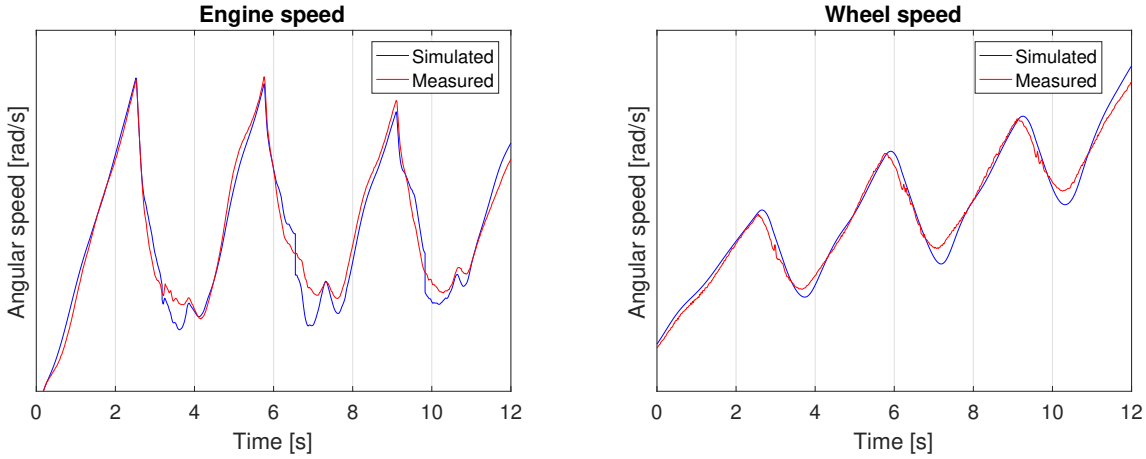

(a) Simulated and measured engine speed.

(b) Simulated and measured wheel speed.

Figure B.9: Simulated and measured engine and wheel speed.

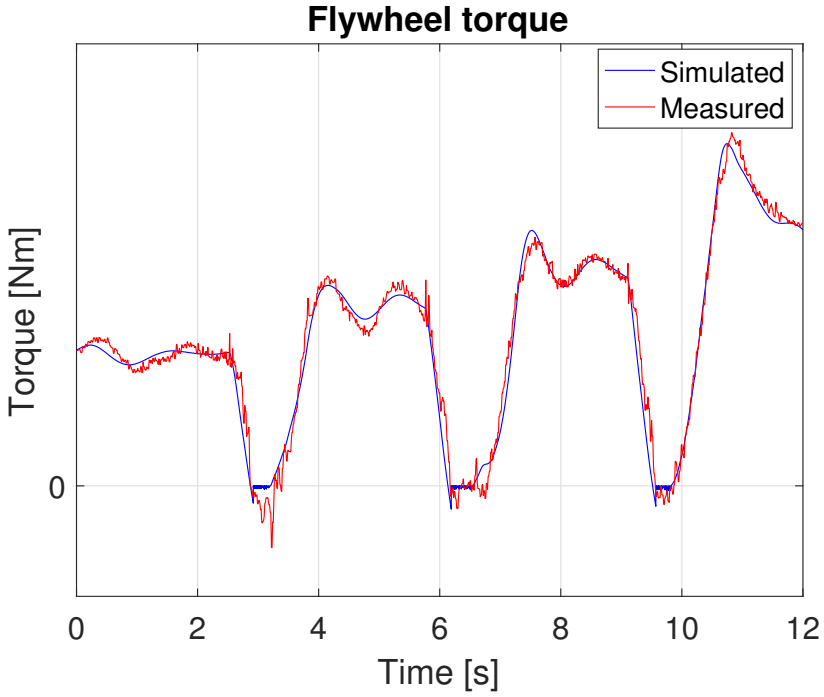

Figure B.10: Simulated and measured flywheel torque.

The figures show that the powertrain behaviour was good. When the clutch was disengaged the model did not perform which was expected. The final parameters for the powertrain are displayed in Table B.3.

Table B.3: Powertrain parameters.

Parameter	**Result**
$k_{\mathrm{d}}(Nm/rad)$	$1.0755 \cdot 10^5$
$c_{\mathrm{d}}(Nms/rad)$	2000
$b_{\mathrm{e}}(Nms/rad)$	0
$b_{\mathrm{w}}(Nms/rad)$	75

Bibliography

[1] Magnus Pettersson. "Driveline Modeling and Control". PhD dissertation. Department of Electrical Engineering, Linköping University, 1997.

[2] Lars Eriksson and Lars Nielsen. *Modeling and Control of Engines and Drivelines*. Automotive (Wiley). Wiley, 2014. ISBN: 9781118479995.

[3] M. Pettersson and L. Nielsen. "Gear Shifting by Engine Control". In: *IEEE Transactions on Control Systems Technology* Vol. 8.Num. 3 (2000).

[4] E. Jonsson Holm. *Vehicle Mass and Road Grade Estimation Using Kalman Filter*. Masterś thesis. Department of Electrical Engineering, Linköping University, 2011.

[5] H. Akçay and S. Türkay. "Active Suspension Design for an Idealized Truck Cabin". In: *Proceedings of the European Control Conference 2009 in Budapest, Hungary* (2009).

[6] W. Evers et al. "Controlling active cabin suspensions in commercial vehicles". In: *2009 American Control Conference at Hyatt Regency Riverfront, St. Louis, MO, USA* (2009).

[7] Anders Forsén. "Heave Vehicle Ride and Endurance - Modelling and Model validation". PhD. Department of Vehicle Engineering, Royal institute of Technology, 1999.

[8] Jo Yung Wong. *Theory of ground vehicles, 3rd ed.* John Wiley & Sons, Inc., 2001. ISBN: 9780471354611.

[9] Henrik Abrahamsson, Peter Carlson. *Robust Torque Control for Automated Gear Shifting in Heavy Duty Vehicles*. Master's thesis. Linköping University, 2008.

[10] Thomas D. Gillespie. *Fundamentals of vehicle dynamics*. Fourth Printing, 1992. ISBN: 1560911999.

[11] David González et al. "Speed Profile Generation based on Quintic Bézier Curves for Enhanced Passenger Comfort". In: *International Conference on Intelligent Transportation Systems (ITSC)* (2016).

[12] Paolo Giani et al. "Automatic Gear Shifting in Sport Motorcycles". In: *IEEE Transactions on Vehicular Technology , Vol. 63, No. 5, June 2014* (2013).

[13] Xiukun Wei et al. "Rail vehicle ride comfort prediction based on bogie acceleration measurements". In: *Control and Decision Conference (CCDC)* (2013).

[14] Marlene Sandström. *Investigation of and Compensation for Time-Delays in Driveline Control Systems*. Master's thesis. Royal Institute of Technology, 2014.

[15] Lars Eldén and Linde Wittmeyer-Koch. *Numeriska beräkningar*. Studentlitteratur, 2001. ISBN: 978-91-44-02007-5.

[16] Peter Christensen. *Elementär mekanik Del 2: Stelkroppsmekanik*. Tekniska högskolan vid Linköpings Universitet.

[17] Peter Christensen. *Elementär mekanik Del 1: Masspunkters mekanik, Jämviktslära*. Tekniska högskolan vid Linköpings Universitet.

[18] Martin Enqvist and Torkel Glad and Svante Gunnarsson and Peter Lindskog and Lennart Ljung and Johan Löfberg and Tomas McKelvey and Anders Stenman and Jan-Erik Strömberg. *Industriell reglerteknik Kurskompendium*. Reglerteknik, Istitutionen för systemteknik, Linköpings Universitet, 2014.

[19] Torkel Glad and Lennart Ljung. *Reglerteknik - Grundläggande teori*. Studentlitteratur, 2006. ISBN: 9789144022758.

[20] Fredrik Gustafsson, Lennart Ljung, and Mille Millnert. *Signal Processing*. Studentlitteratur, 2011. ISBN: 9789144058351.